

## Politecnico di Torino

Sustainable processes and chemical engineering 2024/2025

December 2025 Graduation Session

# TREATMENT OF FLY ASHES FOR INERTIZATION AND ADSORBENT PURPOSES

Ball milling on MSWI fly ash: impact on heavy metal leaching and acid gas adsorption properties

Supervisor:

Francesca Demichelis

Co-Supervisor:

Antonio Nieto Marquez Ballesteros

Candidate:

Alessandra Lodi

## Summary

| 1 | INTR    | ODUCTION  | 9   |
|---|---------|---|-----|
|   | 1.1.    | Ashes production and actual disposal  | 10  |
|   | 1.2.    | Objectives  | 13  |
|   | 1.3.    | Novelty   | 14  |
| 2 | WAS     | TE INCINERATION   | 16  |
|   | 2.1. Ho | w does a waste incinerator work?  | 17  |
|   |         | posal methods with focus on incineration plants and fly ash management in the Europerented on Spain and Italy |     |
| 3 | СОМ     | PARATIVE ANALYSIS OF WASTE ADMISSION CRITERIA IN EUROPE   | 27  |
| 4 | MAT     | ERIALS AND METHODS  | 36  |
|   | 4.1.    | Properties of ashes   | 36  |
|   | 4.2.    | Inertization and activation tests   | 38  |
|   | 4.3.    | Leaching tests  | 44  |
|   | 4.4.    | Analysis of the leaching liquid   | 47  |
|   | 4.5.    | Acid-base curve analysis  | 61  |
|   | 4.6.    | Brunamer-Emmet-Teller method: BET analysis  | 65  |
|   | 4.7.    | Sulphur dioxide adsorption test   | 67  |
|   | 4.8.    | Hydrogen sulphide adsorption test   | 76  |
| 5 | RESU    | ILTS  | 80  |
|   | 5.1.    | Fly ashes characterisation  | 80  |
|   | 5.2.    | Inertization and activation   | 85  |
|   | 5.3.    | Leaching results  | 86  |
|   | 5.4.    | Acid-base curve results   | 92  |
|   | 5.5.    | BET results   | 94  |
|   | 5.6.    | Adsorption tests  | 96  |
| 6 | CONCLU  | ISIONS AND FUTURE IMPROVEMENT   | 105 |
| В | IBLIOGR | APHY  | 108 |

## Sommario

| 1 | INTR     | ODUZIONE  | 9    |
|---|----------|---|------|
|   | 1.1.     | Produzione di ceneri e smaltimento effettivo  | . 10 |
|   | 1.2.     | Obiettivi   | . 13 |
|   | 1.3.     | Novelty   | . 14 |
| 2 | INCE     | NERIMENTO DI RIFIUTI  | . 16 |
|   | 2.1. Cor | ne funziona un inceneritore?  | . 17 |
|   | volanti  | todi di smaltimmento incentrati su impianti di incenerimento e sulla gestione delle ceneri<br>nell'Unione Europea, in particolare Spagna e Italia | . 23 |
| 3 | ANA      | LISI COMPARATIVA DEI CRITERI DI AMMISSIONE DEI RIFIUTI IN EUROPA  | . 27 |
| 4 | MAT      | ERIALI E METODI   | . 36 |
|   | 4.1.     | Proprietà delle ceneri  | . 36 |
|   | 4.2.     | Inertizzazione e attivazione  | . 38 |
|   | 4.3.     | Prove di lisciviazione  | . 44 |
|   | 4.4.     | Analisi del liquido di lisciviazione  | . 47 |
|   | 4.5.     | Curva acido-base  | . 61 |
|   | 4.6.     | Metodo Brunamer-Emmet-Teller: BET analisi   | . 65 |
|   | 4.7.     | Test di adsorbimento dell'anidride solforosa  | . 67 |
|   | 4.8.     | Test di adsorbimento dell'acido solfidrico  | . 76 |
| 5 | RISU     | .TATI   | . 80 |
|   | 5.1.     | Caratterizzazione delle ceneri volanti  | . 80 |
|   | 5.2.     | Inertizzazione e attivazione  | . 85 |
|   | 5.3.     | Risultati analisi del liquido di lisciviazione  | . 86 |
|   | 5.4.     | Risultati curva acido-base  | . 92 |
|   | 5.5.     | Risultati dell'analisi BET  | . 94 |
|   | 5.6      | Risultati adsorbimento  | 06   |

| 6 CONCLUSIONI E MIGLIORAMENTI FUTURI | 105 |
|--------------------------------------|-----|
| BIBLIOGRAFIA                         | 108 |

#### Table index

- Table 1: Limit values for concentrations in a leachate (BOE-A-2020-7438).
- Table 2: Limit values for total content of organic parameters (BOE-A-2020-7438).
- Table 3: Limit values for concentrations in a leachate (Legislative decree 3<sup>rd</sup> September 2020, n. 121 Annex 3).
- Table 4: Limit values for total content of organic parameters (Legislative decree 3<sup>rd</sup> September 2020, n. 121 Annex 3).
- Table 5: Size and weight of the balls used in the different tests with respective standard deviation.
- Table 6: Experimental conditions for the four ball milling tests.
- Table 7: Preparation of lead measurement standards by atomic absorption.
- Table 8: Example of a procedure for 1000 ppm of  $SO_2/N_2$  to insert in the experimental protocol.
- Table 9: Flow rate of  $SO_2/N_2$  and  $N_2$  for different concentrations of  $SO_2$ .
- Table 10: Flow rate of  $H_2S/N_2$  and  $N_2$  for different concentrations of  $H_2S$ .
- Table 11: Example of a procedure for 1000 ppm of  $H_2S/N_2$  to insert in the experimental protocol.
- Table 12: Characterisation of the original fly ash based on the leaching test, comparing it with the values established in legislation for different types of landfills [27].
- Table 13: Characterisation of the FA1-ST-WAT based on the leaching test, comparing it with the values established in legislation for different types of landfills [28].
- Table 14: Adsorption isotherm data for FA-ST-WAT.
- Table 15: Ball milling resulting ashes.
- Table 16: UFA1 chlorine content result.
- Table 17: UFA2 chlorine content result.
- Table 18: IFA1 chlorine content result.
- Table 19: IFA2 chlorine content result.
- Table 20: Chlorine contents results summarize.
- Table 21: UFA1 lead content result.
- Table 22: UFA2 lead content result.
- Table 23: IFA1 lead content result.
- Table 24: IFA2 lead content result.

- Table 25: Lead contents results summarize.
- Table 26: Results of the BET analysis.
- Table 27: SO₂ adsorption isotherm data.
- Table 28: Calculation results of partial pressure and partial pressure/adsorption capacity data of the graph.
- Table 29: Fitting parameters of the Langmuir model for IFA2.
- Table 30: Calculations result of  $log(P_p)$  and log(q) data of the graph.
- Table 31: Fitting parameters of the Freundlich model.
- Table 32: Adsorption isotherm of Hydrogen sulphide.
- Table 33: Calculation results of partial pressure and partial pressure/adsorption capacity.
- Table 34: Fitting parameters of the Langmuir model.
- Table 35: Calculation results of  $log(P_p)$  and log(q) data of the graph.
- Table 36: Calculated parameters from Freundlich fitted mode.

## Figure index

- Figure 1: Ternary diagram showing relative proportions of  $SiO_2$ ,  $Al_2O_3$  and CaO,  $K_2O$ ,  $Na_2O$ , MgO and  $Fe_2O_3$  in various fly (FA) and bottom (BA) ashes RDF refuse derived fuel, MSWI municipal solid waste incineration (Brännvall & Kumpiene, 2016).
- Figure 2: Probable uses of fly ashes after the mechanochemical treatment (Grabias-Blicharz & Franus, 2023).
- Figure 3: Market size in dollars versus Years, divided by continents (Grand View Research, 2024).
- Figure 4: Municipal waste incinerator scheme (Lam et al., 2010).
- Figure 5: Waste management pyramid (Waste Framework Directive, Official EU website).
- Figures 6 & 7: Comparison of ball sizes used in the ball milling experiment on the left large balls, on the right mixed-ball size.
- Figure 8: Retsch ball mill S100 year 2002.
- Figure 9: Determination of chlorine on a fly ash sample.
- Figure 10: Thermo Scientific iCE 3000 series spectrometer.
- Figure 11: BET isotherms adsorption and desorption curve types [34].
- Figure 12: TGA Equipment Models SDT Q-600 with Iberfluid Instruments Flow Controller.
- Figure 13: Gas cylinder of hydrogen sulphide with a concentration of 3000 ppm  $H_2S/N_2$ .
- Figure 14: Acid-base curve of the blank for FA-ST-WAT.

Figure 15: Acid-base curve of FA-ST-WAT.

Figure 16: BET isotherm graph of FA-ST-WAT.

Figure 17: Adsorption isotherm graph for FA-ST-WAT.

Figure 18: UFA1 and UFA2 mL AgNO3 versus derivative of the potential.

Figure 19: IFA1 and IFA2 mL AgNO3 versus the derivative of the potential.

Figure 20: Blank curve analysis of IFA2.

Figure 21: Curve analysis of IFA2.

 ${\it Figure~22: Isotherm~linear~plot~of~BET~analysis~of~IFA2.}$ 

Figure 23: Isotherm graph adsorption of  $SO_2$  for IFA2.

Figure 24: Graph of Langmuir model with fitted line equation.

Figure 25: Graph of Freundlich model with fitted line equation.

Figure 26: Isotherm graph adsorption of  $H_2S$  for IFA2.

Figure 27: Graph of Langmuir model with fitted line equation.

Figure 28: Graph of Freundlich model with fitted line equation.

## **ABBREVIATIONS**

| ACRONYM       | MEANING   |
|---------------|---|
| MSWI          | Municipal solid waste incinerator   |
| FA            | Fly ashes   |
| S/S           | Stabilization/solidification  |
| LOI           | Loss of ignition  |
| ANC           | Acid neutralization capacity  |
| DOC           | Dissolved organic carbon  |
| TDS           | Total dissolved solids  |
| FA1           | Untreated fly ash   |
| FA-ST-<br>WAT | Batch inertized fly ash   |
| UFA1          | Inertized and activated with ball milling starting from FA1 and with the use of big ball mills.   |
| UFA2          | Inertized and activated with ball milling starting from FA1 and with the use of small ball mills. |
| IFA1          | Only activated with ball milling starting from FA-ST-WAT and with the use of big ball mills.      |
| IFA2          | Only activated with ball milling starting from FA-ST-WAT and with the use of small ball mills.    |

#### 1 INTRODUCTION

The increasing generation of municipal solid waste incinerator (MSWI) fly ash, classified as hazardous waste due to its high content of heavy metals and soluble salts, poses a significant environmental challenge. Traditional disposal through landfilling is becoming increasingly unsustainable, not only because of the declining availability of landfill capacity, but also owing to the risk of pollutant leaching and long-term environmental contamination. In the context of the circular economy, the transformation of MSWI fly ash from a waste product into a valuable secondary raw material represents a strategic priority. However, the highly heterogeneous composition of fly ash complicates its handling and disposal, often requiring tailored management pathways depending on its physicochemical characteristics. This study investigated ball milling as an innovative dual-purpose treatment for MSWI fly ash, targeting both inertization (detoxification) and activation (enhancement of surface area and adsorption properties). Mechanochemical treatments are nowadays promising, achieving metastable materials with no solvent involved and modest energy consumption. Ball milling was tested under four different conditions, with two different ash feedstock type and two milling ball dimensions combined. The effectiveness of inertization was evaluated by measuring the quantity of chlorine and lead in leachates, as they are the only two components exceeding the toxic threshold in untreated fly ash. Chlorine and lead content are assessed using potentiometric titration and atomic absorption spectroscopy, respectively. Activation performance was evaluated through SO<sub>2</sub> and H<sub>2</sub>S adsorption tests, complemented by acid-base curves and surface area analysis. Results demonstrated that ball milling effectively reduced 80 % of chlorines and 55 % of lead leaching content in untreated fly ash, with higher yields achieved with bigger balls. However, when applied to pre-inertized ash, the process facilitated the release of chlorine with both ball sizes. Whereas for lead, occurred only with larger balls and decreased with smaller ones (29 %). Only with a reduction in ball size and a pre-treatment, it is achieved an ash that does not exceed both toxic pollutant thresholds. Ball milling improved surface area and enhanced adsorption capacity for SO<sub>2</sub> and H<sub>2</sub>S. This was proven with good maximum adsorption capacity for both pollutants (42,02 mg SO<sub>2</sub>/g FA and 19,61 mg H<sub>2</sub>S/g FA). The acid-base curve provided valuable insights into ash categorization in a type C material, and coupled with BET analysis, some mechanisms governing surface interactions with target gases were discovered. Ball milling represents an economical and environmentally sustainable treatment option with promising performance outcomes. Conversely, optimal results require integration with complementary treatment processes to maximize both inertization efficiency and activation potential for MSWI fly ash valorisation.

#### **1.1.** Ashes production and actual disposal

Ashes are residual materials generated from a thermal process and are characterized by a complex physicochemical structure. This can present substantial environmental management challenges, contingent upon the concentration of toxic components. Varying properties of combustion, gasification, or pyrolysis, like feedstock materials, operational parameters, and point of collection (bottom ashes or fly ashes) produce a heterogeneous nature of this material, causing complications in management, disposal and valorisation pathways. Ash generation occurs across multiple sectors with annual global production estimated to exceed 550 million tonnes per year. Ashes can be produced from power generation such as coal combustion residuals dominating the global production volumes with a high silica and alumina content and varying concentrations of calcium oxide (1-12%) depending on coal type [1]. Biomass combustion ashes are often enriched in potassium, phosphorus, and calcium reflecting the biological origin of the starting mass as some types could be reused as fertilizer [2]. Ashes can also be produced in industrial processes like metallurgical slag with iron oxide (FeO) contents ranging from 15-38 %, depending on the steelmaking process. A re-integration in chemical industry residues and cement/lime production byproducts often contain specialized catalytic materials and cement production byproducts with high calcium oxide concentrations (20-50 %) [3]. The municipal solid waste incineration ashes produce complex residues reflecting the eclectic matrix and location of the plant. In contrast, bottom ash is composed of similar aggregates and composition used in concrete structures. Fly ashes are primarily composed of glass structure, basic salts and heavy metals [4].

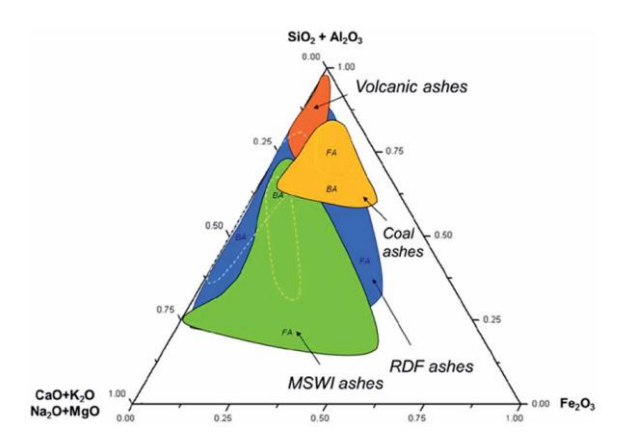


Figure 1: Ternary diagram showing relative proportions of  $SiO_2$ ,  $Al_2O_3$  and CaO,  $K_2O$ ,  $Na_2O$ , MgO and  $Fe_2O_3$  in various fly (FA) and bottom (BA) ashes RDF refuse derived fuel, MSWI municipal solid waste incineration (Brännvall & Kumpiene, 2016).

Nowadays, with an increase in global consciousness about climate change, lower land filling areas and higher restrictions from European governments, valorisation has a forced shift in waste management philosophy, trending with the circular economy. Based on transforming what was once considered a problematic waste stream into a valuable secondary resource. Recent advances in material science and processing technologies have enabled multiple pathways for ash reutilization as an actual common example, the construction sector. Ash (particularly coal fly and bottom ash) serves as a crucial partial replacement for Portland cement, reducing CO<sub>2</sub> emissions by up to 30% in concrete production while simultaneously improving durability and sulphate resistance [5].

The ecological impact of improper ash disposal is multifaceted and long lasting, with difficulties in predicting the exact value. Particulate emissions from dry ash storage facilities present respiratory health concerns for surrounding communities, requiring enclosed spaces. On the other hand, when ashes encounter water, the result is contamination plumes with extensions of several kilometres from disposal sites. A small-scale reproduction of unmanaged ash deposits could be represented with leaching studies. This test demonstrates potential mobilization of heavy metals, including lead, chromium and selenium with concentrations favouring exceeding regulatory thresholds by 1-2 orders of magnitude [6]. These challenges are compounded by transportation, physical volume occupied (0,7-1,2 m³/tonne depending on compaction), consuming valuable land resources, and creating long-term management liabilities spanning decades to centuries of monitoring conditions. Economic analyses, further reveal and states truth about conventional disposal approaches, which have different costs based on the type of ashes. An industry could spend \$ 2,5 billion per year creating a substantial financial burden while simultaneously wasting a potential secondary resource [7].

Traditional ash management strategies remain prevalent in many regions, with landfilling historically constituting the primary disposal methodology. In the European Union the council directive 1999/31/EC of 26<sup>th</sup> of April 1999 states that the correct points to follow for disposal start with the classification of the ashes as solid residues. Later categorization under hazardous, non-hazardous, or inert waste classes depends on their composition (Annex II, III criteria) with assurances that each classification can only be deposited in places that meet certain thresholds. Information on requirements design and operation for ash ponds must cover liners and leachate collection systems for preventing groundwater contamination, gas control systems for sites containing organic material, and strict controls on emissions.

Modern engineered landfills are containment systems incorporating multiple protective elements with composite bottom liners typically consisting of 2,00 mm HDPE geomembranes overlying 1,00 m compacted clay barriers, achieving a hydraulic conductivity value of 10<sup>-9</sup> m/s or lower. Leachate collection systems maintain a maximum hydraulic head below 30 cm and real-time monitoring networks with groundwater sampling every 100-300 m intervals [8].

Advanced containment technologies have further emerged as intermediary solutions, particularly for challenging ash types containing elevated levels of mobile contaminants, with a pre-treatment consisting of chemical stabilization to lower the concentration of hazardous substances. Permitting to reduce the leachability of critical elements by 90 to 99 % in standardized test procedures [9]. These approaches, while environmentally preferable to conventional disposal, still represent end-of-life management rather than true valorisation. More progressive solutions include controlled storage facilities designed for potential future recovery when technology and market conditions permit resource extraction, effectively functioning as anthropogenic ore deposits.

This thesis aims to treat fly ash (FA), the fine particulate matter captured from flue gases during municipal solid waste (MSW) incineration, which represents one of the most significant environmental challenges in modern waste management systems. These ashes are classified as hazardous waste in most countries due to their high content of heavy metals, soluble salts, and potential organic pollutants, which pose substantial risks to human health and the environment if improperly managed [10].

The primary concern with fly ash disposal is its volatility and leaching potential. When exposed to air, are easily inhaled, and in contact with water, toxic elements such as lead (Pb), cadmium (Cd), arsenic (As), mercury (Hg), and chromium (Cr) can be released into the environment, potentially contaminating soil and water resources [7]. According to the European Waste Catalogue, fly ash from municipal waste incineration is classified under code 19 01 13\* (marked with an asterisk to indicate its toxic nature), requiring specialized handling and disposal.

This also represents a challenge to the overall economic viability of waste-to-energy systems, where high production of residues, landfill taxes, and increasingly stringent environmental regulations have further escalated the financial burden of fly ash as a waste, creating an urgent demand for more sustainable and cost-effective reuse.

#### 1.2. Objectives

This research constitutes part of an ongoing project within the Department of Mechanical, Chemical Engineering, and Industrial Design at the Escuela Técnica Superior de Ingeniería y Diseño Industrial, Universidad Politécnica de Madrid, titled "Valorización de cenizas volantes de incineración de RSU" (Valorisation of Municipal Solid Waste Incineration Fly Ash).

The fly ash (FA) samples utilized in this investigation were sourced from "Servicio de Incineración de Residuos Urbanos S.A. (SIRUSA)", an incineration facility located in Tarragona, Catalonia. According to Article 8 of Law 7/2022 (April 8th) concerning waste and contaminated soils, these fly ashes were classified as hazardous waste due to their content of pollutants and harmful substances to environmental systems and human health. Preliminary elemental analysis and leaching tests conducted on these samples, following relevant regulatory protocols, have confirmed this classification [10].

This thesis pursues two interconnected research objectives:

#### 1. Development of an effective fly ash stabilisation process

The first objective aims to develop and optimize a treatment methodology that can effectively reduce the toxic component content of incineration fly ash, thereby potentially reclassifying this material from hazardous to non-hazardous waste. This would enable its diversion from specialized hazardous waste landfills to conventional waste management facilities, in compliance with Spain's regulatory limits.

The research builds upon and extends methodologies established in previous investigations, particularly focusing on ball milling techniques identified through a comprehensive literature review as the most promising approach for laboratory implementation. The proposed treatment framework implements an integrated strategy that combines separation and immobilization of soluble salts, stabilization of heavy metals, and processing with sodium

carbonate (Na₂CO₃) solutions to promote inertization, as previous lab tests confirmed the efficacy of this reagent.

#### 2. Valorisation of Treated Fly Ash as Gaseous Pollutant Adsorbent

The second objective explores the valorisation route for inertized fly ash as an adsorbent material for contaminated gas streams. This application leverages the increased specific surface area achieved through the activation process to enhance adsorption capacity. Activation is induced with sodium hydroxide (NaOH) solutions (also previously tested) and hopefully in a single step with inertization.

The research will evaluate the adsorption performance of the treated fly ash through systematic experimentation with two model pollutant gases: Sulphur dioxide (SO<sub>2</sub>) and hydrogen sulphide (H<sub>2</sub>S).

Performance assessment will be conducted under varying initial adsorbent concentrations to determine optimal operating parameters and establish efficacy of the boundaries, for a subsequential process design.

#### 1.3. Novelty

This thesis proposes and assesses an innovative path to fly ash treatment that simultaneously addresses two critical challenges: reduction in environmental hazard and enhancing its potential for beneficial reuse for adsorption purposes.

In specific these two processes must be accomplished:

- 1. **Inertization**: transform crystalline phases into further steady structures to encapsulate heavy metals into stable mineral phases, reducing leaching potential and toxicity.
- 2. **Activation**: reduce the size of solid particles, consequently increasing specific surface area/porosity and creating reactive sites. Adsorption capacity and pozzolanic reactivity are developed enabling its application as an adsorbent for gaseous pollutants.

For reaching those goals, previous research conducted at the laboratory level worldwide was tested. The aim of this project is to evaluate the effectiveness of ball milling combined with the adding of

potential chemical additives. This work is achieved with the help of rotating grinding balls within a cylindrical chamber that uses collision, impact, and friction to favour chemical reaction and mixing.

One-pot ball milling approach offers several potential advantages over conventional treatment methods. Direct reaction routes can propagate alone, with no need for solvent and heat, resulting in low energy consumption and no need for solvent regeneration. Mechanochemistry is also known for discovering unique and metastable materials that cannot be synthesized in conventional techniques [11].

The goal is to develop a technically viable and economically feasible process that can be scaled up for industrial implementation, contributing to sustainable fly ash conversion practices in Spain, Italy, and beyond.



Figure 2: Probable uses of fly ashes after the mechanochemical treatment (Grabias-Blicharz & Franus, 2023).

#### 2 WASTE INCINERATION

Waste incineration is a critical element of contemporary waste management strategies worldwide. It sits at the intersection of environmental protection, energy recovery, and waste reduction being a subject of varying opinions regarding the management of dry waste material. However, the production of potentially hazardous ashes and toxic fumes is a cause for concern.

In an era of increasing urbanization and consumption, municipal solid waste generation continues to rise globally, with projections suggesting an increase from 2,01 billion tonnes in 2016 to 3,40 billion tonnes by 2050 [12]. High-density population regions have limited terrain capacity and growing environmental concerns, with waste-to-energy incineration emerging as the only solution for management. The European Union, plus many other continents, have embraced incineration technology to reduce waste volume and generate energy, with a global waste-to-energy market valued at approximately \$ 35,1 billion in 2021 and with prospects of increasing.



Figure 3: Market size in dollars versus Years, divided by continents (Grand View Research, 2024).

Controlled combustion of municipal waste is the working principle of an incinerator. The volume of waste is reduced up to 90 %, reaching temperatures in the range of 900-1200 °C. The heat generated

can be harnessed for electricity production, and the remainder could be saved into district heating systems. These facilities produce ashes and fumes as byproducts. Both require careful pretreatment before disposal or release in the environment. Ashes can be divided into bottom and fly ash, two fundamentally different residues with distinct physical, chemical, and environmental properties. Bottom ash, comprising approximately 80-90 % of solid residues from incineration, consists primarily of non-combustible materials that accumulate at the base of the combustion chamber, permitting a low concentration of toxic substances. These ashes are easily reintroduced into the economy market [13]. In contrast, fly ash, airborne particulate matter captured by air pollution control systems, represents only 10-20 % of total ash but often contains higher concentrations of heavy metals, salts, and other potentially hazardous substances (Chandler et al., 1997).

The gaseous emissions from incineration facilities present another treatment challenge, with release of acid gases (HCl, SO<sub>2</sub>, NO<sub>x</sub>), heavy metals (mercury, cadmium, lead), particulate matter, and organic toxic compounds such as dioxins and furans. Despite regulatory frameworks governing these emissions continue to evolve and stringent standards being implemented across developed countries. This combined with significant technological advances in air pollution control systems over recent decades, including electrostatic precipitators, fabric filters, scrubbers, and selective catalytic reduction systems, public concern regarding emissions remains a limiting factor in the broader adoption of incineration technology (Vehlow, 2015).

As the filtration technology on incinerators improves, the concentration of toxic contaminants in the ash increases. Fly ash is especially toxic, although there is less of it (about 3-5 per cent of the original waste by weight and about 5-15 per cent of all the ash produced), it must be treated with great care. It is classified as special waste, currently that means a double lined landfill in a location as dry as possible, and every effort is taken to reduce exposure to water and to capture and store leachate [9].

#### 2.1. How does a waste incinerator work?

The fundamental operation of an incinerator is easily understood through several interconnected subsystems.

#### Waste reception and pre-treatment

The incineration process begins with waste reception facilities where municipal solid waste (MSW) is delivered and temporarily stored in bunkers. The design capacity must be sufficient to meet the incinerator's waste demand for 7-10 days of storage autonomy, as waste dumping does not occur daily due to holidays or reduced waste production. A fixed constant input in the combustion chamber is important to maintain. It avoids several problems occurring in the startup and shutdown phase. The system is huge, and reaching high temperatures is not immediate, plus waste must be completely burned. After a certain number of days, the waste tends to rot. This issue is overcome with a slight depression with an air intake. The air which is now polluted with odours is used for combustion, this recycle avoids air treatment and the depression costs are paltry. The pressure given by the amount of waste on the top makes the formation of percolate inevitable, a grid system ensures that polluted water can flow, liquid is then collected and sent to water treatment in modest quantities. Pieces that can be re-evaluated or that could cause combustion difficulties are separated by an overhead crane. With this operation, combustion efficiency is improved, and problematic emissions downstream are reduced. The waste is also homogenized through mixing and shredding to optimize combustible content and homogeneous combustion [13].

#### **Combustion system**

The area can be divided into three connected zones:

- 1. Feeding system: calibrates the input of residues and controls the quality to maintain optimal combustion [13].
- 2. Primary combustion chambers: the waste is burned as it travels on a mechanically operated grate system while allowing the air flow through the bed (time of permanence around 30 min). The energy content of municipal solid waste is 10000 kJ/kg, and a typical performance of an incinerator plant is 45 tons of waste per day (USDA, 2016). This zone could be described as coarse biphasic, where ash and fumes come out, fumes are sent to the afterburner and then energy recovery, while ash is disposed.

The inclination of the grill depends on the process that is taking place inside the incinerator. In the first part, water is removed, and the initial content is 25-30%. The increase in temperatures when the matrix is dry, proceeds towards a substantial heating until reactions begin to develop around 800 °C. This is the widest area with an inclination of 8-12 °, lowering

the inclination increases the residence time. The last area has an even lower inclination, about 5  $^{\circ}$  up to 8  $^{\circ}$ , here, the temperature decreases as some reactions are completed. At the end the presence of an extinguishing tank lowers bottom ash temperature (600-700  $^{\circ}$ C) till equilibrium with the ambient.

Usually at least two main lines are needed, resulting in equal principles of working yet the currents of raw material are different. In case of maintenance, at least one is operating on full range. The normative imposes control only at the end, on the ashes where the maximum organic carbon remaining is tested (not on the grated system).

#### Maintenance issues:

- Startup: the optimal temperature (850-1200 °C) is not reached with the oxidation of waste but with external energy (e.g. fossil fuel), which involves time favouring good accumulation of residues.
- Shutdown: before stopping the process, it is necessary to complete the combustion as much as possible for cleaning and maintenance, which usually takes months [7].
- 3. Secondary combustion chamber: this section recovers the heating value from unburned substances which are not at the maximum degree of carbon oxidation also called PICs. It's a thermal combustion on a gas stream with a time of permanence of at least two seconds, given by law directives, and sufficient excess oxygen 6-11%. It is the sole location where controls can be implemented. As in other parts, the temperature is excessively high, and a significant amount of heterogeneity is present. The temperature is measured at the wall (minimum temperature), depending on the halogens present in the fume (more frequent are chlorines and fluorides, both in organic and acid form) [13].

#### **Energy recovery system**

Modern facilities capture and utilize the thermal energy generated with a vapour cycle, allowing the production of thermal and electric energy.

The stream of hot gases lowers its temperature till 200-250 °C, in some points water could be condensed, and some pollutants could dissolve in non-negligible concentrations, which must then be reduced. At first, a heat transfer system with water-filled boiler tubes that absorb heat from hot combustion gases, generates high-pressure steam. Superheated steam has a low exchange coefficient, as it behaves as a gas. The power generation consists of steam driving turbines connected to electrical generators, where the expansion of the vapour is till 0,1 bar and a

temperature of 30 °C for recovering the maximum work possible. The typical efficiency in the conversion of vapour expansion to electrical energy is 20-30 % depending on heat capacity, the plant design, and scale. A big part is lost due to the condensation of water.

A vapour cycle is chosen for polluting problems of the gas and a cogeneration mode, producing both electricity and recovering lower-grade heat for district heating systems or industrial processes is implemented raising overall energy efficiency to 60%.

The number of lines of combustion does not add up to other turbines, a unique turbine works, as the regulation has a wide range [13].

#### Flue gas treatment system

Combustion gases undergo extensive treatment before atmospheric release, starting with particulate removal with dimensions lower than 1  $\mu$ m. Electrostatic precipitators are employed for this purpose, reaching 99% efficiency, fly ash is included in this separation. This equipment is chosen because they are the best option for large flow rates and high temperatures, with the option of adding/subtracting modules.

Composites with acid behaviour, such as HCl, HF and SO<sub>2</sub>, can be removed with the same reaction but with 3 different conditions:

- Dry treatment: reagents such as NaHCO<sub>3</sub> or CaO are injected at a solid state. These components react and form products such as NaCl, NaF, Na<sub>2</sub>SO<sub>3</sub>, Na<sub>2</sub>SO<sub>4</sub> or CaCl<sub>2</sub>, CaF<sub>2</sub>, CaSO<sub>3</sub>, CaSO<sub>4</sub>.
  - NaHCO<sub>3</sub> dissociates at high temperatures, leaving a porous matrix inside, ideal for a high contact surface area and production of Na<sub>2</sub>CO<sub>3</sub>, the main component that reacts with acidic gases. The carbonate is used in excess and must be removed at the end of the treatment.
- Semi-dry treatment: reagents are in solution or in suspension, and the content of water it's completely vaporized during the operation. The products are solids. It is used to save water, but difficulties are encountered in adjustments.
- Humid treatment: water content is so high that even products are found in the form of suspension or solution.

The calorific value of waste increases, causing a rise in temperatures inside the combustor. The result is a higher production of  $NO_x$  as the Equation 1 is favoured to the right.

$$N_2 + O_2 \leftrightarrow 2NO$$

Equation 1: Reaction of the production NO.

The solution is reducing NO to nitrogen by a redox process that uses ammonia (or urea). This is a selective reaction that can be developed with or without the help of a catalyst.

SNCR (selective non-catalytic reduction) or SCR (selective catalytic reduction) functions as the reagent is directly injected into the secondary combustor chamber, and an excess of oxygen is present.

$$2NH_3 + NO + O_2 \rightarrow \frac{3}{2}N_2 + 3H_2O$$

Equation 2: NOx abatement's reaction.

Parasite reaction or other parallel reaction can occur, with the presence of the catalyst are avoided.

Heavy metals and dioxin capture (PCDD and PCDF) are usually removed with chemical adsorption. The most worrying is the presence of mercury, which has a low boiling point (357 °C), it is encountered at vapour phase and comes mainly from batteries (nowadays can also be collected separately). PCDD and PCDF are formed due to the presence of chlorine. The chemical adsorption is irreversible because the bond created is covalent. At the end, a continuous emissions monitoring system is mandatory. It tracks and verifies compliance with regulatory emission limits in real-time [13].

#### Residue handling system

A pre-treatment of the two primary solid residues:

1. Bottom ash collection: Non-combustible materials accumulate at the base of the combustion chamber. The composition of these ashes is primarily of inorganic materials, yet it can contain unburned organic matter. Obviously, this composition depends on the incineration process and input waste mass but generally contains some valuable materials alongside a few hazardous substances like heavy metals. The ashes are cooled (often through water quenching to control dust) before conveyor transport to storage or processing areas. Metals and other recyclable materials are separated using screening and sieving (for larger metals) and magnets (for ferrous metals). Bottom ashes are stabilized and cleaned through washing, ageing, binder addition and thermal treatment.

2. Fly ash management: Lighter particulate matter captured by air pollution control systems is carefully stored and stabilized through treatments before disposal due to its potentially hazardous nature [13].

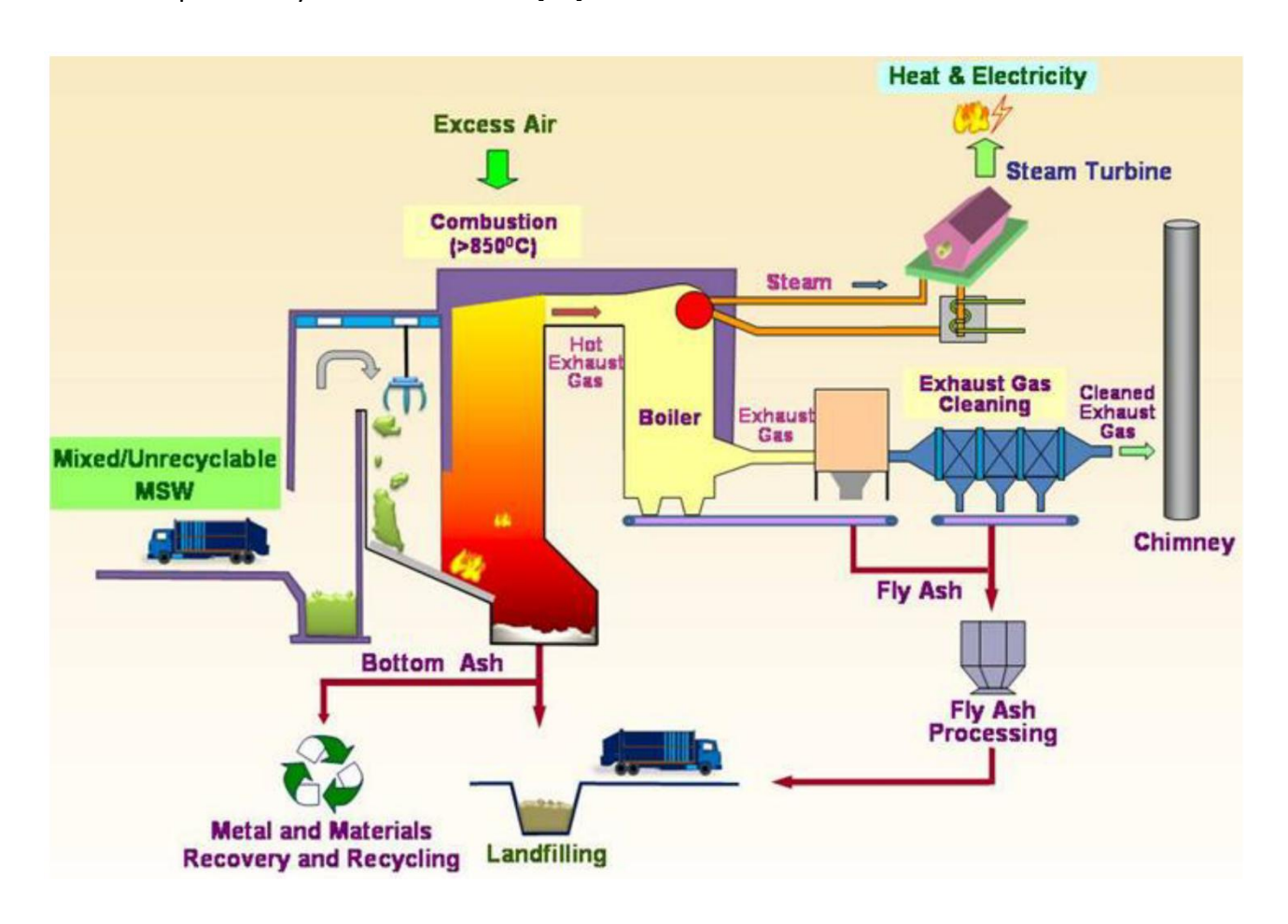


Figure 4: Municipal waste incinerator scheme (Lam et al., 2010).

These highly integrated systems collectively enable modern incinerators to process waste with significantly improved environmental performance compared to historical facilities.

## 2.2. Disposal methods with focus on incineration plants and fly ash management in the European Union centred on Spain and Italy

Spain produces roughly 22 million tonnes of urban waste per year, with every Spanish citizen producing 455 kg/cap (European average is 505 kg/cap). The actual major disposal method is landfill, even if it is in slow decrease (52 % in 2020). Other main approaches of handling waste are recycling and composting, which are in a growing trend (36,4 % in 2020) and incinerators with 2,5-2,8 million tonnes treated (12 % in 2020). The main problem for Spain is the reliability in mechanical biological treatment plants, consisting of a process that separates and treats mixed waste. Thought, 40 % of the fractional residual is organic material that could be composted, only 55 plants of 143 treat organic matrix separated plus 74 % of waste in landfilling sites comes from waste process of industries. In essence, Spain has a rather static waste management system, with a strong dependence on landfills and room for improvement in the separate collection of organic waste [15].

Italy generates about 30 million tonnes of municipal waste annually with every Italian citizen producing 503 kg/cap (slightly above European medium). The main disposal method is recycling and composting/digestion (51 % in 2019), then landfilling with a total amount of 6,3 million tonnes (20,9 % in 2019), nearly the same amount of waste was processed by incinerators (with 20 % in 2019). The issue with Italy is its regional differences where in the north it can be encountered 63 % recycling (Veneto) ad in the south till 93 % could be landfilled or not corrected disposal (Sicily) [14].

In 2016, in the European Union the active incinerators plants were 512 with 251 combined heat and power source, 161 just electricity producers and 94 heat-only generators (Eurostat, 2018). These numbers have certainly increased with a landfill directive (1999/31/EC as amended by Directive (EU) 2018/850) requiring the limitation of landfilled waste by 10% of the total residue generate in 2035. Across its member states, Germany, France, Netherlands, Sweden, Italy and United Kingdom accounts for three quarters of EU's incineration capacity. These facilities collectively process around 90 million tonnes of waste annually, generating energy and heat for local communities and 1,8 million tonnes of fly ash (CEWEP, 2023). Although, a reduction of 10-15 % in global emissions is estimated and could be achieved through solid waste management, a big part (> 30%) of EU's municipal waste is landfilled with differences across the Member States (IPCC, 2022). The distribution of waste to energy plants is uneven across the EU, with Northern and Western European countries finding most developed incineration infrastructure compared to Eastern and Southern

regions, though this gap has been narrowing with recent investments in modern facilities and still evolving.

Spain and Italy both operate under EU regulations but applied through national/regional rules and standards, practice varies by region and by the ash's origin or quality.

Spain has roughly 12 operational MSWI, with a focus on developing specialized treatment for bottom ashes, based on recovering metal and using treated ash as a secondary aggregate in construction application. In the last decade a significant growth in waste incineration capacity reached 2,19 million tonnes of solids treated per year [16]. These facilities are primarily situated in northeastern regions, Catalonia and Balearic Islands.

Consequently, 44000 tonnes of fly ashes are annually generated and must be properly managed in accordance with Spanish Royal Decree 646/2020 on waste disposal through landfill deposition. This legislation establishes strict leaching limits for various heavy metals and other components, in most cases landfilling of untreated ashes is impossible.

Italy is home to approximately 40 incineration plants. A more extensive waste incineration infrastructure compared to Spain. Low landfilling area available forces to pioneer innovative approaches to fly ash management, where some facilities privilege the stabilization and solidifying of toxic components before final disposal. Italy generally achieves higher rates of FA recycling compared to Spain, albeit the significant regional disparities. Italy's incineration capacity exceeds 6 million tonnes per year, producing circa 120000 tonnes of fly ashes annually [17].

Italian regulations on solid landfilling are governed by Legislative Decree 152/2006 (Environmental Code) and subsequent amendments. These regulations also classify fly ashes as hazardous waste requiring specialized treatment before disposal.

Before adopting a treatment process for a residue, the important part is to determine the shortand long-term conditions expected for the scenario. When evaluating a single option is also crucial to examine and predict the new waste stream created by the process into account. For the future of treated FA, another variable to consider is the characterisation of the changes in leaching behaviour caused by pH dependence tests, as it provides a direct measure for every environmental condition. Each method of current approaches to fly ash management presents distinct advantages and limitations in terms of efficiency, cost, and environmental impact.

The categorization is into three main strategies:

- Stabilization/solidification (S/S) represents the most widely implemented treatment
  method for fly ash worldwide. Various technologies have been tried and proposed but the
  common is mixing with a variety of hydraulic binders (cement and/or lime, blast furnace slag,
  etc.) This approach also gives the possibility of reusing the final materials, chemical reagents
  reduce the mobility of hazardous components and fix them through physical encapsulation
  and chemical immobilization mechanisms [18].
  - In Spain, approximately 70 % of fly ash is treated through cement-based S/S processes before being disposed of in controlled landfills. While it is relatively low-cost, easy of application and technologically mature, it substantially increases the waste volume (by 1,5 to 2 times) and does not effectively address all contaminants, particularly soluble salts like chlorides and sulphates [18].
- Thermal treatments encompass various high-temperature processes, including vitrification, sintering, and melting. These methods reduce its volume, producing a high-density melted product. Melting at extreme temperatures induces changes in physical and chemical state, detoxifying heavy metals and decomposing organic pollutants. This can effectively transform fly ash into a stable glass-like material with significantly reduced leaching potential. However, their implementation needs to be improved in certain area. It is limited by high energy requirements, substantial capital investment, and the potential for volatilization of certain pollutants during the heating process [19].
  - In Italy, several thermal treatment facilities have been established, particularly in the northern regions, processing approximately 15% of the country's fly ash production. While these treatments provide superior stabilization compared to conventional S/S methods, their high operational costs (typically €300-500 per tonne) have limited their wider adoption.
- Chemical extraction methods were also popular as their easy operation. The aim is to remove hazardous components from fly ash through washing processes using water, acids, or chelating agents [20]. Environmentally and economically seems a benefit the extract and detoxify hazardous elements, but generating secondary liquid waste streams is onerous cause further treatment is needed. This process usually does not address all hazardous

| components. An example is the FLUWA process, developed in Switzerland and implemented in several European countries, which uses acid washing to remove heavy metals from fly ash. |
|---|
|   |
|   |
|   |
|   |
|   |
|   |
|   |
|   |

## 3 COMPARATIVE ANALYSIS OF WASTE ADMISSION CRITERIA IN EUROPE

The European Union has established the Waste Framework Directive for the disposal of residue through the Landfill Directive (1999/31/EC) and subsequent updated Council Decision 2003/33/EC, which differentiates and set baseline acceptance criteria for the different classes of landfills.

While previous waste directives focused primarily on disposal, Directive 2008/98/EC shifts the emphasis toward prevention and resource efficiency. It applies a hierarchy for companies to respect, based on reducing consumerism and preventing waste, promoting the use of less material, manufacturing products with a long-life span and avoid the production of toxic substances.

Re-use with appropriate repairing/cleaning and recycling based on creating a new product from a waste, these are all favoured processes instead of recovery (extracting energy from residues) and landfilling.

## **Waste hierarchy**



Figure 5: Waste management pyramid (Waste Framework Directive, Official EU website).

The definition of waste is any substance that holds/requires discarding. The EU framework establishes three landfill categories: inert, non-hazardous, and hazardous. Every class belongs to a

range of corresponding waste acceptance criteria that define threshold values for various parameters in waste leachate. Council Decision 2003/33/EC provides the baseline values that all member states must implement as minimum standards.

#### In Spain

The Royal Decree 646/2020 regulates the management of waste in landfills in Spain. It has the objective to limit the disposal of residues, maintaining strict adherence to European classifications. It introduces specific nuances tailored to national conditions and aims to reduce the environmental impact, and people's health. Characterisation and prior treatment are mandatory. The Spanish system places particular emphasis on dissolved organic carbon limits and implements additional parameters for evaluating biodegradable waste streams.

In article 3(a) of Law n°22/2011, waste is defined as "any substance or object that the owner disposes of or has the intention or obligation to do so." Royal decree 646/2020 combined with Law n°22/2011 distinguishes several categories of waste and specific disposal methods according to waste hazardousness:

- Inerts: Non-hazardous waste that does not undergo significant physical, chemical, or biological transformations with time. Inert waste is not soluble, combustible, or biodegradable. It does not react with the materials it encounters, either physically, chemically, or in any other way, nor does it adversely affect other materials with which it comes into contact. In any way, this waste cannot lead to environmental contamination or harm human health. Inert waste must have a negligible contaminant content and leaching potential. Inert waste and its leachates must not pose a risk to the quality of surface and/or groundwater.
- Non-toxics: those that do not present the dangerous characteristics listed in Annex I of Law 7/2022, of April 8.
- Toxic: waste that presents one or more of the hazardous characteristics listed in Annex I.

The decree establishes specific acceptance criteria for each landfill type, with detailed threshold values for leachate concentrations of potentially harmful substances. The classification system is further refined through provisions from Law 7/2022 of 8<sup>th</sup> April, on waste and contaminated soil for circular economy transposes Directive (EU) 2018/851, amending Directive 2008/98/EC on waste (Waste Framework Directive). The hazardous details of characteristics in Annex I, including flammable, toxic, and reactive properties, are listed in Table 1.

Additionally, the regulations include comprehensive evaluation procedures for waste characterisation, addressing aspects such as loss on ignition (LOI), acid neutralization capacity (ANC), and pH stability requirements. Table 7 of the decree synthesizes the various landfill categories and subcategories, including specialized facilities for inert, non-hazardous, biodegradable wastes, explosives and inflammables, demonstrating Spain's commitment to implementing the European waste hierarchy while addressing its unique environmental challenges. Furthermore, Royal Decree 646/2020 stipulates the limiting values for the concentrations of various compounds in leachate, following the ratio: Liters of leaching liquid/kg of ash = 10 L/kg.

| Component    | Inert (mg/Kg FA) | Non-Toxic (mg/Kg FA) | Toxic (mg/Kg FA) |
|--------------|------------------|----------------------|------------------|
| As           | 0,50             | 2,00                 | 25,00            |
| Ва           | 20,00            | 100,00               | 300,00           |
| Cd           | 0,04             | 1,00                 | 5,00             |
| Cr Total     | 0,50             | 10,00                | 70,00            |
| Cu           | 2,00             | 50,00                | 100,00           |
| Hg           | 0,01             | 0,20                 | 2,00             |
| Мо           | 0,50             | 10,00                | 30,00            |
| Ni           | 0,40             | 10,00                | 40,00            |
| Pb           | 0,50             | 10,00                | 50,00            |
| Sb           | 0,06             | 0,70                 | 5,00             |
| Se           | 0,10             | 0,50                 | 7,00             |
| Zn           | 4,00             | 50,00                | 200,00           |
| Chlorides    | 800,00           | 15000,00             | 25000,00         |
| Fluorides    | 10,00            | 150,00               | 500,00           |
| Sulphate     | 1000,00 (*)      | 20000,00             | 50000,00         |
| Phenol Index | 1,00             | -                    | -                |
| DOC**        | 500,00           | 800,00               | 1000,00          |
| TDS***       | 4000,00          | 60000,00             | 100000,00        |

Table 1: Limit values for concentrations in a leachate (BOE-A-2020-7438).

\*Even if the waste does not meet this value for sulphate, it may be considered to meet the admission criteria if leaching does not exceed any of the following values: 1500 mg/L in CO with an L/S ratio of 0,1 L/kg and 6000 mg/kg with an L/S ratio of 10 L/kg. The percolation test will be required to determine the limit value with an L/S ratio of 0,1 L/kg under initial equilibrium conditions, while the

value with an L/S ratio of 10 L/kg may be determined either by a batch leaching test or by a percolation test under conditions close to local equilibrium.

\*\* If the waste does not meet these dissolved organic carbon (DOC) values at its own pH, it may alternatively be tested with an L/S ratio of 10 L/kg and a pH between 7,5 and 8,0. The waste may be considered compliant with the DOC acceptance criteria if the result of this determination does not exceed 500 mg/kg.

\*\*\* It is possible to choose during the authorization phase, at the request of the manager, if to use the TDS value or the single values for sulphates and chlorides.

In addition to the leachability limits in aqueous media indicated in the previous section, waste must comply with the additional limit values indicated in the table in this section, relating to organic substances soluble in organic solvents (UNE-EN 14039, UNE-EN 15308, and UNE-EN 15527), as well as total organic carbon.

| Parameter                    | Inert waste | Non-toxic waste | Toxic waste       |
|------------------------------|-------------|-----------------|-------------------|
| TOC (Total Organic Carbon)   | 3000,00*    | Maximum 5% on   | Maximum 6% on dry |
|                              | mg/Kg FA    | dry matter **   | matter***         |
|                              |             |                 |                   |
| DTEV /Domestic Ethydhomestic | 6.00 mg//g  |                 |                   |
| BTEX (Benzene, Ethylbenzene, | 6,00 mg/Kg  | -               | -                 |
| Toluene and Xylenes)         | FA          |                 |                   |
| PCB (Polychlorobiphenyls)    | 1,00 mg/Kg  | -               | -                 |
|                              | FA          |                 |                   |
| Mineral Oil (C10 to C40)     | 500,00      | -               | -                 |
|                              | mg/Kg FA    |                 |                   |
| PAHs (Polycyclic Aromatic    | 55,00 mg/Kg | -               | -                 |
| Hydrocarbons)                | FA          |                 |                   |
| рН                           | -           | >=6             | -                 |
| ANC                          | -           | ***             | ****              |
| LOI                          | -           | -               | Maximum 10% on    |
|                              |             |                 | dry matter        |

Table 2: Limit values for total content of organic parameters (BOE-A-2020-7438).

- \* In the case of soil, subject to the approval of the competent environmental authority of the autonomous community, a higher limit value may be applied provided that the DOC reaches a maximum value of 500 mg/kg at L/S = 10 L/kg, either with the waste's own pH or with a pH between 7,5 and 8,0.
- \*\* If this value is exceeded, subject to the approval of the competent environmental authority of the autonomous community, a higher limit may be applied provided that the DOC reaches a maximum value of 800 mg/kg at L/S = 10 L/kg, either at the material's own pH or at a pH between 7,5 and 8,0.
- \*\*\* The basic waste characterisation procedure must assess its ANC. The competent environmental authority of the autonomous community may waive testing for this parameter when sufficient information is available or it is not considered relevant, considering the pH conditions likely to be induced by the other waste admitted to the landfill.
- \*\*\*\*If this value is exceeded, with the agreement of the competent environmental authority of the autonomous community, a higher limit value may be applied, provided that the DOC reaches a maximum value of 1000 mg/kg at L/S = 10 L/kg, either pH of the residue, or with a pH between 7,5 and 8,0
- \*\*\*\*\* In the basic waste characterisation procedure, its ANC. The competent environmental body of the autonomous community may exempt from testing for the verification of this parameter when sufficient information is available or is not considered relevant considering the expected pH conditions induced by the other accepted residues in the landfill.

#### In Italy

Italy's implementation of EU regulations occurs primarily through Legislative Decree 36/2003, updated in 2020 with the legislative decree n°121 of September 3<sup>rd</sup>, implementing the Directive 2018/850/EU on waste landfills. It establishes strict acceptance criteria for carrying out the verification directly at the place of production, with procedures for admission to landfill and adopts specific technical parameters to establish when waste treatment is necessary. Italy has developed

a more granular subcategorization system for non-hazardous waste landfills, reflecting its industrial diversity and dense population distribution.

Concentration limits in the eluate for acceptability in landfills for inert waste are found in Table 3.

| Component | Inert (mg/Kg FA) | Non-Toxic (mg/Kg FA) | Toxic (mg/Kg FA) |
|-----------|------------------|----------------------|------------------|
| As        | 0,050            | 0,200                | 2,500            |
| Ва        | 2,000            | 10,000               | 30,000           |
| Cd        | 0,004            | 0,100                | 0,500            |
| Cr Total  | 0,050            | 1,000                | 7,000            |
| Cu        | 0,200            | 5,000                | 10,000           |
| Hg        | 0,001            | 0,020                | 0,200            |
| Мо        | 0,050            | 1,000                | 3,000            |
| Ni        | 0,040            | 1,000                | 4,000            |
| Pb        | 0,050            | 1,000                | 5,000            |
| Sb        | 0,006            | 0,070                | 0,500            |
| Se        | 0,010            | 0,050                | 0,700            |
| Zn        | 0,400            | 5,000                | 20,000           |
| Chlorides | 80,000           | 1500,000             | 2500,000         |
| Fluorides | 1,000            | 15,000               | 50,000           |
| Sulphate  | 100,000          | 5000,000             | 5000,000         |
| DOC       | 50,000 *         | 100,000 ***          | 100,000 *        |
| TDS **    | 400,000          | 10000,000            | 10000,000        |

Table 3: Limit values for concentrations in a leachate (Legislative decree 3<sup>rd</sup> September 2020, n. 121, Annex 3).

- \*If the waste does not respect the reported values for DOC at their pH value, they can be subjected to test with a liquid/solid proportion L/S = 10 L/kg and with a pH between 7,5 and 8,0. Waste can be considered compliant with the eligibility criteria for organic carbon dissolved if the test result does not exceed 50 mg/L.
- \*\* It is possible to choose during the authorization phase, at the request of the manager, if to use the TDS value or the single values for sulphates and chlorides.
- \*\*\* The concentration limit for the DOC parameter does not apply to the following types of waste:
- a. Sludge produced by the treatment and preparation of foods identified by the codes of the European list of wastes 020301, 020305, 020403, 020502, 020603, 020705, sludge and waste deriving from production and processing of pulp, paper and cardboard (codes of the European list

of waste 030301, 030302, 030305, 030307, 030308, 030309, 030310, 030311 and 030399), septic tank sludge (200304), provided and treated through processes suitable for significantly reducing the content of organic substances.

- b. Sludge identified by the codes in the European waste list: 040106, 040107, 040220, 050110, 050113, 070112, 070212, 070312, 070412, 070512, 070612, 070712, 170506, 190812, 190814, 190902, 190903, 191304, 191306. Previously treated through processes, suitable for significantly reducing the content of organic substances.
- c. Waste produced by treatment of urban wastewater identified by the codes of the European list of waste 190801 and 190802.
- d. Waste from sewer cleaning 200306.
- e. Waste produced by cleaning chimneys and chimneys identified by the European Waste List Code 200141.
- f. Waste resulting from mechanical treatment (e.g., selection) identified by code 191212.
- g. Waste resulting from treatment of organic municipal waste, identified by codes 190501, 190503, 190604 and 190606, if compliance with what is guaranteed provided for by the Regional Programs referred to in Article 5 of this decree and presents a potential dynamic breathing index (determined according to UNI/TS11184) not exceeding 1000 mg  $O_2$ /kg VSh.
- h. Sludge produced by wastewater treatment urban (European Waste List Code 190805) provided have an IRDP value not exceeding 1000 mg O<sub>2</sub>/ kg VSh.

If the waste does not comply with the values reported for the DOC at their own pH value, can be tested, with a proportion L/S=10 L/kg and with a pH between 7,5 and 8,0. Waste can be considered compliant with the criteria of eligibility for dissolved organic carbon if the result test does not exceed 100 mg/L.

The supplementary threshold value, indicated in Table 4, are relating to organic substances soluble in organic solvents, as well as total organic carbon.

| Parameter                            | Inert waste<br>(mg/kg) | Non-toxic waste (mg/kg) | Toxic waste (mg/kg) |
|--------------------------------------|------------------------|-------------------------|---------------------|
| TOC (Total Organic Carbon)           | 30,0000 *              | 5%                      | 6%                  |
| BTEX (Benzene, Ethylbenzene, Toluene | 6,0000                 | -                       | 1                   |
| and Xylenes)                         |                        |                         |                     |
| PCB (Polychlorobiphenyls)            | 1,0000                 | 10,0000 ***             | 50,0000 ***         |
| Mineral Oil (C10 to C40)             | 500,0000               | -                       | -                   |
| PCDD/PCDF**                          | 0,0001                 | 0,0020 ***              | 0,0100              |
| Dry material                         | -                      | ≥25%                    | ≥25%                |
| рН                                   | -                      | ≥6                      | -                   |

Table 4: Limit values for total content of organic parameters (Legislative decree 3<sup>rd</sup> September 2020, n. 121 Annex 3).

#### **Comparisons**

Significant variations exist in how member states implement these directives, a comparison across Spain and Italy is outlined:

- Heavy metals, halogens and sulphates: Italy applies stricter standards with one order of magnitude lower than Spain's. As an example, the examination of the parameters that will then be analysed in this procedure and results are lead (Pb) and chlorides (Cl). The nonhazardous landfills for Pb have a limit of 10,00 mg/kg in Spain and 1,00 mg/kg in Italy, for chlorides 15000,00 mg/kg in Spain and 1500,00 mg/kg in Italy.
  - Spain maintains the EU-standard, while Italy indicates a more conservative environmental and health protection.
- Organic parameters: Spain is consistently more permissive, allowing 6-10 times higher concentration.
- pH and acid neutralization capacity: Spain contains provisions for evaluating pH stability and ANC as determinants for waste acceptance. Italy's approach focuses on long-term leaching behaviour under varying pH conditions. Additional tests are required for residues with pH values outside the range 5,5-12.
- Regional flexibilities: Spain allows autonomous communities to establish higher threshold values for certain parameters, particularly for organic carbon content in specific waste types.

<sup>\*</sup>For land the competent authority can accept a higher value limit, if the value of 500 mg/kg is not exceeded for dissolved organic carbon at pH 7 (DOC7).

<sup>\*\*</sup> The values are calculated according to the equivalence factors of which to Table 1 of Annex P.

<sup>\*\*\*</sup> For persistent organic pollutants other than PCBs PCDD/PCDF the concentration limits set out in Annex IV apply to Regulation 2019/1021.

| Italy implements a regionally variable system with northern regions enforcing stricter criteria than the national baseline, especially for industrial waste streams. |
|--|
|  |
|  |
|  |
|  |
|  |
|  |
|  |

#### **4 MATERIALS AND METHODS**

#### 4.1. Properties of ashes

This section is structured to detail the source and describe pre-applied procedures of fly ashes used in the following procedures. Ball milling experiments were conducted using two distinct fly ash samples: FA1 and FA-ST-WAT, both originating from the same municipal solid waste incineration facility located in Tarragona, Spain (SIRUSA). The primary difference between these samples lies in their pretreatment history. FA1 represents untreated fly ash, while FA-ST-WAT corresponds to FA1 that has undergone stabilization through a batch inertization process.

The ash samples (FA1) were collected from pre-wash particulate trap systems of flue gases during the process of incineration of the rejected fraction of municipal solid waste. The material exhibits a characteristic grey, black to brown coloration with extremely fine particle size distribution. It results in a powdery texture, and the moisture content is approximately 41 % [11]. FA1 were conserved in a closed barrel and were transferred into a sealed jar with appropriate safety devices. This facilitates the weighing of the material moreover safety as fly ashes might contact the mucous membranes and prove toxicity.

FA-ST-WAT were already available in a closed container and visually appear as fine particle size distribution and a light grey colour.

The experimental protocol implemented to FA1 to obtain FA-ST-WAT is a batch inertization process and is detailed below to ensure reproducibility [21].

#### **Materials:**

- Crystallizer
- 2 graduated flasks 2 L
- 2 test pieces 250 mL
- Beaker 3 L
- 2 beakers 250 mL
- Beaker 400 mL
- Kitasato flask
- Spatula/spoon

- Magnet
- Glass rod
- Funnel Büchner
- Filter paper ALBET 145 (7 11 μm)
- PRAT DUMAS filter paper (0,45 μm)
- Mask FFP3
- Gloves

# **Equipment:**

- Thermostatic bath, Selecta TECTRON 200
- Grenade scale KERN 440-47N.
- Stove J.P. Selecta S.A.
- Vacuum pump
- Desiccator
- Magnetic stirrer plate
- pH meter, LPG 21 CRISON, CRISON electrode
- CRISON Conductometer Basic 30

### **Reactants:**

- $Na_2CO_3$  anhydrous, labkem (99,5-100,5 %; MM = 105,99 g/mol)
- Distilled water
- FA1

## Methodology:

- 1. Preparation of a thermostatic bath at 30 °C containing a sodium carbonate (Na₂CO₃) solution.
- 2. Introduction of 300 g of fly ash into the carbonate solution under controlled temperature conditions.
- 3. Continuous manual agitation of the mixture for 5 minutes using a glass rod.
- 4. Vacuum filtration using a Büchner funnel and filter paper with a pore diameter of 7–11 μm.

- 5. Washing of the retained ash with distilled water in a 1:1 ratio (300 mL of water per 300 g of original ash) after the initial filtration.
- 6. Secondary filtration using cellulose acetate filter paper (pore diameter:  $0,45 \mu m$ ) to capture fine precipitates formed during the treatment process.
- 7. Drying of the treated ash at 110 °C for 24 hours, followed by cooling in a desiccator.

This method was previously designed and tested by the Department of Chemical Engineering and Industrial Design at the 'Escuola Técnica Superior de Ingeniería y Diseño Industrial', Universidad Politécnica de Madrid. The object is to facilitate the removal of chlorides through a carbonate-based reaction, thereby reducing the concentration of soluble salts in the processed fly ash. The chlorine and lead content were measured with procedures described in paragraphs 4.3 and 4.4 [21].

### 4.2. Inertization and activation tests

Ball milling is a mechanochemical process which involves grinding materials that collides with the material to reduce particle size and induce physicochemical changes. The structure of fly ashes is altered through compression, collision, friction, and shear accompanied by heating (ca. 60 °C). For this reason, the efficiency depends on critical parameters including milling time, speed and dimension of the milling balls, with optimal peaks. For example, prolonged milling time improves reactivity but potentially cause particle agglomeration, which has a negative impact performance [22].

This innovative method has the potential to produce new materials and develop eco-friendly and economical technologies, advancing the field of recovering of fly ashes. However, the need for pre-and/or post-treatments optimization to achieve optimum performance is usually required and possible contamination from milling media can occur.

The mill used has grinding jars in the centrifugal ball mills and move in a horizontal plane. Grinding gives primarily impact and friction because generated centrifugal forces propel the balls against the wall of the jar, rolling over the product. The device has also an automatic reversal effect if wanted to overcome the possible agglomeration and favour homogenization [23].

It also represents a dual-purpose approach, with the possibility of simultaneously achieving inertization and activation.

Inertization involves the reducing of hazardous components such as heavy metals through encapsulation mechanisms. Previous laboratory studies have identified sodium carbonate (Na<sub>2</sub>CO<sub>3</sub>) as the most optimal reactant to incorporate during the stabilization process. Carbonate is primarily responsible for removing chlorides from ash through solubilization reactions, where Na<sub>2</sub>CO<sub>3</sub> in the aqueous phase reacts with chlorides to form sodium chloride (NaCl) according to the reaction:

$$Na_2CO_3 + 2Cl^- \rightarrow 2NaCl + CO_3^{2-}$$
 Equation 3: Inertization reaction with chlorides.

Additionally, carbonate reacts with heavy metals to form insoluble carbonate precipitates, effectively immobilizing these contaminants within the ash matrix through reactions (where M

represents heavy metal cations).

$$Na_2CO_3 + M^{2+} \rightarrow 2Na^+ + MCO_3$$
  
Equation 4: Inertization reaction with heavy metals.

The activation process is favoured by particle size reaching submicron scale, allowing the break and reconstruction of interfacial bonds and molecular arrangements, hopefully increasing oxygen defects on the adsorbent surface for attracting environmental pollutants. Ball milling of fly ashes results in an ultra-fine ash powder with more uniform particle size distribution, improving the final product's quality, consistency, and longevity [22]. Sodium hydroxide (NaOH) is used as the alkaline activating agent. It dissolves the silica and alumina matrix and other metal oxides, converting fly ash into a valuable reagent that can sustain circular economy principles. Self-sustaining reactions in exothermic (dissolution of NaOH in water) power mixtures are induced. In this case, the heat activation enhances pozzolanic reactivity by increasing surface area and promoting amorphization of the ash matrix. Specifically, the depolymerization of SiO<sub>2</sub> and Al<sub>2</sub>O<sub>3</sub> networks, generates soluble silicate and aluminate species that, upon precipitation, form new crystalline aluminosilicate structures [11].

The treatment methodology was implemented with the same time and speed through two approaches: a one-pot solution that simultaneously inerts and activates the ash (FA1), or a single step activation on previously inertized ash (FA-ST-WAT).

The efficiency of both reactants and the overall mechanochemical process has been researched through previous articles. The experimental variables are the ball dimensions and initial fly ash

characteristics. Results are systematically investigated to optimize treatment parameters, maximize environmental safety and material performance outcomes.

The steel balls used in the ball milling tests vary in dimension. Table 5, presents the specifications of the different ball types employed across the various experiments, categorized by size classification.

| Description           | Mass (g) | STD dev. | Diameter (cm) | STD dev. | Quantity | Material |
|-----------------------|----------|----------|---------------|----------|----------|----------|
| Macro balls           | 11,00    | ± 0,05   | 2,00          | ± 0,02   | 8,00     | Ceramic  |
| Mixed dimension balls | 3,54     | ± 0,01   | 0,95          | ± 0,01   | 15,00    | Steel    |
|                       | 2,03     | ± 0,01   | 0,80          | ± 0,01   | 15,00    | Steel    |

Table 5: Size and weight of the balls used in the different tests with respective standard deviation.



Figure 6 & 7: Comparison of ball sizes used in the ball milling experiment on the left large balls, on the right mixed-ball size.

# **Equipment**

- Retsch ball mill Type: S100 year 2002

- Mill balls

- Granatory balance KERN 440-47N

- Oven J.P Selecta S.A.

- Vacuum filtration system

### **Materials**

- Spoon or spatula
- graduated cylinder
- 3 beakers
- Filter 7-11 micrometres
- Sealed container for storage of FA
- Labels
- Parafilm

### Reagents

- NaOH, Labkem (>98,0 %; MM=40 g/mol)
- Na<sub>2</sub>CO<sub>3</sub> anhydrous, Labkem (99,5-100,5 %; MM=105,99 g/mol)
- Fly ashes
- Distilled water

### **Calculation of reactive**

Before starting the experiment, it is necessary to derive the right quantity of reactants. Sodium carbonate ( $Na_2CO_3$ ) is used to neutralize the quantity of chlorides present in the ash. According to Technical Report 22-782-IN [11], the original ashes measured by ion chromatography have a content of  $18 \pm 2\%$  of soluble chlorides.

As an example, 17 grams of ash are treated, and considering the properties of the compounds, the amount of carbonate required is obtained by following Equation 5.

[Cl<sup>-</sup>]=18%

Molecular Mass Cl<sup>-</sup> =35,5 g/mol

Molecular Mass Na<sub>2</sub>CO<sub>3</sub> =105,99 g/mol

Purity of Na<sub>2</sub>CO<sub>3</sub>=100%

$$\begin{split} m \, N a_2 C O_3 = 17 \, g \, FA \cdot \frac{18 \, g \, C l^-}{100 \, g \, FA} \cdot \frac{1 \, mol \, C l^-}{35,5 \, g \, C l^-} \cdot \frac{1 \, mol \, N a_2 C O_3}{2 \, mol \, C l^-} \cdot \frac{105,99 \, g \, N a_2 C O_3}{1 \, mol \, N a_2 C O_3} \\ m \, N a_2 C O_3 = 4,568 \, g \end{split}$$

Equation 5: Formula to obtain the amount of  $Na_2CO_3$ .

For the volume of water (the stabilizer of the solution), a rule is known, stating the ratio of ash grams over litres of solution stabilizer as 150 g FA/L liquid stabilizer. To determine the litres of solution in which the carbonate is diluted, Equation 6 is respected.

mL solution of stabilizer = 
$$17g \, FA \cdot \frac{1000 \, mL \, stabilizing \, liquid}{150 \, g \, FA} = 113,33 \, mL$$

Equation 6: Formula to obtain the volume of water.

For the activation, it is used sodium hydroxide (NaOH). The volume of NaOH 3,5 N is calculated with the right ratio mass of FA and mL of solution, which is 8 mL of solution for every gram of FA.

mL solution of NaOH = 20 g FA 
$$\cdot \frac{8 \text{ mL solution of NaOH}}{1 \text{ g FA}} = 136 \text{ mL NaOH } 3,5 \text{ M}$$

Equation 7: Formula for the calculation of the volume of NaOH.

Then the mass of NaOH is calculated considering the purity of NaOH at 98%, its concentration and molar mass.

$$mass\ NaOH\ =\ 3,5\ \frac{mol}{L} \cdot L\ solution\ NaOH\ \cdot\ 40\ \frac{g}{mol} \cdot \frac{100g}{98g} =\ 19,429g\ NaOH\ 98\%\ pure$$

Equation 8: Formula for the calculation of the mass of NaOH.

# **Procedure**

# 1. Reagent preparation

The required quantities of reagents are calculated in proportion to the mass of volatile ash to be treated. All reagents are weighted using an analytical balance, with measurements recorded to three decimal places to ensure accuracy.

**Safety considerations:** Due to the toxic nature of fly ash, a FFP2 respiratory mask was worn during handling. Immediately after weighing, beakers containing ash samples were covered with parafilm to prevent volatilization. Sodium hydroxide is handled expeditiously to minimize atmospheric moisture absorption due to its hygroscopic properties.

### 2. Milling Process

All reagents and milling balls are placed in the mill chamber. The ball mill is set to operate at 580 rpm for 60 minutes in unidirectional rotation. The process is immediately initiated to take advantage of the exothermic heat generated from sodium hydroxide dissolution in water.

# 3. Post Milling and vacuum filtration

Milling balls are carefully removed from the slurry, trying to avoid sample loss. A vacuum filtration system is assembled using a 7-11  $\mu$ m filter. The empty filter capsule is pre-weighed, and the tare weight is recorded for subsequent mass balance calculations. This is not mandatory, but useful for the next steps.

# 4. Drying

The filtered cake in the pre-weighed capsule is placed in an oven maintained at 110 °C for 24 hours to achieve complete moisture removal.

## 5. Final processing

The capsule is removed from the oven and allowed to cool in a desiccator to prevent moisture re-absorption. The final mass was recorded to determine the remaining fly ash quantity for subsequent analyses. The processed ash is then transferred to a properly sealed container with complete identification information for traceability.



Figure 8: Retsch ball mill S100 year 2002.

This process was conducted 4 times with these 4 different parameters (Table 6), producing 4 different types of ashes.

|         | Fly ashes | Ball size   |  |
|---------|-----------|-------------|--|
| 1° test | FA1       | Macro balls |  |
| 2° test | FA1       | Mixed balls |  |
| 3° test | FA-ST-WAT | Macro balls |  |
| 4° test | FA-ST-WAT | Mixed balls |  |

Table 6: Experimental conditions for the four ball milling tests.

# 4.3. Leaching tests

This phenomenon is crucial for areas of studies like environmental engineering and waste management. It allows examining the quantity of soluble hazardous components mobilized when exposed to aqueous solutions, recreating a similar natural behaviour. Leaching tests are based on the contact between a solid material and a liquid solvent for a fixed set time and ratio, this encounter gives the opportunity for soluble substances to be extracted. The remaining liquid (solvent + soluble substances) is called the leachate, which is analysed to determine its chemical composition. Multiple factors govern the leaching behaviour such as pH, temperature, contact time, particle size distribution, and chemical composition of solid matrix/leaching medium. Understanding these correlation mechanisms is essential for predicting the long-term environmental fate of disposed materials and assisting potential groundwater contamination risks [24].

The analysis of the leachate is crucial for determining the type of waste and the appropriate disposal method, in alternatively the probable re-use of the solid material in recovery applications.

The European Committee for Standardization has established several leaching test methods. Each is designed for specific waste types and application scenarios to ensure reproducibility and comparability of results across different laboratories. For this investigation, Standard UNE-EN 12457-4:2003 was implemented. A one-stage batch leaching test procedure utilizing a liquid-solid ratio of 10 L/kg for materials with particle sizes below 10 mm.

The resulting leachate compositions will be evaluated against the criteria established in Royal Decree 646/2020 to determine the hazard classification index of the four-ball milled fly ash samples.

This leaching analysis will be conducted exclusively on treated ash samples that have undergone stabilization and activation processes, as the composition of FA1 and FA-ST-WAT samples has been previously characterized in Technical Report 22-782-IN [11] [21]. The effectiveness of the treatment

methods applied will be evaluated by comparing the leaching behaviour between the different conditions, providing insights into the most effective optimization of waste treatment through ball milling.

# **Equipment**

- Granatory balance KERN 440-47N
- Stirring plate
- Vacuum filtration system

#### **Materials**

- Crucible
- 250 mL beaker
- 250 mL measuring cylinder
- Magnet
- Glass rod
- Parafilm
- Kitasato flask
- Butchner funnel
- ALBET 145 filter paper (7-11  $\mu$ m)
- PRAT DUMAS filter paper (0.45 μm)

# Reagents

- Dried ball milled fly ashes
- Distilled water

If the treated and dried fly ash has been stored a period longer than 6–12 months, it will be necessary to return it to the oven for 24 hours to remove the moisture content that it may have adsorbed.

## **Procedure**

## 1. Reagent calculation and measurement

The mass of processed ash samples from the ball milling treatment (typically 10,00 g) is accurately weighted using an analytical balance. The required volume of deionized water

was calculated according to the liquid-solid ratio of 10 L/kg as specified in Standard UNE-EN 12457-4:2003 and measured with a graduated pipette.

volume 
$$H_2O(L) = mass \ ashes \ (kg) \cdot 10 \ \frac{L}{kg}$$

Equation 9: Calculation of the volume of water to dilute the FA.

For example, if it is chosen to treat 0,01 kg of ashes, the amount of water is 0,1 L.

#### 2. Mixing

The ash sample and deionized water are combined in a clean beaker (250 mL). A magnetic stirrer is employed to maintain continuous agitation at a speed sufficient to ensure complete particle suspension and effective solid-liquid contact while preventing solution splashing. For minimizing evaporation losses and contamination during the extended contact period, the vessel is sealed with parafilm.

The mixing is maintained continuously for 24 hours at room temperature (25  $\pm$  2 °C) to achieve equilibrium conditions between the solid and liquid phases, as required by the standard protocol.

#### 3. Filtration

The suspension is subjected to sequential vacuum filtration to separate the leachate from the solid residue.

The filtration process is conducted in two stages:

- Initial filtration through filter paper with a pore size of 7-11  $\mu m$  to remove coarse particulates and suspended solids.
- Secondary filtration of the initial filtrate through a 0,45  $\mu$ m membrane filter to remove fine particulates and ensure solution clarity for successive analytical procedures.

The final filtered leachate represents the extractable fraction of the treated fly ash under the specified test conditions. The leachate volume is measured using a graduated cylinder and recorded for mass balance calculations. The clarified leachate was transferred to a clean, labelled beaker and covered with parafilm to prevent contamination and evaporation prior to chemical analysis.

The solid residue retained on the filters was disposed of according to laboratory waste management protocols, as it no longer contained extractable components of analytical interest.

# 4.4. Analysis of the leaching liquid

The leaching test was conducted to simulate potential environmental exposure conditions and evaluation. To assess the environmental safety of the treated fly ash, chlorine and lead concentrations were analysed in the leachate liquid. The measure of these key parameters determines if the ball milling treatment was effectively implemented. The goal is to reach the material's suitability for safe disposal and good properties for reuse applications.

# **4.4.1.** Determination of chlorine with potentiometry

Potentiometry can determine total solubilized chloride content with titration using silver nitrate solution (for environmental reasons, mercury nitrate is avoided). The method is based on the measurement of the electrical potential generated by changes in silver ion concentration during a precipitation titration. The procedure employs a manual titration with silver nitrate (AgNO<sub>3</sub>) as the titrant and utilizes a suitable reference electrode (typically Ag/AgCl or calomel electrode) to monitor potential changes throughout the titration [25].

When the silver nitrate titrant is added to the sample solution, chloride ions react with silver ions according to the precipitation reaction illustrated in Equation 10.

$$Ag_{(aq)}^+ + Cl_{(aq)}^- \rightarrow AgCl$$

Equation 10: Precipitation reaction of AgCl.

The silver chloride precipitate formed is highly insoluble ( $K_{sp} = 1,77 \times 10^{-10}$  at 25 °C), effectively removing chloride and silver ions from solution [21]. During the initial stages of the titration, the electrical potential remains relatively stable as the silver ions are consumed by the precipitation reaction, maintaining a low concentration of free Ag<sup>+</sup> ions in solution.

The equivalence point occurs when all chloride ions in the sample have been consumed. Any additional silver nitrate causes a dramatic increase in free silver ion concentration, since there are no more chloride ions available for precipitation. This sudden change results in a sharp, characteristic inflection of the electrical potential curve, detected by the potentiometric system [25].

The volume of AgNO₃ solution consumed up to the equivalence point is directly proportional to the chloride content in the sample, as in any titration. Using the stoichiometric relationship from the

Equation 10 (1:1 molar ratio of Ag<sup>+</sup> to Cl<sup>-</sup>) and the known concentration of the silver nitrate titrant. The chloride concentration in the original sample can be calculated using the formula:

$$[Cl^-] = \frac{volume \ of \ AgNO_3 \cdot molarity \ AgNO_3}{volume \ sample}$$

Equation 11: Calculation of the chlorine concentration in the sample.

This potentiometric approach offers high precision and accuracy, with the added advantage of being suitable for coloured or turbid solutions where visual endpoint detection would be problematic.

# **Determination of the blank sample**

## **Equipment:**

- Potentiometer/pH meter with mV capability
- Magnetic stirrer and stir bar

#### Materials:

- 250 mL beakers
- Various pipettes and graduated cylinders

### **Reactants:**

- 0,1 M AgNO<sub>3</sub> solution
- 0,1 M HNO₃ solution
- Distilled water

#### **Procedure:**

## 1. Electrode and equipment preparation

Rinse the probe and magnet that will be used for titration with distilled water and gently blot dry, calibrate the potentiometer according to manufacturer's instructions.

## 2. Sample preparation

Prepare the nitration mixture in a 250 mL beaker by adding reagents in the following order: 50 mL distilled water (using a 50 mL graduated cylinder) and 5 mL of 0,1 M HNO<sub>3</sub> (using a 5 mL pipette). The order of addition is critical for reproducibility and to ensure proper sample matrix conditions.

## 3. Titration Set Up

Place the magnetic stir bar in the beaker and insert both electrodes into the solution, ensuring they do not contact the stir bar or beaker walls. Begin gentle magnetic stirring (avoid creating a vortex) and allow the potential reading to stabilize and record the initial potential.

### 4. Titration Procedure

Add 0,02 mL of 0,1 M AgNO<sub>3</sub> solution incrementally using a pipette and record the potential right after each addition once it stabilizes, as the equivalent point approaches (indicated by larger potential changes) mark the value and continue adding silver nitrate until the potential change is minimal. The volume of titrant added at the time of the jump is the amount of interest when performing the calculations.

## 5. Cleaning and repeatability

Turn off the stirrer and carefully remove electrodes rinsing them with distilled water, clean all glassware with appropriate solvents.

Repeat the entire procedure in triplicate to ensure reproducibility.

## Determination of chlorine in the sample

## **Equipment:**

- Potentiometer/pH meter with mV capability
- Magnetic stirrer and stir bar

## **Materials:**

- 250 mL beakers
- Various pipettes and graduated cylinders
- Sample solution (leachate)

#### Reactants:

- 0,1 M AgNO₃ solution
- 0,1 M HNO₃ solution

#### **Procedure**

### 1. Electrode and equipment preparation

The probe and magnet are rinsed and will be used for titration with distilled water. Gently blot dry and calibrate the potentiometer according to manufacturer's instructions.

### 2. Sample preparation

The nitration mixture is prepared in a 250 mL beaker by adding reagents in the following order:

- 50 mL distilled water (using a 50 mL graduated cylinder)
- 5 mL sample solution (using a 100-1000 μL micropipette)
- 5 mL of 0,1 M HNO<sub>3</sub> (using a 5 mL pipette)

The order of addition is critical for reproducibility and to ensure proper sample matrix conditions.

#### 3. Titration Set Up

The magnetic stir bar is placed in the beaker. The electrode is inserted into the solution, ensuring there is no contact with the stir bar or beaker walls. Gentle magnetic stirring is started (avoid creating a vortex) and the potential reading is allowed to stabilize with the recording of the initial potential.

### 4. Titration Procedure

A volume of 0,02 mL of 0,1 M AgNO<sub>3</sub> solution is added incrementally using a pipette and the potential is noted right after each addition once it stabilizes. As the equivalent point approaches (indicated by larger potential changes) mark the value and continue adding silver nitrate until the potential change is minimal. The volume of titrant added at the time of the jump is the amount of interest when performing the calculations.

# 5. Cleaning and repeatability

The stirrer is turned off and the electrode carefully removed and rinsed with distilled water. All glassware is cleaned with appropriate solvents. Repeat the entire procedure in duplicate to ensure reproducibility. If the data do not match, it is recommended to repeat the procedure another time.

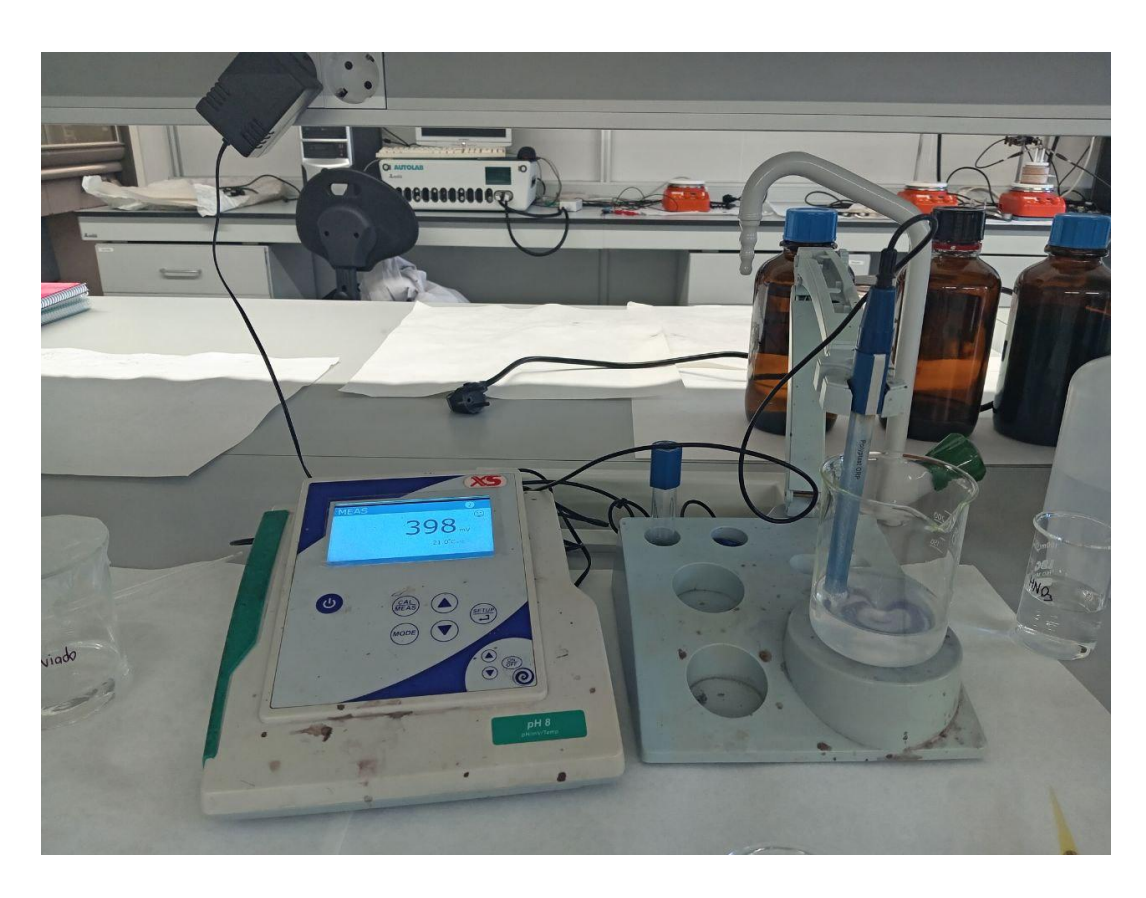


Figure 9: Determination of chlorine on a fly ash sample.

## **Example of real chlorine concentration calculation**

The data excerpt from the titration are disposed in two columns, one addressing the volumes of  $AgNO_3$  added, the second corresponding to the potential readings. The location of the peak of interest is estimated and for a more accurately value, the method of derivatives is used. It consists in finding the highest potential difference caused by the addition of the volume of the titrant. This is achieved by creating a column with a formula, representing the quotient between the two values  $\Delta E$  and  $\Delta V$ . Where  $\Delta V$  is the difference in volume added and  $\Delta E$  is the measured potential difference. From here, the calculated quotient is plotted against the added volume. The equivalence point is now clearly visible, researching the maximum peak of the quotient of the derivatives corresponds to the volume of titrant being sought. With the volume of the titrant, the concentration of chlorines is calculated following Equation 12.

An example with a volume of  $AgNO_3$  that results in the greatest change in potential as 0,46 mL, is used.

Vol AgNO $_3$  = 0,46 mL

 $[AgNO_3] = 0.1 M$ 

Volume of the sample = 1 mL

 $MM(Cl^{-}) = 35,5 \text{ g/mol}$ 

$$[Cl^{-}] = 0,46 \ ml \ Ag^{+} \cdot \frac{1 \ L}{1000 \ mL} \cdot \frac{0,1 \ mol \ Ag^{+}}{1 \ L \ Ag^{+}} \cdot \frac{1 \ mol \ Cl^{-}}{1 \ mol \ Ag^{+}} \cdot \frac{35,5 \ g \ Cl^{-}}{1 \ mol \ Cl^{-}} \cdot \frac{1}{10^{-3} \ L \ sample}$$
 
$$= 1,633 \ \frac{g \ Cl^{-}}{L}$$

Equation 12: Calculation of the concentration of Cl<sup>-</sup> from the volume of AgNO<sub>3</sub>.

Since the permitted limit values according to regulations are stipulated in mg of substance per kg of ash, the resulting value must be converted.

$$[Cl^{-}] = 1,633 \frac{g \ Cl^{-}}{L} \cdot \frac{1000 \ mg \ Cl^{-}}{1 \ g \ Cl^{-}} \cdot \frac{10 \ L \ stabilizing \ liquid}{1 \ kg \ of \ fly \ ashes} = 16330 \frac{mg \ Cl^{-}}{kg \ fly \ ashes}$$

Equation 13: Conversion of the concentration from g/L to mg/kg.

This value will be compared with the waste admission criteria in Table 1.

# **4.4.2.** Determination of lead with atomic absorption spectroscopy

Atomic absorption spectroscopy is a widely used analytical technique for the quantitative determination of chemical elements, specifically metals, in liquid, solid, or gaseous samples. It is a high-throughput and non-destructive method. Also, it presents high sensitivity and selectivity for the detection of trace metals, with limits in the parts per million or even parts per billion range.

The theoretical basis of atomic absorption spectroscopy is based on the absorption of electromagnetic radiation by atoms in a gaseous state. When a sample is atomized and brought to a gaseous state, it is irradiated with light of a specific wavelength corresponding to the electronic

transition of interest in the element being analysed. The atoms selectively absorb this light at a characteristic frequency, causing a decrease in the intensity of the incident radiation. The amount of light absorbed is directly related to the concentration of atoms of the element in the sample, thanks to the Beer-Lambert law. Beer-Lambert discovered the direct proportionality of the amount of light absorbed with the concentration of the analyte present and the optical path length through the sample. The amount of absorbed light is measured using a detector, such as a photodiode or photomultiplier, and compared to a reference signal to determine the concentration of the element in the sample. For this reason, a calibration line is necessary for comparison and reliability of the results, minimizing spectral interferences with background correction [21].

The experimental procedure follows UNE Standard 12506:2004, regarding the characterisation of residues in an eluate. This test consists of four sections to accurately measure the lead concentration in the sample.

# Preparation of standard solutions of Pb(NO<sub>3</sub>)<sub>2</sub> [1000 ppm] + HNO<sub>3</sub> 2%

#### **Materials**

- 9 volumetric flasks (50 mL)
- 3 beakers (100 mL)
- 3 volumetric flasks (100 mL)
- Pasteur pipettes
- 3 beakers (250 mL)
- Kartell Pluripet micropipette (20-200 μL)
- Easy 40 Elite micropipette (100-1000 μL)
- Easy 40 Elite micropipette (1-5 mL)
- Magnet

### Reactants

- HNO₃ PanReac AppliChem 2% mass
- Distilled water
- Pb<sup>2+</sup> 1000 ppm

The preparation of standard solutions (known lead concentrations) is necessary to calibrate the atomic absorption equipment. This calibration constructs a line that relates the lead concentration to the sample's absorbance, so that when the absorbance of the test solution is measured, the equipment returns its corrected concentration. The program generally recommends the concentrations of the standards to be measured. However, these can be edited and adjusted according to the range of values to be measured.

For this study, the standards to be prepared contain lead nitrate concentrations of 0,10; 0,25; 0,50; 1,00; 3,00; 5,00; 7,00 and 10,00 ppm and another 8,00 ppm to ensure the measurement is correct.

The stock-solution is a standard solution of 1000 ppm of Pb<sup>2+</sup>.

$$V_1 \cdot C_1 = V_2 \cdot C_2$$

Equation 14: Dilution formula where subscript 1 indicates the stock solution and 2 indicates the sample to be prepared.

The calibration solutions will be prepared in 50- or 100-mL volumetric flasks ( $V_2$ ), with their corresponding concentrations ( $C_2$ ). The stock solution concentration is known (1000 ppm =  $C_1$ ). The only unknown left to calculate is the volume of stock solution required for each standard.

An example of this would be:

$$V_1(\mu L) \cdot 100(ppm) = 50 (\mu L) \cdot 10(ppm)$$
  
 $V_1 = 5 mL$ 

Equation 15: Example of a dilution calculation.

These calculations are grouped in Table 7.

|                      | 0,10   | 0,25   | 1,00  | 3,00   | 5,00   | 7,00   | 8,00   | 10,00  |
|----------------------|--------|--------|-------|--------|--------|--------|--------|--------|
| C <sub>2</sub> (ppm) |        |        |       |        |        |        |        |        |
|                      | 100,00 | 100,00 | 50,00 | 50,00  | 50,00  | 50,00  | 50,00  | 50,00  |
| V <sub>2</sub> (mL)  |        |        |       |        |        |        |        |        |
|                      | 10,00  | 25,00  | 50,00 | 150,00 | 250,00 | 350,00 | 400,00 | 500,00 |
| V₁(μL)               |        |        |       |        |        |        |        |        |

Table 7: Preparation of lead measurement standards by atomic absorption.

These volumes (V1) must be added to each correspondent 50- or 100-mL flask.

Micropipettes with different measuring ranges are used depending on the quantity to be added, the right amount of Pb<sup>2+</sup> is poured into the correspondent flasks, then filled till the mark with the 2% HNO<sub>3</sub> solution. The standards are now ready for measurement.

# Preparation of the lead measurement sample

This procedure describes the preparation of leachate samples for lead concentration analysis. The method involves pH adjustment and dilution to ensure compatibility with analytical instrumentation requirements and to achieve optimal measurement accuracy within the calibrated range. The critical parameters that must be evaluated are a pH below 2,0 (specified by the equipment manufacturer's guideline) and final lead concentrations falling within the calibrated standard range of 0,10-10,00 ppm to ensure reliable measurements.

### Equipment

- Calibrated pH meter
- Magnetic stirrer and stir bars

## **Materials**

- 100 mL beakers
- 100 mL volumetric flasks
- Graduated cylinders
- Parafilm or appropriate stoppers for sample coverage

#### Reactants

- 2% HNO₃ solution
- EDTA solution
- Distilled water
- Leachate sample

#### **Procedure:**

- 1. **Initial sample transfer:** A volume of leachate is measured and transferred using a graduated cylinder into a 100 mL beaker. The volume is recorded and keep.
- 2. **Initial pH assessment:** While maintaining continuous magnetic stirring, the initial pH is measured using a pre-calibrated pH meter. This value is recorded and verified whether it falls below the required threshold of 2,0. The leachate of ashes is typically basic, so a value of pH around 12-14 is expected.
- 3. **pH adjustment:** Since leachate samples typically exhibit basic characteristics, pH reduction is necessary so 1 mL of 2% HNO<sub>3</sub> solution is added to the sample, the new pH value is measured and recorded while maintaining stirring. This process is repeated incrementally until the pH reaches approximately 1,75. It is important to maintain a detailed record of the total nitric acid volume added to track the cumulative solution volume.
- 4. **Dilution process**: 1 mL of EDTA solution is added to the acidified sample (pH value is recorded). Incremental dilutions are performed by adding 5 mL aliquots of distilled water, and the pH is monitored after every addition to ensure the pH is below 2. If pH exceeds the threshold, another 1 mL of 2% HNO<sub>3</sub> solution is added, if not continue the dilution process until the total solution volume reaches approximately 95 mL. It is also indispensable to maintain a detailed record of the total water added.
- 5. **Final sample preparation:** Transfer the prepared solution from the beaker to a 100 mL volumetric flask and dilute to the mark with distilled water.

Prepared dilutions should be analysed promptly after preparation to prevent potential sample degradation and quality assurance. All samples, whether in beakers during preparation or in volumetric flasks after dilution, must be covered with Parafilm or appropriate stoppers to minimize volatilization losses and protect any lab worker from potential toxic risk. Other safety precautions are handling nitric acid solutions with appropriate personal protective equipment, ensure adequate ventilation when working with acid solutions, and follow institutional safety protocols for chemical handling and disposal.

#### Lead measurement

This procedure outlines the analytical protocol for lead concentration determination using atomic absorption spectrometry. The method employs flame atomization with acetylene fuel gas and follows standardized calibration and measurement protocols to ensure accurate quantitative analysis.

## **Equipment**

- Thermo Scientific iCE 3000 series spectrometer
- Magnetic stirrer
- pH meter, GLP 21 CRISON pH meter, CRISON electrode
- Fume hood

Prior to analysis, ensure the following solutions are properly prepared and positioned within the spectrometer sample compartment:

- Calibration standard solutions (0,10, 0,50, 1,00, 3,00, 5,00, 7,00 and 10,00 ppm Pb)
- Prepared sample dilutions
- 2% HNO<sub>3</sub> solution (blank)
- Distilled water (system cleaning)

### **Equipment setup and initialization**

- System startup: in this order the acetylene fuel gas cylinder valve is opened, the air compressor connected to the spectrometer system is activated, the spectrometer instrument is powered on, the fume extraction hood is activated to ensure proper ventilation. The computer system is initialized, launching the SOLAAR analytical software only when the instrument is already completely working.
- Method configuration: the acetylene-air flame is ignited following manufacturer's safety protocol. The analytical method selection interface is accessed within the SOLAAR software, measurement parameters including standard concentration range (0,1-10 ppm) are configured with analytical wavelength specific to lead detection and fuel gas flow rate as recommended by manufacturer specifications. Lead (Pb) is selected as the target analyte

from the element database, plus the corresponding lamp is visually controlled if it is working. A descriptive experiment name is assigned corresponding to the sample set, verify all parameters and then proceed to measurement phase.

### Calibration protocol and standard solution analysis

- System conditioning and blank measurement: The distilled water is aspirated by the instrument to establish system baseline and remove any residual contamination. The solvent used (10% HNO<sub>3</sub> solution) is measured to establish system background correction factor and account for matrix interferences.
- **Standard solutions analysis:** Execute the following protocol for each calibration standard (0,10, 0,50, 1,00, 3,00, 5,00, 7,00 and 10,00 ppm):
  - 1. Sample preparation: Each standard solution is mixed to ensure homogeneity.
  - 2. Aspiration: Complete submersion of the aspiration tube is ensured in the standard solution.
  - 3. Measurement: Sufficient aspiration time is allowed for stable signal acquisition.
  - 4. System maintenance: The aspiration line is cleaned with absorbent paper between each standard measurement to prevent cross-contamination.

### **Calibration curve validation**

- Linearity assessment: The software will automatically generate a calibration curve plotting lead concentration (ppm) versus absorbance, the correlation coefficient (R²) must be higher than 0,995.
- Accuracy verification: A quality control standard of known concentration is analysed (e.g.,
  in this case 8 ppm) within the calibration range, the measurement concentration is verified
  to fall within ±10% of the known value.

### Sample analysis

• **Triplicate analysis:** Each prepared sample is analysed three times to ensure measurement precision. The complete dataset is exported in Excel format for statistical analysis and reporting.

- **Data acquisition:** The software automatically records absorbance values and calculate corresponding concentrations based on the established calibration curve.
- Quality control: Monitor measurement consistency across replicates, some data might be outliers (specially the firsts).

## Procedure for system shutdown protocol (important to execute in this order):

- The acetylene-air flame is extinguished using proper safety procedures.
- The SOLAAR analytical software is properly closed.
- The spectrometer instrument is shut down.
- The fume extraction system is deactivated.
- The computer system is turned off.
- The acetylene cylinder valve is closed.
- The air compressor is turned off.

## Quality assurance considerations and safety protocols

New calibration standards are needed for each analytical session to ensure accuracy. Cleaning procedures are implemented between measurements and triplicate measurements to assess precision and identifying potential outlier. A regular verification of calibration accuracy using certified reference materials should be implemented.

For safety reasons it is important to ensure adequate ventilation during all flame operations, follow proper procedures for acetylene handling and storage, maintain appropriate personal protective equipment throughout the analysis and implement emergency shutdown procedures in case of equipment malfunction.



Figure 10: Thermo Scientific iCE 3000 series spectrometer.

# Example of the real lead concentration calculation

The lead concentration values obtained from atomic absorption spectrometry require mathematical correction to account for sample dilution and unit conversion to express results in regulatory-compliant units. It is needed to consider that the spectrometer provides lead concentrations for diluted sample preparations, the concentrations are reported in parts per million (ppm) or milligrams per litre (mg/L), but regulatory limits require expression in milligrams of compound per kilogram of ash (mg/kg).

The spectrometer provides three lead concentration values in ppm, an arithmetic mean of triplicate measurements is calculated to obtain the representative diluted sample concentration. In this example, the mean value is 7 ppm. This value corresponds to the dilution of 20 mL of sample in 100 mL of solution.

$$7 ppm = 7 \frac{mg Pb}{L dissolution} \cdot \frac{0.1 L dissolution}{0.02 L sample} = 35 \frac{mg Pb}{L sample}$$

Equation 16: From ppm to mg of lead in one litre of sample.

Since the limit values are established by regulation in mg of compound per kg of ash, and the ratio of litres of stabilizing liquid per kg of ash is 10 L/kg.

$$35 \frac{mg Pb}{L sample} \cdot \frac{10 L stabilizing liquid}{1 kg FA} = 350 \frac{mg Pb}{kg FA}$$

Equation 17: Converting in mg Pb over kg FA so this value can be compared to Waste Framework Directive.

# 4.5. Acid-base curve analysis

The acid-base curve analysis constitutes a fundamental technique for determining the material's acid neutralization capacity and establishing optimal pH conditions for its valorisation across diverse applications, including stabilization and solidification of hazardous materials. This approach is important to account as it quantifies the buffering capacity of the ash, a property that directly governs material performance in pH-sensitive applications. Thereby necessary for optimizing performance parameters and environmental issues.

In this case, treated fly ash is wanted to be used as an adsorber. The objective of the acid-base curve analysis is to understand the surface chemistry, comprehend functional groups and their acid-base properties. Also, giving information on the distribution and strength of basic sites that will neutralize acidic gases and how surface properties change with pH during the adsorption process.

This could also predict adsorption performance, and the combination of the two methodologies could confirm or missing deductions. Materials with higher basicity and greater buffer capacity results in better adsorption capacity of SO<sub>2</sub> and H<sub>2</sub>S, due to their acidic behaviour that require basic

sites for effective chemisorption. Sulphur dioxide requires basic sites to form sulphides or sulphates, whereas hydrogen sulphide reacts with basic sites to form sulphides [26].

The curve analysis is also linked with process control and design. Changes in pH during actual operation, state how long the adsorbent will remain effective before saturation, or whether regeneration is an option. It can be predicted which gases will be preferentially absorbed based on their relative acidity strengths.

Completing valorisation of fly ashes, help draw conclusion on how effective the ball milling treatment increases basicity and if the desired surface proprieties are created as expected.

The initial pH of the ash suspension provides baseline alkalinity information, while the acid neutralization capacity, expressed in milliequivalents of acid per gram of material, quantifies the total buffering potential. The buffering range identifies the pH interval where the material maintains stable condition. Furthermore, the titration curve reveals dissolution kinetics of alkaline phases inherent to fly ash composition, including calcium oxide, magnesium oxide, and various silicate minerals that contribute to overall alkalinity.

The ball milling pretreatment should enhance material reactivity through increased specific surface area and exposure of fresh reactive surfaces. These physical modifications could be seen in the acid-base curve through improved neutralization kinetics and potentially enhanced buffering capacity compared to untreated material [27]. This comprehensive characterisation enables prediction of long-term environmental behaviour, optimization of dosage requirements for practical applications, and verification of compliance with environmental regulations governing pH buffering in industrial processes utilizing valorised fly ash.

The acid-base curve analysis employed a standardized potentiometric titration procedure. The experimental protocol comprised three distinct phases:

- 1. Solution preparation.
- 2. Blank curve calibration to validate the experimental setup and establish baseline conditions.
- 3. Sample analysis using the validated methodology.

#### Blank curve

# **Equipment**

- pH meter, GLP 21 CRISON pH meter, CRISON electrode

#### **Materials**

- 250 mL beaker
- Burette
- Pipette
- Magnetic stirrer
- Standard pH solutions (4, 7 and 10 pH)

## Reagents

- NaOH 0,1 M
- NaCl 0,1 M
- HCl 0,1 M

#### **Procedure:**

## 1. Equipment setup

The equipment is switched on. The electrode and the thermal probe are rinsed with distilled water. After, they are dried gently with a clean tissue. The pH meter is calibrated using standard buffer solutions with a pH of 4, 7 and 10. A measurement of a standard solution is tried to verify if the calibration has been done correctly.

# 2. Initial solution preparation

Using a volumetric pipette, exactly 50,0 mL of NaCl 0,1 M solution are transferred into the 250 mL beaker. The beaker is placed on the magnetic stirrer and stirring occurs at the faster velocity. Using a micropipette 0,5 mL of NaOH 0,1 M are added to the beaker and it is let mixing for 30 seconds. The pH electrode is inserted into the solution, ensuring it is properly immersed but the walls and stirring bar are not touched. The initial pH and temperature are recorded (this is the starting point with 0 mL HCl added).

## 3. Titration process

A volume of 0,005 mL of HCl is supplemented using a micropipette. The value of pH is recorded after a waiting for its stabilization. The steps 1 and 2 are repeated until the pH reaches nearly 2,5. All equipment are cleaned thoroughly between replicates.

The entire procedure is repeated at least one time if the curves are similar, if not at least other 2. The pH is plotted versus the cumulative HCl volume to generate the blank curve. This blank curve served as a reference to account for the acid consumption by the background electrolyte and any systematic errors in the measurement system.

## Sample acid-base curve

## Equipment

- pH meter, GLP 21 CRISON pH meter, CRISON electrode
- Balance KERN 440-47N granulating scale

#### **Materials**

- 250 mL beaker
- Burette
- Pipette
- Magnetic stirrer

### Reagents

- NaOH 0,1 M
- NaCl 0,1 M
- HCl 0,1 M
- Treated fly ashes

#### **Procedure**

### 1. Initial solution preparation:

In an analytical balance, exactly 0,025 g of pre-treated fly ashes are weighted in a 250 mL beaker. The calibration of the pH meter should be already done previously for the blank curve. Using a volumetric pipette, 50,0 mL of NaCl 0,1 M solution are transferred into the

250 mL beaker then place the beaker on the magnetic stirrer and the mixing is started. Using a micropipette, 0,5 mL of NaOH 0,1 M are added to the beaker, and the mixing occurs for 30 seconds. At this point, the electrode is cleaned and inserted into the solution, ensuring it is properly immersed but not touching the stirring bar or the walls. The initial pH and temperature are recorded (this is the starting point: 0 mL HCl added).

## 2. Titration process

A volume of 0,005 mL of HCl is supplemented using a micropipette. When the pH is stabilized, the value is recorded. These steps are repeated until the pH reaches nearly 2,5. All equipment are cleaned thoroughly between replicates and at least another analysis is accomplished. If the data correspond, the analysis is finished. If not, another one is needed to guarantee precise results.

For data processing, the volume of HCl 0,1 M added is plotted against the pH. With this graph, the point of zero charge and the buffering zones are easily visual detected.

# 4.6. Brunamer-Emmet-Teller method: BET analysis

For characterizing adsorbent materials, it is crucial to know their specific surface area, pore volume and pore size distribution. For achieving these parameters BET analysis are used and basically consists in physical adsorption of inert gases (usually nitrogen) and this process can be represented as a monolayer adsorption with Langmuir theory but with three modifications:

- 1. Infinite multilayer adsorption states that gas molecules undergo physical adsorption on a solid surface, forming multiple layers without limit.
- 2. Layer independence where distinct layers do not interact with each other.
- 3. Universal applicability meaning that Langmuir theoretical concept can be applied individually to each adsorption layer.

Another result of this analysis is the gas adsorption and desorption isotherm curve. This trend can be compared with one of the six types in the IUPAC classification. Observing how the adsorbent material responds under these phases could be useful for understanding the structure, morphology and designing processes. The overall shape indicates pore structure, viewing the amount adsorbed at different adsorption pressures. Indicating a higher gain in mass for low pressure and low gain for higher pressures as a microporous material, on the contrary, for macro-porous or non-porous

materials. With these assumptions, we can divide type I with microporous structures, type II for non-porous or macro-porous, and type IV as mesoporous (a shape between the other two).

Another classification is the presence of a hysteresis, which represents a separation between adsorption and desorption branches, representing an anticipation or delay in the desorption behaviour [28].

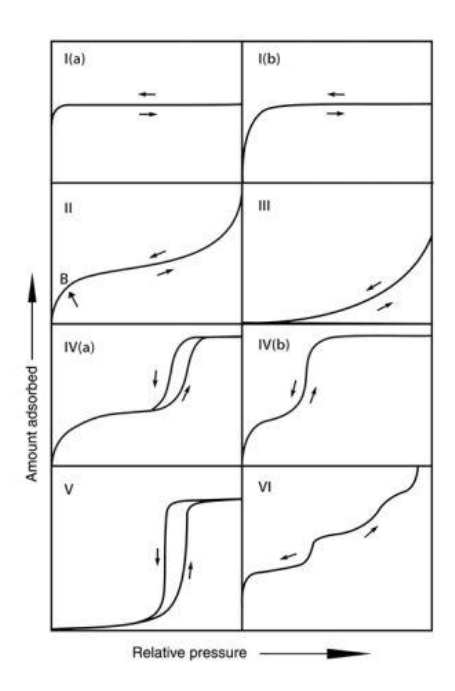


Figure 11: BET isotherms adsorption and desorption curve types [34].

# **Equipment**

- Micromeritics ASAP 2020 (Accelerated Surface Area and Porosimetry System), specifically version 4.02, operating in MicroActive 5.02 software

### **Materials**

- Treated fly ashes

#### Procedure

- **1. Sample preparation and degassing:** The material is weighed and placed in a glass vial, degassed under vacuum conditions while the temperature is maintained at 400 °C for six hours. Water vapour and other gases adsorbed are removed from the sample surface.
- 2. **Cryogenic cooling:** Interaction between gas and solid interface is weak at ambient conditions. To favour adsorption and making it measurable, the sample is cooled to cryogenic temperatures with liquid nitrogen.
- 3. **Gas adsorption process:** Nitrogen gas is incrementally introduced into the sample using a calibrated piston and ensuring that the relative pressure ranges from 0 to 1. Where relative pressure is calculated as equilibrium pressure divided by the saturation pressure. When relative pressure reaches 1, saturation pressure is reached, revealing in a no additional adsorption even with further pressure increases.
- 4. **Adsorption sequence:** First micropores are filled (< 2 nm diameter) then mesopores (2-50 nm diameter), third macropores (> 50 nm diameter) and last a complete monolayer of molecules is formed in the entire sample surface.
- 5. **Desorption and data collection:** The nitrogen environment is heated, realising the adsorbed nitrogen which is precisely quantified. Collected data generates a BET isotherm and thanks to the trend of the curve the adsorbent can be classified.

# 4.7. Sulphur dioxide adsorption test

Adsorption is a surface phenomenon characterized by the accumulation of adsorbate molecules (gas or liquid phase) onto the surface of an adsorbent (solid phase) through van der Waals forces, electrostatic interactions, or chemical bonding. This process occurs because of unsatisfied valence forces present at the solid-gas interface, creating an energetically favourable condition for molecular adhesion. The mechanism has gained significant attention as an effective approach for atmospheric pollutant control, particularly for the removal of sulphur dioxide (SO<sub>2</sub>) from fume treatment, a primary contributor to acid precipitation and adverse respiratory health effects. Previous studies have demonstrated that treated fly ash can serve as a cost-effective alternative to conventional adsorbents for SO<sub>2</sub> capture applications, the low porosity and surface reactivity can be improved [29].

In this study, fly ash samples have been subjected to ball milling treatment, a mechanical activation process designed to increase specific surface area and create new microporous structures through particle size reduction and surface fracturing. Ball milling is expected to modify the morphological characteristics of fly ash, including the generation of fresh reactive sites through the breakdown of larger particles and the creation of surface defects. The result is a structural imperfection or deviation from the original fly ashes where defects are built. Oxygen from alumina or silica structures is modified into non-stoichiometric composition, either oxygen is missing, in excess or in unusual coordination environment within the material crystal or surface. This behaviour creates sites that typically react as Lewis basic sites, donating electrons to adsorbent molecules. Modification of local electronic structures also creates new energy levels that enhance binding interaction with specific molecules [29].

The primary objective of this experimental investigation is to quantitatively assess the SO<sub>2</sub> adsorption capacity of modified fly ash samples that have been previously characterized and classified as non-hazardous materials in accordance with regulatory frameworks. Specifically, this study aims to:

- Determine the maximum adsorption capacity of treated fly ash under controlled laboratory conditions
- Evaluate the kinetic behaviour of the adsorption process
- Compare experimental results with literature values to validate the adsorbent performance
- Assess the potential of fly ash as a sustainable adsorbent for industrial SO2 removal applications and for a potential new inert and stable material

The experimental approach employs gravimetric analysis to quantify  $SO_2$  uptake by measuring the mass variation of fly ash samples during exposure to a controlled  $SO_2$ -containing gas stream. The adsorption capacity is calculated using the relationship in Equation 18, where q is the adsorption capacity,  $m_1$  is the mass after the adsorption process, and  $m_0$  is the initial dry mass of the adsorbent [21].

$$q = \frac{m_1 - m_0}{m_0}$$

 ${\it Equation~18: Formula~for~obtaining~the~adsorption~capacity}.$ 

The experimental conditions are monitored to ensure reproducibility and accuracy of results. Key parameters include:

• SO<sub>2</sub> inlet concentration maintained at predetermined levels using certified gas mixtures

- Gas flow rate regulated to ensure adequate contact time while preventing mass transfer limitations
- Temperature and pressure are monitored continuously to account for environmental variations
- Contact time is optimized based on preliminary kinetic studies

## **Equipment:**

- TGA Equipment Models SDT Q-600
- Iberfluid Instruments Flow Controller

#### Materials:

- 2 platinum capsules
- 2 alumina discs
- Fly ashes
- Tweezers
- Spatula

### **Reactants:**

- Bottle of N<sub>2</sub>, Air Liquide (>99,995%)
- SO<sub>2</sub> bottle, Praxair (2% v/v in N<sub>2</sub>)
- Fly ashes

#### **Procedure:**

# • Equipment setup and preparation

Before initiating any experimental procedures, the gas supply system must be properly configured. Both nitrogen ( $N_2$ ) carrier gas and sulphur dioxide/nitrogen ( $SO_2/N_2$ ) mixture connections are established according to the instrument specifications. Due to the single flow meter limitation of the thermogravimetric analyser, an additional external flow meter is integrated into the gas delivery system to ensure accurate flow control and monitoring.

Instrument initialization and sample preparation

The experimental sequence commences with the activation of the thermogravimetric analyser equipment, followed by computer initialization and the running of the TA Instruments Explorer software package. The furnace chamber is opened to allow placement and clean, contamination-free platinum sample crucibles are placed into the microbalance system. The experimental configuration employs a dual-crucible setup where the distant crucible serves as the reference standard while the proximal crucible contains the fly ash sample. The furnace is now sealed, and the balance system is tared to establish baseline measurements. The furnace is subsequently reopened to facilitate sample loading, wherein the sample crucible is carefully removed and filled with approximately 50 % of its capacity using the ball-milled fly ash. The loaded crucible is repositioned on the microbalance, and the system registers the sample mass, which is maintained within the optimal range of 10-40 mg to ensure measurement accuracy and minimize experimental error. Consistent sample masses across all experimental trials are maintained to reduce inter-test variability.

# • Experimental protocol implementation

With the crucibles properly positioned, and the furnace chamber secured, the experimental protocol is programmed using the integrated software interface. The complete experimental procedure consists of two distinct phases: the sample conditioning phase (preparation), where thermal drying and degassing of the fly ash sample to remove residual moisture and volatile compounds occur. The second is the adsorption phase, where controlled exposure to SO<sub>2</sub>-containing gas stream to quantify uptake capacity.

| Procedure   | N <sub>2</sub><br>(mL/min) | $SO_2/N_2$ (mL/min) | Description  |
|-------------|----------------------------|---------------------|--|
| Preparation | 120,00                     | 0,00                | I step: from room temperature to 105°C with 5°C/min ramp II step: 5-minute isotherm III step: from 105°C to 35°C with a 20°C/min ramp IV step: isotherm until the mass is stable |
| Adsorption  | 114,00                     | 6,00                | Isotherm until the mass is stable  |

Table 8: Example of a procedure for 1000 ppm of  $SO_2/N_2$  to insert in the experimental protocol.

The gas flow rates are controlled and varied according to the SO₂ concentrations wanted.

While the methodology remains consistent across all experimental trials, specific flow rate parameters are adjusted to achieve the desired concentration profiles, found in Table 9.

## Post-experimental procedure

Upon completion of the programmed experimental sequence, the furnace chamber is opened, and the sample crucibles are carefully removed from the microbalance system. The computer software is properly shut down, followed by systematic deactivation of the thermogravimetric analyser equipment to ensure instrument longevity and maintain calibration stability.

Due to the toxic and corrosive nature of sulphur dioxide, comprehensive safety measures are implemented throughout the experimental procedure. The exhaust gas stream is neutralized using a 0,1 M sodium hydroxide scrubbing solution system designed according to standard laboratory safety protocols.

### Calculation of flow rates according to the required concentration

The experimental investigation encompasses a comprehensive concentration range of sulphur dioxide from 500 to 8000 ppm to evaluate the adsorption behaviour across various pollutant loading conditions. Gas flow rates are precisely monitored and controlled using calibrated flowmeters installed at the gas inlet connections to ensure accurate concentration delivery throughout the experimental duration.

The gas mixing system utilizes a certified SO<sub>2</sub>/N<sub>2</sub> mixture containing 2 % sulphur dioxide by volume (20000 ppm) as the source gas, which is diluted with air to achieve the desired test concentrations. The total gas flow rate is maintained constant at 120 mL/min to ensure consistent contact conditions across all experimental trials.

The individual flow rates for each gas stream are calculated using the dilution relationship.

$$1000 \ ppm \ SO_2 \rightarrow \frac{1000 \ mL \ SO_2}{10^6 \ mL \ solution} \cdot 120 \ mL \ solution \cdot \frac{100 \ mL \ \frac{SO_2}{N_2}}{2 \ mL \ SO_2} = 6 \ mL \ \frac{SO_2}{N_2}$$
Fountion 19: Formula for calculation the age stream of SO:

Equation 19: Formula for calculating the gas stream of SO<sub>2</sub>.

To achieve a concentration of 1000 ppm  $SO_2$  in 120 mL/min of total dissolution, 6 mL/min are required from the  $SO_2/N_2$  cylinder and 114 mL/min of air.

This systematic approach ensures precise concentration control while maintaining consistent hydrodynamic conditions throughout the experimental matrix.

| (O. (nnm)             | Total flow rate (m) (min) | Flow rate of SO <sub>2</sub> /N <sub>2</sub> | Air's flow rate |  |
|-----------------------|---------------------------|--|-----------------|--|
| SO <sub>2</sub> (ppm) | Total flow rate (mL/min)  | (mL/min)                                     | (mL/min)        |  |
| 500,00                | 120,00                    | 3,00   | 117,00          |  |
| 1000,00               | 120,00                    | 6,00   | 114,00          |  |
| 2500,00               | 120,00                    | 15,00  | 105,00          |  |
| 4000,00               | 120,00                    | 24,00  | 96,00           |  |
| 6000,00               | 120,00                    | 36,00  | 84,00           |  |
| 8000,00               | 120,00                    | 48,00  | 72,00           |  |

Table 9: Flow rate of  $SO_2/N_2$  and  $N_2$  for different concentrations of  $SO_2$ .

The thermogravimetric analyser continuously records mass changes throughout the experimental procedure, generating characteristic profiles that exhibit distinct phases corresponding to sample conditioning and  $SO_2$  adsorption. The adsorption phase is characterized by a positive mass increment, indicating successful  $SO_2$  uptake by the fly ash sample.

$$q = \frac{mg \ SO_2}{g \ CV} = \frac{m_1 - m_0}{m_0} \cdot 1000$$

Equation 20: Formula to calculate the adsorbent capacity in [mg SO2/g adsorbent] where  $m_1$  is the mass after adsorption and  $m_0$  is the mass before adsorption.

Adsorption capacity serves as the primary performance metric for evaluating adsorbent materials, providing a quantitative assessment of their effectiveness for pollutant removal applications. This parameter enables direct comparison between different adsorbent materials and facilitates optimization of operational parameters, including contact time, adsorbent dosage and inlet concentration ranges.

From a fundamental perspective, adsorption capacity provides valuable insights into the surface properties, pore structure, and chemical reactivity of the adsorbent material. Higher capacity values

typically correlate with increased surface area, favourable pore size distribution and enhanced surface chemistry. This parameter enables comprehensive cost-benefit analysis by establishing performance benchmarks on a per-unit-mass or per-unit-volume basis. Similar information is crucial for industrial applications where economic viability depends on the trade-off between adsorbent performance and material costs, facilitating the design of the treatment systems with the determination of optimal regeneration or replacement schedules.

Understanding the saturation limits of the adsorbent material allows efficient process design and minimizes operational costs associated with premature adsorbent replacement or inadequate treatment performance.

The experimental data will be analysed using established adsorption isotherm models to elucidate the adsorption mechanisms and predict system behaviour under varying operational conditions. The Langmuir and Freundlich models represent the most applied theoretical frameworks for describing adsorption equilibrium: the Langmuir Model assumes monolayer adsorption on homogeneous surfaces with finite adsorption sites instead Freundlich Model describes multilayer adsorption on heterogeneous surfaces with exponential site energy distribution.

Model selection is based on statistical analysis of experimental data fitting, with each model providing complementary insights into adsorption mechanisms and practical capacity limitations. The chosen model will inform scale-up considerations and provide predictive capability for system optimization under industrial operating conditions.

### Langmuir model

The Langmuir equation relates the amount of substance adsorbed to the gas pressure or the concentration of the substance in the fluid phase. This equation assumes that adsorption reaches equilibrium, where the rate of adsorption is equal to the rate of desorption. Adsorbent surface is supposed flat and homogeneous, plus the adsorbate is an ideal gas at the considered temperature [31].

$$q = \frac{q_{max} \cdot K \cdot P_p}{1 + K \cdot P_p}$$

Equation 21: Langmuir fitted model.

#### Where:

- Q adsorbed quantity (mg SO<sub>2</sub>/g FA)
- Q<sub>max</sub> maximum adsorption capacity (mg SO<sub>2</sub>/g FA)
- K Langmuir constant
- P<sub>p</sub> partial pressure of the adsorbent (atm), calculated with Equation 22

$$P_n = P_{tot} \cdot x$$

Equation 22: Formula for partial pressure.

Linearizing the equation to determine the unrecognized parameters results in:

$$\frac{P_p}{q} = \frac{1}{K \cdot q_{max}} + P_p \cdot \frac{1}{q_{max}}$$

Equation 23: Langmuir model linearized.

As it can be seen in the Equation 23 representing  $P_p/q$  and  $P_p$ , the slope and the ordinate are obtained with parameter fitting. The only unknown parameters at this point are the maximum adsorption capacity and the Langmuir constant that can be calculated from the graph.

# Freundlich model

The Freundlich isotherm model describes multilayer adsorption processes occurring on heterogeneous surfaces characterized by sites with exponentially distributed adsorption energies. This model fundamentally differs from the Langmuir approach in its treatment of the concentration-adsorption relationship and underlying surface assumptions. While the Langmuir equation predicts saturation behaviour that asymptotically approaches a maximum capacity (q<sub>max</sub>) due to monolayer coverage limitations, the Freundlich equation describes continuous, gradually increasing adsorption even at elevated concentrations. This pattern reflects the model's accommodation of multiple adsorption layers and the energetic heterogeneity of binding sites, where high-energy sites are occupied first, followed by progressively weaker sites [31].

The Freundlich equation is expressed as:

$$q = K_F \cdot P_p^{\frac{1}{n}}$$

Equation 24: Freundlich equation.

#### Where:

Q: adsorbed quantity (mg SO<sub>2</sub>/g FA)

- K<sub>F</sub>: Freundlich constant

- P<sub>p</sub>: partial pression of adsorbate (atm)

- n: exponential factor (describes the affinity between adsorbate and adsorbent)

For parameter determination, this power-law relationship is linearized by logarithmic transformation.

$$\log(q) = \log(K_F) + \frac{1}{n} \cdot \log(P_p)$$

Equation 25: Linearized Freundlich equation.

When log(q) is plotted against log( $P_p$ ), an ideal straight line is obtained from which the Freundlich constants can be extracted. The slope of this linear plot directly provides 1/n, known as the heterogeneity factor or adsorption intensity, where values closer to 0 represents more heterogeneous surfaces and stronger adsorption. The y-intercept yields log( $K_F$ ) with  $K_F$  representing the Freundlich adsorption capacity constant (expressed in  $(\frac{mg}{g} \cdot \frac{L}{mg})^{\frac{1}{n}}$ ) that quantifies the relative adsorption capacity of the adsorbent and indicates the strength of the adsorbate-adsorbent interaction. Higher  $K_F$  values signify greater adsorption capacity and stronger binding affinity.



Figure 12: TGA Equipment Models SDT Q-600 with Iberfluid Instruments Flow Controller.

# 4.8. Hydrogen sulphide adsorption test

The hydrogen sulphide adsorption investigation follows an analogous experimental approach to the SO<sub>2</sub> testing protocol, with modifications in values of concentration of the stream gas and a higher caution associated with H<sub>2</sub>S handling. Hydrogen sulphide presents greater health hazards due to its extreme toxicity at low concentrations.

The hydrogen sulphide experimental setup utilizes a certified hydrogen sulphide/nitrogen ( $H_2S/N_2$ ) mixture as the source gas containing 3000 ppm  $H_2S$  in nitrogen (ALPHAGAZ). Due to the lower stability and higher reactivity of  $H_2S$  compared to  $SO_2$ , the source gas cylinders require more frequent verification of concentration accuracy and may exhibit gradual concentration drift over time.



Figure 13: Gas cylinder of hydrogen sulphide with a concentration of 3000 ppm  $H_2S/N_2$ .

The gas dilution calculations follow the same fundamental principles as the  $SO_2$  system in Equation 19, the only parameter that changes is the concentration of the cylinder of hydrogen sulphide/nitrogen (3000 ppm).

As Table 9, the concentration adopted for the H<sub>2</sub>S adsorption are collected in Table 10.

| H <sub>2</sub> S (ppm) | Total flow rat | e Flow rate of H <sub>2</sub> S/N <sub>2</sub> | Flow rate N <sub>2</sub> |
|------------------------|----------------|--|--------------------------|
|                        | (mL/min)       | (mL/min)                                       | (mL/min)                 |
| 250,00                 | 120,00         | 10,000   | 110,00                   |
| 500,00                 | 120,00         | 20,00  | 100,00                   |
| 1000,00                | 120,00         | 40,00  | 80,00                    |

Table 10: Flow rate of  $H_2S/N_2$  and  $N_2$  for different concentrations of  $H_2S$ .

# Modified experimental procedure for H₂S testing

The  $H_2S$  adsorption experiment follows a modified two-phase structure that differs from the  $SO_2$  protocol based on preliminary experimental observations, where the sample conditioning phase with thermal drying and degassing until 105 °C is conducted under pure nitrogen flow to eliminate moisture-induced mass variations that were viewed in preliminary tests using ambient air. As the hydrogen sulphide adsorption phase starts, the gas atmosphere is switched to ambient. At the same time, when the input of the gas stream containing  $H_2S$  enters the thermo-gravitational chamber. This atmospheric transition was implemented after thermogravimetric analysis revealed abnormal mass gains during the preparation phase when air was used initially, and a gain in mass was attributed to humidity adsorption from atmospheric moisture. The modified protocol ensures accurate baseline establishment, eliminating humidity-related mass artifacts, while maintaining the integrity of the  $H_2S$  adsorption measurements through the strategic use of air atmosphere only during the actual adsorption phase.

The same methodology as in 4.7 paragraph is followed, apart from the sample preparation and adsorption phases viewed in Tables 10 & 11.

| Procedure   | N <sub>2</sub><br>(mL/min) | Air<br>(mL/min) | H <sub>2</sub> S/Air<br>(mL/min) | Description  |
|-------------|----------------------------|-----------------|----------------------------------|--|
| Preparation | 120,00                     | 0,00            | 0,00                             | I step: from room temperature to 105°C with 5°C/min ramp II step: 5-minute isotherm III step: from 105°C to 35°C with a 20°C/min ramp IV step: isotherm until the mass is stable |
| Adsorption  | 0,00                       | 80,00           | 40,00                            | Isotherm until the mass is stable  |

Table 11: Example of a procedure for 1000 ppm of  $H_2S\,/N_2$  to insert in the experimental protocol.

The thermogravimetric data analysis follows identical principles to the SO<sub>2</sub> testing, with mass changes recorded continuously throughout the experimental procedure. The characteristic adsorption profile exhibits a positive mass increment during H<sub>2</sub>S exposure.

The H<sub>2</sub>S adsorption results will be analysed in comparison with SO<sub>2</sub> data to evaluate the selectivity and versatility of the ball-milled fly ash adsorbent. Key comparative parameters include the adsorption capacity differences between H<sub>2</sub>S and SO<sub>2</sub> under equivalent conditions, kinetic behaviour variations reflecting different molecular interactions and temperature effects on adsorption performance for both gases.

The modified analytical approach for H<sub>2</sub>S testing provides comprehensive characterisation of fly ash adsorption performance across multiple sulphur containing pollutants, demonstrating the versatility and practical applicability of the modified adsorbent material.

The fitting models used to characterize the adsorption process in paragraph 4.7 are re-used for this case adsorption (Langmuir and Freundlich approaches).

# **5 RESULTS**

# 5.1. Fly ashes characterisation

Untreated fly ashes were characterised with crystallographic analysis conducted via X-ray diffraction revealing a predominantly crystalline composition, with major mineral phases identified as sodium chloride (NaCl), calcium carbonate (CaCO<sub>3</sub>), potassium chloride (KCl), calcium hydroxide (Ca(OH)<sub>2</sub>), and calcium oxide (CaO) [11]. Table n°12 presents the characterisation of the original fly ash based on the leaching test performed, comparing the values with those set out in Spain's legislation for different types of waste disposal sites.

| Compound  | FA1<br>(mg/kg<br>FA) | Hazardous<br>waste landfill | Non-hazardous<br>waste landfill | Inert waste landfill | Classification         |
|-----------|----------------------|-----------------------------|---------------------------------|----------------------|------------------------|
| Chlorides | 100905,00            | 25000,00                    | 15000,00                        | 800,00               | hazardous<br>waste     |
| Sulphates | 9140,00              | 50000,00                    | 20000,00                        | 1000,00              | non-hazardous<br>waste |
| Pb        | 46,10                | 50,00                       | 10,00                           | 0,50                 | hazardous<br>waste     |
| Ва        | 16,99                | 300,00                      | 100,00                          | 20,00                | inert waste            |
| Zn        | 44,96                | 200,00                      | 50,00                           | 4,00                 | non-hazardous<br>waste |
| As        | <2                   | 25,00                       | 2,00                            | 0,50                 | non-hazardous<br>waste |
| Cd        | <0,42                | 5,00                        | 1,00                            | 0,04                 | non-hazardous<br>waste |
| Мо        | 1,98                 | 30,00                       | 10,00                           | 0,50                 | non-hazardous<br>waste |
| Cr        | 0,48                 | 70,00                       | 10,00                           | 0,50                 | inert waste            |
| Ni        | 0,17                 | 40,00                       | 10,00                           | 0,40                 | inert waste            |
| TDS       | 349026,67            | 100000,00                   | 60000,00                        | 4000,00              | hazardous<br>waste     |

Table 12: Characterisation of the original fly ash based on the leaching test, comparing it with the values established in legislation for different types of landfills.

The FA1 samples are classified as hazardous waste due to their elevated concentrations of toxic components, which exceed the permissible thresholds for disposal in hazardous waste landfills. The primary objective of this study is to reduce the concentrations of chlorides and lead, which are the only ones that exceed the toxic threshold with total dissolved solids [11].

FA-ST-WAT samples were prepared using a controlled laboratory-scale batch treatment process, detailed in paragraph 4.1. This procedure was specifically designed to lower the concentrations of toxic and hazardous pollutants present in coal combustion residues, in compliance with the regulatory limits established by Royal Decree 646/2020 [21].

The concentrations of chlorides and lead in the treated FA1-ST-WAT samples are presented in Table 13.

| Compound  | FA-ST-<br>WAT<br>(mg/kg<br>FA) | Hazardous<br>waste landfill | Non-hazardous<br>waste landfill | Inert waste<br>landfill | Classification          |
|-----------|--------------------------------|-----------------------------|---------------------------------|-------------------------|-------------------------|
| Chlorides | 710,00                         | 25000,00                    | 15000,00                        | 800,00                  | Inert waste<br>landfill |
| Pb        | 8,75                           | 50,00                       | 10,00                           | 0,50                    | Non-hazardous<br>waste  |
| TDS       | 15241,90                       | 100000,00                   | 60000,00                        | 4000,00                 | Non-hazardous<br>waste  |

Table 13: Characterisation of the FA1-ST-WAT based on the leaching test, comparing it with the values established in legislation for different types of landfills.

The batch inertization treatment is effective for reducing the concentration of chlorides and lead into a non-hazardous level. For chlorides and SDT, the results deviate considerably from their limits of danger. However, the concentration of lead can be very variable depending on numerous factors such as pattern preparation, temperature and calibration.

Then, despite the result, in other trials may be dangerous, so it is advisable to apply other measurement methods to confirm a repeatability or establish a more effective treatment by removing this component from the ashes.

Acid-base curve of FA-ST-WAT and its correspondent blank are obtained, following the procedure described in paragraph 4.5 .

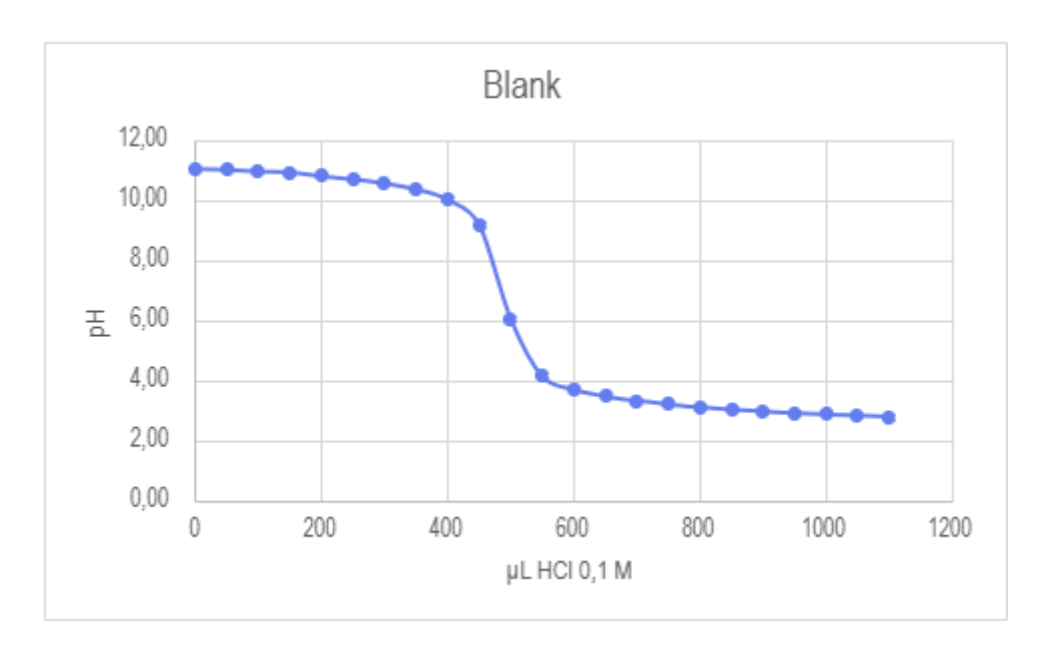


Figure 14: Acid-base curve of the blank for FA-ST-WAT.

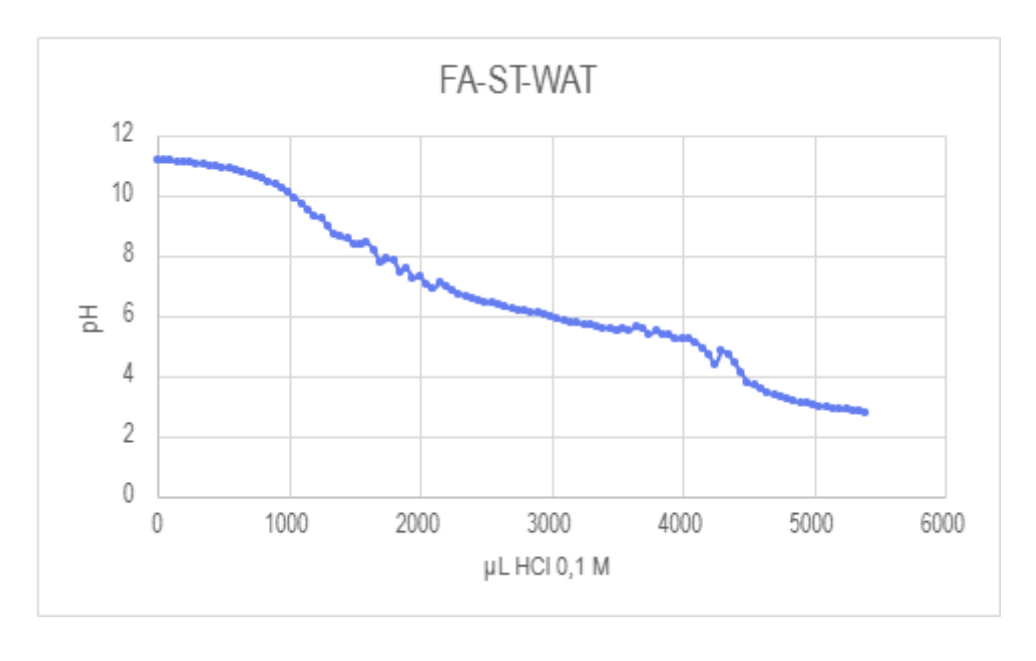


Figure 15: Acid-base curve of FA-ST-WAT.

The acid neutralization capacity is calculated with Equation 26.

$$ANC = \frac{\left(V_{sample} - V_{blank}\right) \cdot [HCl]}{m_{sample}}$$
 
$$ANC = \frac{(0,0054 \, L - 0,0011 \, L)}{0,025 \, g \, FA} \cdot 0,1 = 0,0172 \, \frac{mol \, H^+}{g \, FA} = 17,200 \, \frac{mmol \, H^+}{g \, FA}$$

Equation 26: calculation for acid neutralization capacity of FA-ST-WAT

The titration curve depicts a fly ash with an effective ANC, confirmed with the value of 17,2 mmol  $H^+/g$  FA. FA-ST-WAT has a pH of 12,3 and it is kept approximately constant in a strong base plateau, proving high concentration of CaO and Ca((OH)<sub>2</sub>). Then there is a steep decline, followed by a major buffering region, where carbonates are responsible for high acid consumption without lowering the pH. At the end there is a final drop, where other mineral phases have been consumed.

BET analysis has produced a value of surface area of 10,873  $\text{m}^2/\text{g}$ , a pore volume of 0,024 cm<sup>3</sup>/g and a pore size of 8,56 nm.

#### Isotherm Linear Plot

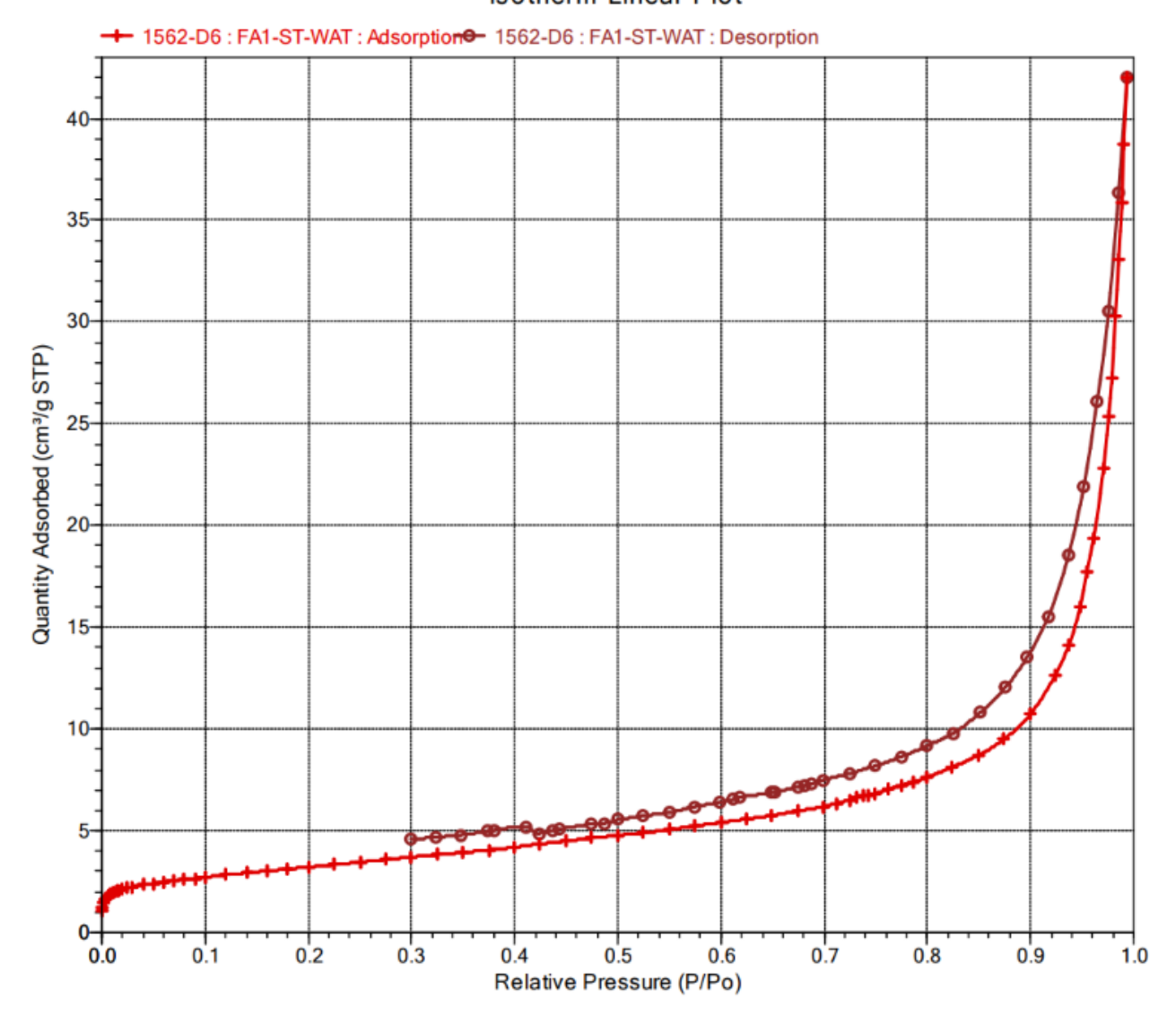


Figure 16: BET isotherm graph of FA-ST-WAT.

FA-ST-WAT exhibits a Type II isotherm according to IUPAC classification, typical for macro porous or non-porous ashes. The extremely low uptake and distinct, horizontal shape suggest an assonance with type III isotherm (characteristic of weak adsorbent-adsorbate interactions), and the low surface area confirms this hypothesis. The hysteresis loop indicates a type IV isotherm and meso-porosity (confirmed by the pore size) [28].

For proving, adsorption tests of SO<sub>2</sub> with the same procedure found in paragraph 4.7, are executed.

| SO <sub>2</sub> ppm | Mass before the adsorption (mg) | Mass after adsorption (mg) | %<br>adsorbed | Adsorption<br>capacity<br>(mg SO <sub>2</sub> /g FA) |
|---------------------|---------------------------------|----------------------------|---------------|--|
| 1000,00             | 32,59                           | 32,63                      | 0,12          | 1,26   |
| 2500,00             | 22,52                           | 22,59                      | 0,28          | 2,82   |
| 6000,00             | 19,39                           | 19,45                      | 0,31          | 3,15   |
| 8000,00             | 14,48                           | 14,53                      | 0,29          | 2,96   |

Table 14: adsorption isotherm data for FA-ST-WAT.

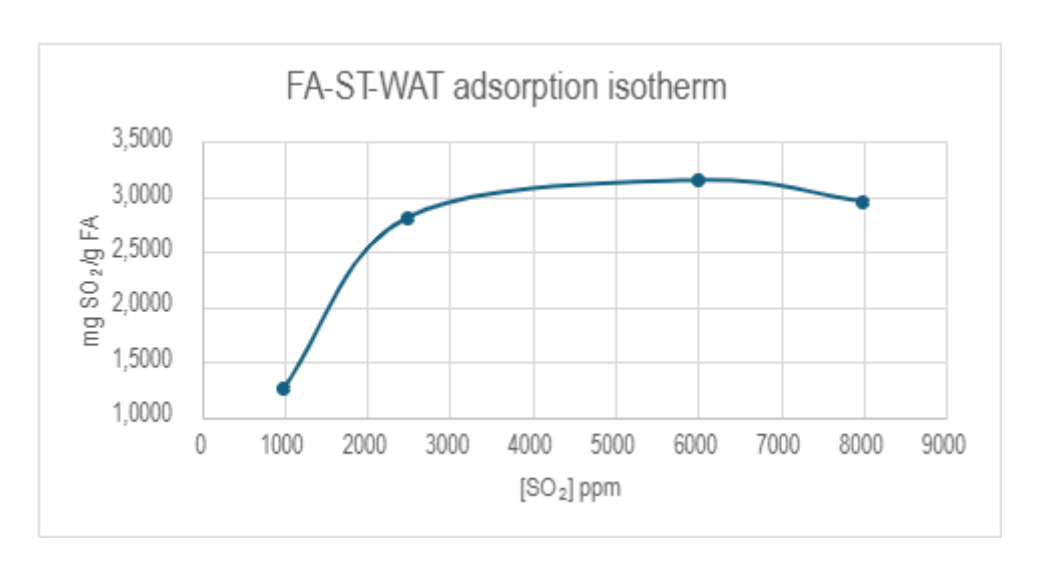


Figure 17: Adsorption isotherm graph for FA-ST-WAT.

FA-ST-WAT shows a low adsorption affinity with SO<sub>2</sub>, it could be improved by a ball milling activation.

## 5.2. Inertization and activation

This project investigated the inertization and activation of fly ash through ball-milling processes. It evaluated the leaching potential of the treated material to determine optimal approaches for waste management or reuse as raw material of fly ashes.

As a result of four different conditions for ball milling, four different ashes were produced, varying in ball size and primary ashes treated, as outlined in Table 6.

To be able to make an effective comparison, the same proportion of reagents and condition (time and speed) of ball milling procedure were used. The resulting treated fly ash samples were designated according to their processing parameters: untreated fly ash with mixed ball sizes (UFA1) and big ball sizes (UFA2), inertized fly ash with mixed ball sizes (IFA1) and big ball sizes (IFA2).

|                     | Mixed balls size Big balls |      |  |  |  |
|---------------------|----------------------------|------|--|--|--|
| <b>Untreated FA</b> | UFA1                       | UFA2 |  |  |  |
| Inertized FA        | IFA1                       | IFA2 |  |  |  |

Table 15: Ball milling resulting ashes.

# 5.3. Leaching results

#### **Chlorine content**

Chloride measurement with potentiometry was performed on the leachate of treated fly ashes. This analysis served first to compare results in the different type of treatments conducted in this project, and second to verify that chloride levels remained below the limits to ensure classification as a non-toxic waste.

The potentiometric titration with 0,1 M AgNO₃ generated an analytical curve called derivative curve, where on the x-axes the volume of 0,1 M AgNO₃ (mL) is found and on the y-axes is plotted the derivative of the potential (dmV/dmL). The derivative method was employed to precisely identify the equivalence point, as it provides a visually sharp peak at the point of maximum potential change during the titration, allowing to calculate the chlorine content. The single lines for every type of ash are a mean of three potentiometry tests, which resulted in similar behaviour.

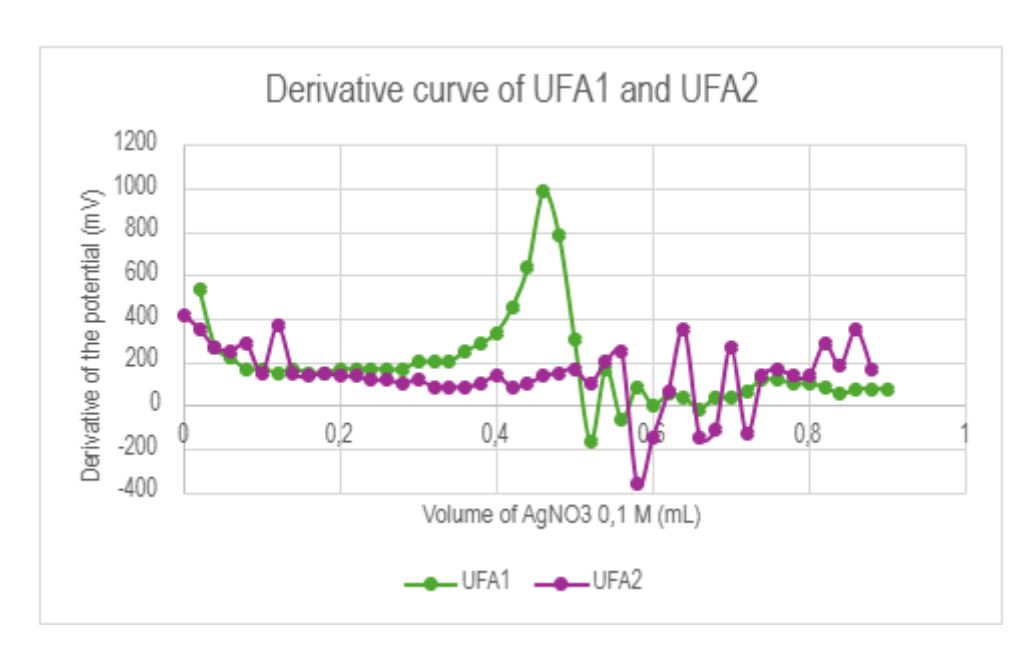


Figure 18: UFA1 and UFA2 mL AgNO3 versus the derivative of the potential.

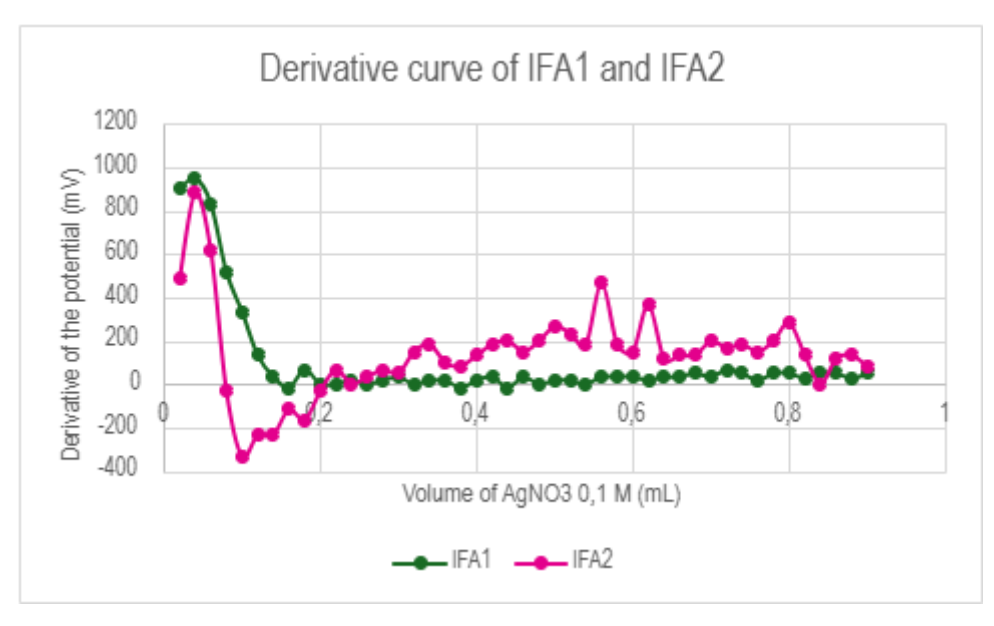


Figure 19: iFA1 and iFA2 mL AgNO3 versus the derivative of the potential.

The tables from n°16 to 20, clast together results and calculation to obtain the concentration of chlorine and their correspondent standard deviation comparable with values in the Royal Decree 646/2020.

| UFA1                                      | 1                  | 2        | 3        | AVERAGE  | DEV. STD |
|---|--------------------|----------|----------|----------|----------|
| Volume of AgNO₃ (mL)                      | 0,46               | 0,48     | 0,46     | 0,47     | 0,01     |
| Concentration of AgNO <sub>3</sub> (N)    | 0,10               | 0,10     | 0,10     | 0,10     | 0,00     |
| Volume of the sample (mL)                 | nL) 1,00 1,00 1,00 |          | 1,00     | 1,00     | 0,00     |
| Molecular mass of Cl <sup>-</sup> (g/mol) | 35,50              | 35,50    | 35,50    | 35,50    | 0,00     |
| [Cl <sup>-</sup> ] in g/L                 | 1,63               | 1,70     | 1,63     | 1,66     | 0,04     |
| [Cl <sup>-</sup> ] in mg/L                | 1633,00            | 1704,00  | 1633,00  | 1656,67  | 40,99    |
| [Cl <sup>-</sup> ] in mg/kg FA            | 16330,00           | 17040,00 | 16330,00 | 16566,67 | 409,92   |

Table 16: UFA1 chlorine content result.

| UFA2                                      | 1        | 2        | 3        | AVERAGE  | DEV. STD |
|---|----------|----------|----------|----------|----------|
| Volume of AgNO <sub>3</sub> (mL)          | 0,68     | 0,60     | 0,60     | 0,63     | 0,05     |
| Concentration of AgNO <sub>3</sub> (N)    | 0,10     | 0,10     | 0,10     | 0,10     | 0,00     |
| Volume of the sample (mL)                 | 1,00     | 1,00     | 1,00     | 1,00     | 0,00     |
| Molecular mass of Cl <sup>-</sup> (g/mol) | 35,50    | 35,50    | 35,50    | 35,50    | 0,00     |
| [Cl <sup>-</sup> ] in g/L                 | 2,41     | 2,13     | 2,13     | 2,22     | 0,16     |
| [Cl <sup>-</sup> ] in mg/L                | 2414,00  | 2130,00  | 2130,00  | 2224,67  | 163,97   |
| [Cl <sup>-</sup> ] in mg/kg               | 24140,00 | 21300,00 | 21300,00 | 22246,67 | 1639,67  |

Table 17: UFA2 chlorine content result.

| IFA1                                      | 1       | 2       | 3      | AVERAGE | DEV. STD |
|---|---------|---------|--------|---------|----------|
| Volume of AgNO <sub>3</sub> (mL)          | 0,04    | 0,04    | 0,02   | 0,03    | 0,01     |
| Concentration of AgNO₃ (N)                | 0,10    | 0,10    | 0,10   | 0,10    | 0,00     |
| Volume of the sample (mL)                 | 1,00    | 1,00    | 1,00   | 1,00    | 0,00     |
| Molecular mass of Cl <sup>-</sup> (g/mol) | 35,50   | 35,50   | 35,50  | 35,50   | 0,00     |
| [Cl <sup>-</sup> ] in g/L                 | 0,14    | 0,14    | 0,07   | 0,12    | 0,04     |
| [Cl <sup>-</sup> ] in mg/L                | 142,00  | 142,00  | 71,00  | 118,33  | 40,99    |
| [Cl <sup>-</sup> ] in mg/kg               | 1420,00 | 1420,00 | 710,00 | 1183,33 | 409,92   |

Table 18: IFA1 chlorine content result.

| IFA2                                      | 1                        | 2       | 3       | AVERAGE | DEV. STD |
|---|--------------------------|---------|---------|---------|----------|
| Volume of AgNO₃ (mL)                      | 0,02                     | 0,04    | 0,04    | 0,03    | 0,01     |
| Concentration of AgNO <sub>3</sub> (N)    | 0,10                     | 0,10    | 0,10    | 0,10    | 0,00     |
| Volume of the sample (mL)                 | nple (mL) 1,00 1,00 1,00 |         | 1,00    | 1,00    | 0,00     |
| Molecular mass of Cl <sup>-</sup> (g/mol) | 35,50                    | 35,50   | 35,50   | 35,50   | 0,00     |
| [Cl <sup>-</sup> ] in g/L                 | 0,07                     | 0,14    | 0,14    | 0,12    | 0,04     |
| [Cl <sup>-</sup> ] in mg/L                | 71,00                    | 142,00  | 142,00  | 118,33  | 40,99    |
| [Cl <sup>-</sup> ] in mg/kg               | 710,00                   | 1420,00 | 1420,00 | 1183,33 | 409,92   |

Table 19: IFA2 chlorine content result.

|      | Initial chlorine content $(\frac{mg}{kg  FA})$ | Final chlorine content $(\frac{mg}{kg\ FA})$ | Waste classification         | % removed compared to the starting fly ash |
|------|--|--|------------------------------|--|
| UFA1 | 100905,00                                      | 16566,70                                     | Hazardous waste landfill     | 83,58                                      |
| UFA2 | 100905,00                                      | 22246,67                                     | Hazardous waste landfill     | 77,95                                      |
| IFA1 | 710,00   | 1183,33                                      | Non-hazardous waste landfill | -66,67                                     |
| IFA2 | 710,00   | 1183,33                                      | Non-hazardous waste landfill | -66,67                                     |

Table 20: Chlorine contents results summarize.

The potentiometric analysis revealed significant differences in chloride concentrations between the treatments. The most notable is the different effect of the mechanochemical treatment on UFA and IFA. While on untreated ashes (UFA) the chloride stabilization/removal reaches values of approximately 80%, assuming an improvement on the leaching behaviour for chlorines but remaining a hazardous waste. In the already inertized ashes (IFA) there is an increase of chlorine in the leachate of 67% (viewed by the minus sign). Luckily, the values remain under non-hazardous conditions. In this case, milling could facilitate the leaching of chlorine, converting compounds from crystalline to an amorphous state and increasing the surface area of the fly ash particles, helping the release of sealed soluble chlorides. The equilibrium constant of dissolution for most compounds is much higher in amorphous state, rather than crystalline. To activate crystals, is needed more than 1 hour of milling, to deliver enough energy [31]. Different physicochemical changes are assumed in these two types of ashes.

The analogy between the two different sizes of balls can be viewed in UFA1 and UFA2, with higher achievements with bigger balls. The physical explanation relies in the impact energy, which depends on the mass and velocity of the ball.

$$E_i = \frac{1}{2}mv^2$$

Equation 27: impact energy formula, where m and v are the mass and the velocity of a single ball

The rotation speed and mill size are fixed, turning less mass to deliver less kinetic energy for each impact. This is translated with smaller balls not generating enough energy to break or plastically deform particles, with lower milling efficiency or slower particle reduction.

The dominant mechanism shifts from impact to abrasion, with smaller balls tending to 'pass' over the powder, causing friction rubbing and not impact [32]. Another variable that needs to be considered is smaller balls having mixed dimensions, randomizing the system with no development of an efficient energy transfer. As examples of this behaviour are smaller balls filling

voids between larger ones (cushioning impacts), less direct collision and less energy, where fly ash acts as a medium for dissipation rather than a transmitting material.

Smaller balls might result in increased total surface area contact, yet friction could increase with energy loss, plus sliding is promoted (not impact motion) [33].

Comparing IFA1 and IFA2, also having different sizes of balls, the gaining in chlorine leaching is not affected. This fact proves primary that the batch stabilization occurred was effective, and secondary the differentiation between initial structure of fly ashes (FA1 and FA-ST-WAT).

#### **Lead content**

Following the procedure described in section 4.4.2 for lead determination by atomic absorption spectroscopy. The results are resumed in Tables 21, 22, 23, 24 and 25 containing the steps of calculations for leachate liquids of treated fly ashes and comparison with the legislative values.

| UFA1                      | 1     |       |       | 2     |       | 3     |       | AVERAGE | DEV. STD |      |      |
|---------------------------|-------|-------|-------|-------|-------|-------|-------|---------|----------|------|------|
| Volume of the sample (mL) |       | 30,00 |       |       | 30,00 |       | 30,00 |         | 30,00    | 0,00 |      |
| Volume of HNO₃ 2% (mL)    |       | 3,00  |       | 3,00  |       | 3,00  |       | 3,00    | 0,00     |      |      |
| Volume of EDTA (mL)       |       | 1,00  |       | 1,00  |       | 1,00  |       | 1,00    | 0,00     |      |      |
| Volume of water (mL)      | 17,00 |       | 17,00 |       | 17,00 |       | 17,00 | 0,00    |          |      |      |
| Volumetric gauging (mL)   |       | 51,00 |       | 51,00 |       | 51,00 |       | 51,00   | 0,00     |      |      |
| [Pb] (mg/L)               | 1,48  | 1,58  | 1,62  | 0,71  | 0,72  | 0,75  | 0,52  | 0,51    | 0,49     | 0,93 | 0,48 |
| [Pb] average (mg/L)       | 1,56  |       | 0,73  |       | 0,51  |       | 0,93  | 0,56    |          |      |      |
| [Pb] real (mg/L)          | 2,66  |       |       | 1,23  |       | 0,86  |       | 1,58    | 0,95     |      |      |
| [Pb] (mg/kg FA)           |       | 26,57 |       |       | 12,33 |       | 8,59  |         | 15,83    | 9,49 |      |

Table 21: UFA1 lead content result.

| UFA2                               |        | 1     |        |       | 2      |       |        | 3     |       | AVERAGE | DEV. STD |
|------------------------------------|--------|-------|--------|-------|--------|-------|--------|-------|-------|---------|----------|
| Volume of the sample (mL)          |        | 35,00 |        | 35,00 |        | 35,00 |        | 35,00 | 0,00  |         |          |
| Volume of HNO <sub>3</sub> 2% (mL) | 43,00  |       | 43,00  |       | 43,00  |       | 43,00  | 0,00  |       |         |          |
| Volume of EDTA (mL)                | 1,00   |       | 1,00   |       | 1,00   |       | 1,00   | 0,00  |       |         |          |
| Volume of water (mL)               | 21,00  |       | 21,00  |       | 21,00  |       | 21,00  | 0,00  |       |         |          |
| Volumetric gauging (mL)            | 100,00 |       | 100,00 |       | 100,00 |       | 100,00 | 0,00  |       |         |          |
| [Pb] (mg/L)                        | 1,16   | 1,78  | 1,20   | 0,68  | 0,71   | 0,76  | 0,40   | 0,43  | 0,42  | 0,84    | 0,46     |
| [Pb] average (mg/L)                |        | 1,38  |        |       | 0,72   |       |        | 0,42  |       | 0,84    | 0,49     |
| [Pb] real (mg/L)                   | 3,94   |       | 2,05   |       | 1,19   |       | 2,39   | 1,41  |       |         |          |
| [Pb] (mg/kg FA)                    |        | 39,38 |        |       | 20,52  |       | 11,88  |       | 23,93 | 14,07   |          |

Table 22: UFA2 lead content result.

| IFA1                      |       | 1      |       |        | 2     |        |       | 3      |       | AVERAGE | DEV. STD |
|---------------------------|-------|--------|-------|--------|-------|--------|-------|--------|-------|---------|----------|
| Volume of the sample (mL) |       | 40,00  |       | 40,00  |       | 40,00  |       | 40,00  | 0,00  |         |          |
| Volume of HNO₃ 2% (mL)    |       | 34,00  |       | 34,00  |       | 34,00  |       | 34,00  | 0,00  |         |          |
| Volume of EDTA (mL)       | 1,00  |        | 1,00  |        | 1,00  |        | 1,00  | 0,00   |       |         |          |
| Volume of water (mL)      | 25,00 |        | 25,00 |        | 25,00 |        | 25,00 | 0,00   |       |         |          |
| Volumetric gauging (mL)   |       | 100,00 |       | 100,00 |       | 100,00 |       | 100,00 | 0,00  |         |          |
| [Pb] (mg/L)               | 1,26  | 1,30   | 1,33  | 0,61   | 0,63  | 0,63   | 0,52  | 0,47   | 0,50  | 0,81    | 0,37     |
| [Pb] average (mg/L)       |       | 1,30   |       | 0,62   |       | 0,50   |       | 0,81   | 0,43  |         |          |
| [Pb] real (mg/L)          | 3,25  |        | 1,56  |        | 1,25  |        | 2,02  | 1,08   |       |         |          |
| [Pb] (mg/kg FA)           |       | 32,48  |       |        | 15,55 | •      | 12,45 |        | 20,16 | 10,78   |          |

Table 23: IFA1 lead content result.

| IFA2                      | 1     |        |       | 2      |       | 3      |       | AVERAGE | DEV. STD |      |      |
|---------------------------|-------|--------|-------|--------|-------|--------|-------|---------|----------|------|------|
| Volume of the sample (mL) |       | 40,00  |       | 40,00  |       | 40,00  |       | 40,00   | 0,00     |      |      |
| Volume of HNO₃ 2% (mL)    |       | 33,00  |       | 33,00  |       | 33,00  |       | 33,00   | 0,00     |      |      |
| Volume of EDTA (mL)       | 1,00  |        |       | 1,00   |       | 1,00   |       | 1,00    | 0,00     |      |      |
| Volume of water (mL)      | 26,00 |        | 26,00 |        | 26,00 |        | 26,00 | 0,00    |          |      |      |
| Volumetric gauging (mL)   |       | 100,00 |       | 100,00 |       | 100,00 |       | 100,00  | 0,00     |      |      |
| [Pb] (mg/L)               | 0,44  | 0,49   | 0,48  | 0,29   | 0,30  | 0,35   | 0,25  | 0,25    | 0,24     | 0,34 | 0,10 |
| [Pb] average (mg/L)       | 0,47  |        | 0,31  |        | 0,25  |        | 0,34  | 0,11    |          |      |      |
| [Pb] real (mg/L)          | 1,17  |        | 0,78  |        | 0,62  |        | 0,86  | 0,28    |          |      |      |
| [Pb] (mg/kg FA)           |       | 11,70  |       |        | 7,81  |        | 6,22  |         | 8,58     | 2,82 |      |

Table 24: IFA2 lead content result.

|      | Initial lead content<br>(mg/kg FA) | Final lead content<br>(mg/kg FA) | Classification               | % removed compared to the starting fly ash |
|------|------------------------------------|----------------------------------|------------------------------|--|
| UFA1 | 46,10                              | 15,83                            | Hazardous waste landfill     | 65,66                                      |
| UFA2 | 46,10                              | 23,93                            | Hazardous waste landfill     | 48,09                                      |
| IFA1 | 8,75                               | 20,16                            | Hazardous waste landfill     | -130,40                                    |
| IFA2 | 8,75                               | 6,22                             | Non-hazardous waste landfill | 28,91                                      |

Table 25: Lead contents results summarize.

Relating the UFA results, about half the leachate lead was removed and this was achieved in only one hour of milling time. As for chlorine results, an increase on lead content is viewed working with smaller ball mills, re-conducting this behaviour to a lower energy impact and more heat dissipation. The IFA results are contrasting, on IFA1 appears a gain in lead content, suggesting a break on the inertization with the use of big balls occurs. Strong mechanical stress could cause fractures and

pulverization of these protective matrices, resulting in an exposure of encapsulated material (including lead). The crystalline phase is amorphized and more reactive, improving diffusion and dissolution rates.

On the other side, IFA2 has a removal of lead of 29% achieved with smaller balls, falling in the non-hazardous waste limit. The explanation is low-energy impacts that leave the stabilized structure intact plus a surface dominated grinding with shear and abrasion, resulting in a gentler mechanical activation [33].

From the analysis on the leachates the only one resulting in non-hazardous ash parameters is IFA2, for this reason, the next experiments for re-evaluation as a primary source were subjected only on this ash.

#### 5.4. Acid-base curve results

Following the procedure of the paragraph 4.561, two curves are obtained in Figures 20 and 21, where the microlitres of HCl 0,1 M are plotted against the pH value.

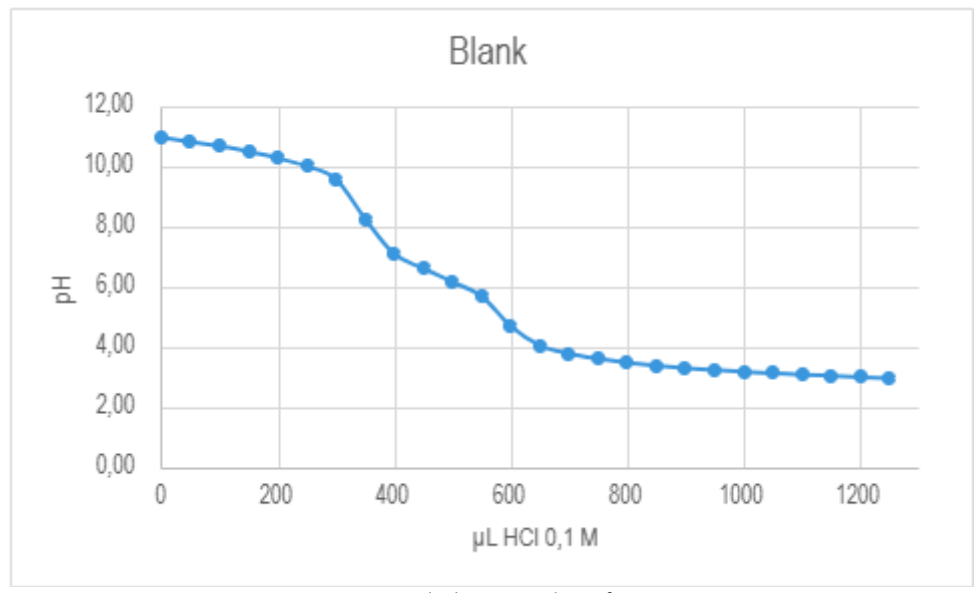


Figure 20: Blank curve analysis of IFA2.

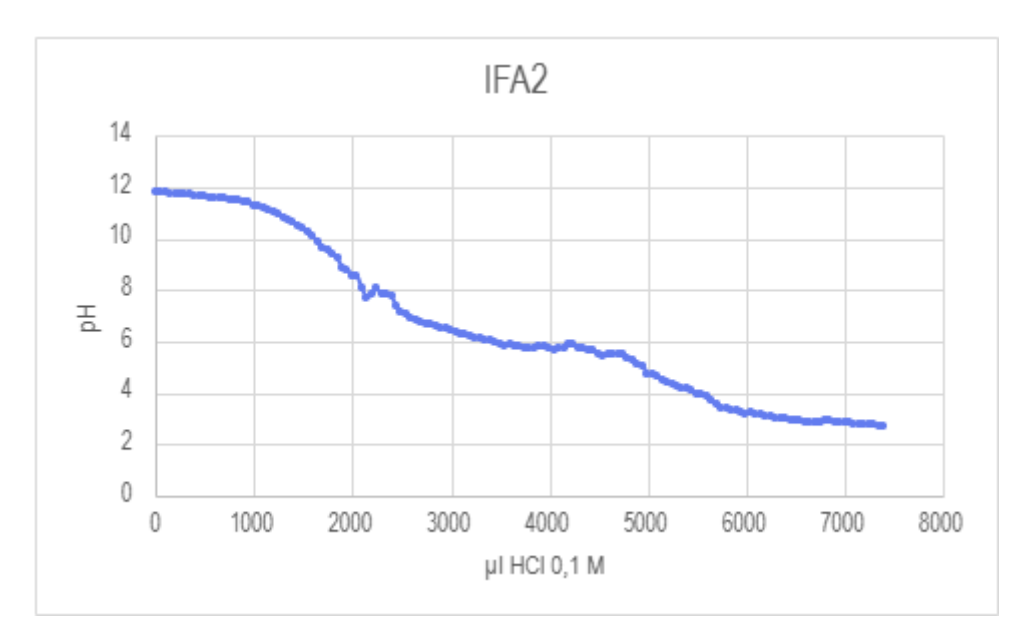


Figure 21: curve analysis of IFA2

From the volume of HCl consumed in the blank and the sample, the acid neutralization capacity (ANC) can be obtained.

$$ANC = \frac{\left(V_{sample} - V_{blank}\right) \cdot [HCl]}{m_{sample}}$$

$$ANC = \frac{(0,006325 L - 0,001250 L) \cdot 0,1 M}{0,025 g FA} = 0,0203 \frac{mol H^{+}}{g} = 20,30 \frac{mmol H^{+}}{g}$$

Equation 28: Formula for acid neutralization capacity with  $V_{sample}$  and  $V_{blank}$  are the volumes of sample and blank of HCl consumed, [HCL] is the concentration of the hydrochloric acid used and  $m_{sample}$  is the mass of the sample.

From Equation 28, it was calculated the ANC for IFA2 corresponding to 20,30 mmol H<sup>+</sup>/g classifying it as a high-calcium fly ash with substantial alkaline content. Significant presence of free lime, calcium hydroxide and carbonates is confirmed.

A buffering region is detected when the solution resists large fluctuations of pH, it is located before the equivalence point on a titration curve. The curve shows three buffering regions, suggesting a heterogeneous distribution of alkaline species with varying reactivity. Specifically:

- pH of 12-10: Reactions dominated by Ca(OH)₂ and CaCO₃ dissolution.
- pH of 6-7: Transitioning region, aluminosilicate surface reactions.

• pH of 2-3: Dissolution of silicate and aluminate phases.

A suitable application with these properties is soil stabilization, pH adjustment or supplementary cementitious material [34].

# 5.5. BET results

From the BET experiment three important characteristics of the fly ashes have been obtained and an isotherm. These parameters are crucial for adsorption properties and classification of the ash.

| Pore surface area $(\frac{m^2}{g})$ | Pore volume $(\frac{cm^3}{g})$ | Pore size (nm) |
|-------------------------------------|--------------------------------|----------------|
| 10,730                              | 0,023                          | 8,753          |

Table 26: Results of the BET analysis.

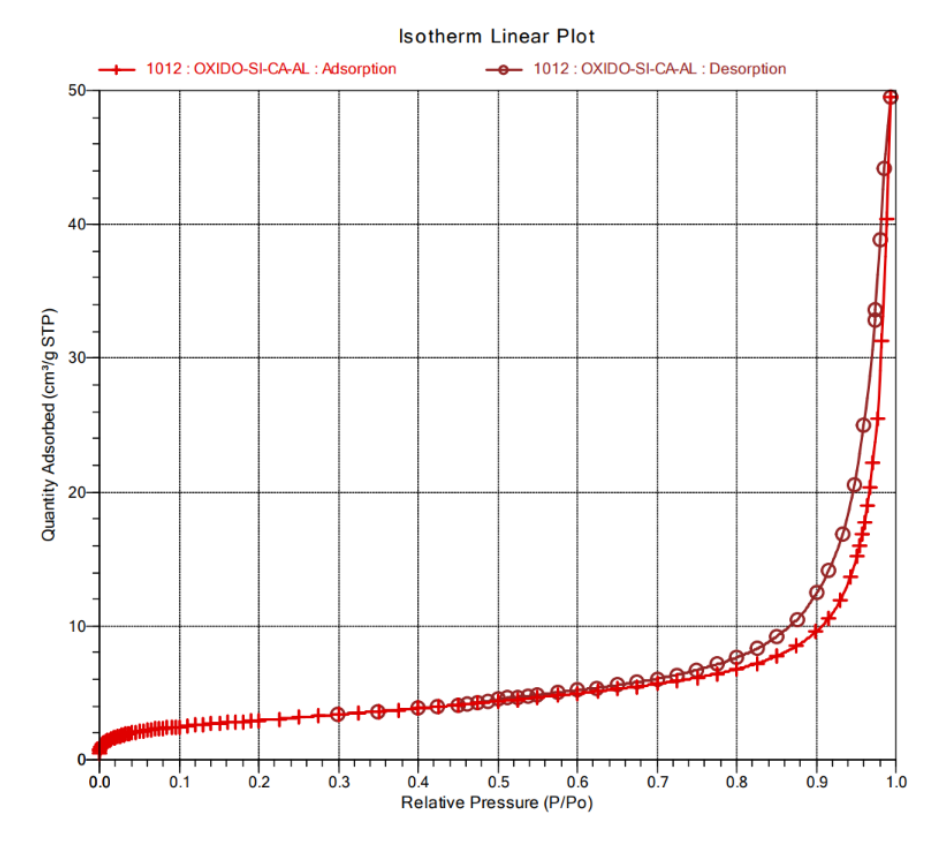


Figure 22: Isotherm linear plot of BET analysis of IFA2.

Fly ashes are classified into Class C or Class F based on their content of calcium oxide and silica-to-alumina ratio. These types of materials are considered to have a morphological smooth and glassy spherical aspect with limited microporosity [34]. The value of the specific surface area is low to moderate, confirming their classification and falling within the ash parameters activated through ball milling (5-50  $\frac{m^2}{g}$ ). This categorisation unfortunately suggests that IFA2 is more suitable for construction applications rather as an adsorption material (usually specific surface area in the order of hundreds  $\frac{m^2}{g}$  are needed) [35].

For an overall view, pore volume and pore size are also compared. The first value results in quite low volume and therefore indicates a macro porous structure where surface area might come from external particle size rather than internal pores. The second parameter classifies the material as mesoporous (2,00 nm < pore diameter < 50,00 nm). The presence of interparticle voids or limited intrinsic porosity is deducted with a low pore volume value. This value also suggests an adsorption kinetics usually relatively fast but limited overall capacity restricted to low surface area. For a designing application, a fly ash with this combination of mesoporous and low-surface-area structure, implicates a use where fast diffusion is more important than maximum adsorption capacity.

For a correct isotherm interpretation, the resulting isotherm is compared with the IUPAC classification represented in Figure 11, resulting in a type II profile and type IV hysteresis behaviour at higher pressure.

In specific at low relative pressure, minimal adsorption indicates a poor quantity of micropores instead at a mid-range pressure a gradual increase is given by the conclusion of monolayer adsorption and the onset of multilayer adsorption. At high pressure rates (> 0,8) a sharp upturn could indicate capillary condensation in mesopores, interparticle condensation and possible presence of macropores or interparticle voids.

A type II isotherm is correlated to a non-porous or macro-porous materials with unrestricted multilayer adsorption in open surfaces. A type IV hysteresis indicates the presence of mesopores, confirmed by the capillary condensation following different pathways during adsorption versus desorption.

The combined view is typical of aggregates of plate-like particles or slit-shaped pores with poreblocking effects. Explaining the delay of desorption affected by pore network effects and interparticle porosity (rather than well-defined pores) [28]. This behaviour is representative of a material which has accessibility to both external surfaces and internal mesopore networks, confirmed by significant value of specific area and low pore volume.

# 5.6. Adsorption tests

## Sulphur dioxide

The procedure described in section 4.7 was followed to analyse the  $SO_2$  adsorption on IFA2, which is the only ash classified as non-hazardous waste for both chlorine and lead parameters. The fumes coming out of the incinerator can contain  $SO_2$  in ranges from a few hundred to thousands of ppm. As the reuse of fly ashes is to be an adsorbent to decrease the concentration of these toxic components, the interval of ppm investigated varies from 500,00 to 8000,00 ppm.

Keeping temperature as a constant while varying the concentration in the gas stream allow isolating the relationship between surface coverage and the driving force for adsorption.

| SO <sub>2</sub> ppm | Mass before the adsorption (mg) | Mass after adsorption (mg) | %<br>adsorbed | Adsorption<br>capacity<br>(mg SO <sub>2</sub> /g FA) |
|---------------------|---------------------------------|----------------------------|---------------|--|
| 500,00              | 21,36                           | 22,16                      | 3,73          | 37,27  |
| 1000,00             | 21,45                           | 22,39                      | 4,37          | 43,68  |
| 2500,00             | 22,20                           | 23,17                      | 4,37          | 43,69  |
| 4000,00             | 21,82                           | 22,71                      | 4,07          | 40,73  |
| 6000,00             | 21,85                           | 22,77                      | 4,20          | 41,97  |
| 8000,00             | 22,79                           | 23,76                      | 4,22          | 42,17  |

Table 27: SO<sub>2</sub> adsorption isotherm data.

Adsorption capacities should increase with adsorbate gas concentration. Figure 23 plotted the adsorption capacity with the concentration. An evident initial sharp rise between 0 and 1500 ppm, followed by a decreasing phase in the gap 1500-4000 ppm and again a rise in the last range of concentrations. An atypical behaviour, that can be explained by a higher adsorption of water at lower concentrations, giving the initial ramp.

The highest adsorption peak is between 1000 and 2500 ppm, for a designing of a capture system, it is needed to consider that the adsorption capacity could drop at higher concentrations. Even if the capacity stays between 37 and 42 mg SO<sub>2</sub>/g FA, with no high changing.

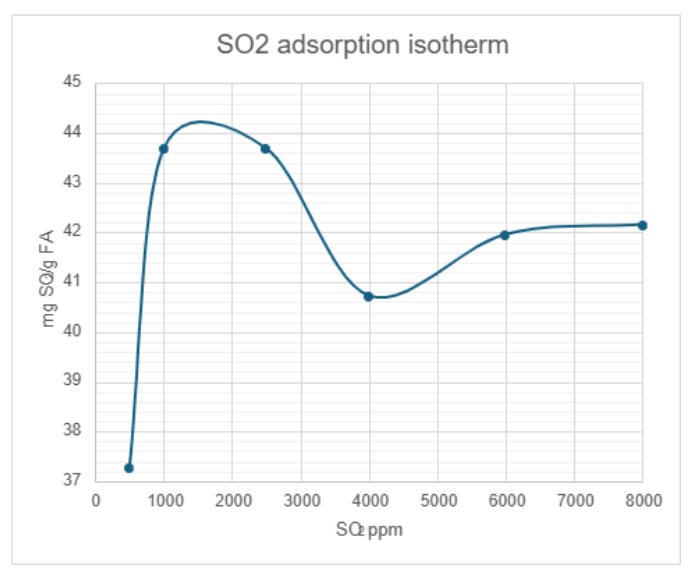


Figure 23: Isotherm graph adsorption for SO2 in IFA2.

In the study of adsorption processes, it is crucial to understand and predict how the adsorbate interacts with the adsorbent. To achieve this, adsorption equilibrium models are used. The maximum adsorption capacity can be determined using the equilibrium equations.

# Langmuir model

As explained in section 4.7, the Langmuir model assumes monomolecular adsorption on a homogeneous surface with a finite number of adsorption sites. Total pressure considered for the calculation is ambient pressure, which is 1,0057 atm. With this value partial pressure (P<sub>p</sub>) is calculated and then plotted against partial pressure divided by adsorption capacity (q), obtaining Table 28 and Figure 24.

| P <sub>p</sub> (Pa) | P <sub>p</sub> /q (Pa/(mgSO2/g FA)) |
|---------------------|-------------------------------------|
| 502,85              | 13,49                               |
| 1005,70             | 23,02                               |
| 2514,25             | 57,54                               |
| 4022,80             | 98,76                               |
| 6034,20             | 143,78                              |
| 8045,60             | 190,80                              |

Table 28: Calculation results of partial pressure and partial pressure/adsorption capacity – data of the graph.

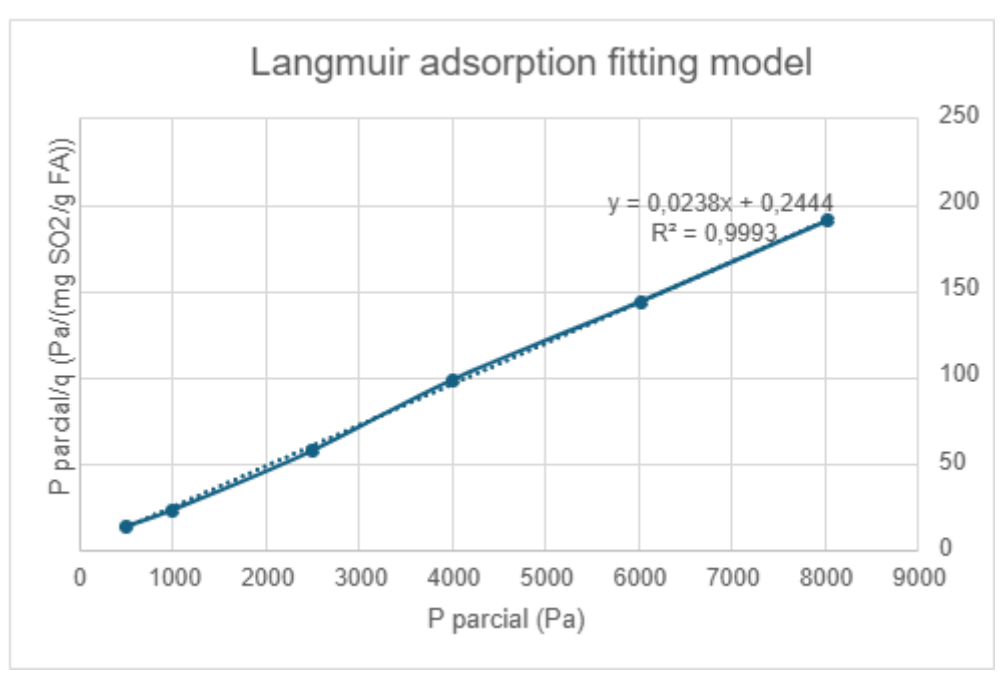


Figure 24: Graph of Langmuir model with fitted line equation.

From Figure 24, a linear relationship between  $P_p/q$  and  $P_p$  can be noticed, with a strong R-square. The Langmuir model is adequate for describing  $SO_2$  adsorption behaviour in this inertized and activated ash. This affinity shows sites of similar energy (e.g., CaO,  $Fe_2O_3$ , unburned carbon) acting uniformly towards  $SO_2$ , monolayer adsorption domination with chemisorbed layer reacting to form sulphides/sulphates rather than multilayer physisorption. There is a maximum number of reactive sites that, once occupied, additional  $SO_2$  cannot be uptake and gives a plateau behaviour.

Substituting the slope and ordinate values into the model equation, the fitting parameters are obtained.

| Maximum adsorption capacity (mg SO <sub>2</sub> /g FA) | 42,02    |
|--|----------|
| K: Langmuir's constant (1/atm)                         | 9,74E-02 |

Table 29: Fitting parameters of the Langmuir model for IFA2.

The maximum adsorption capacity is in a good range for practical low-cost desulfurization applications. It is comparable to modified fly ash systems that include calcium-based additives resulting in a value of  $44,26 \text{ mg SO}_2/\text{g FA}$ . Compared to zeolites, common adsorbents for  $SO_2$  uptake,

the adsorption capacity is 315 mg  $SO_2$ /g which is about 7,5 times higher [36]. The real advantage of IFA2 is economics, not performance. With a decent  $SO_2$  capture from an industrial waste product, making it attractive for large-scale applications where cost matters more than achieving maximum capacity.

In contrast, comparing Langmuir model with the isotherm obtained, these two behaviours are not matching. The isotherm shows a rise, dip and then plateau which suggests experimental problems, competition, or transformation between adsorption mechanisms going from chemical to physical sorption or vice versa. When pores are blocked or diffusion is limited, an apparent capacity loss is seen, might occur on intermediate concentrations. At high concentrations, secondary adsorption sites or multilayer adsorption might start contributing.

In resume the non-smooth, saturating curve is due to the stream of humified air, where higher uptake of water manifests at lower SO<sub>2</sub> concentrations, giving the resulted isothermal curve.

# Freundlich model fitting

This model fits cases where the adsorption energy varies along the surface of the adsorbent, the ambient pressure used for the calculation is 1,0057 atm. The procedure followed in encountered in paragraph 4.7.

| $\log (P_p)$ | $\log(q)$ |
|--------------|-----------|
| 2,70         | 1,57      |
| 3,00         | 1,64      |
| 3,40         | 1,64      |
| 3,60         | 1,61      |
| 3,78         | 1,62      |
| 3,90         | 1,62      |

Table 30: Calculation results of  $log(P_p)$  and log(q) – data of the graph.

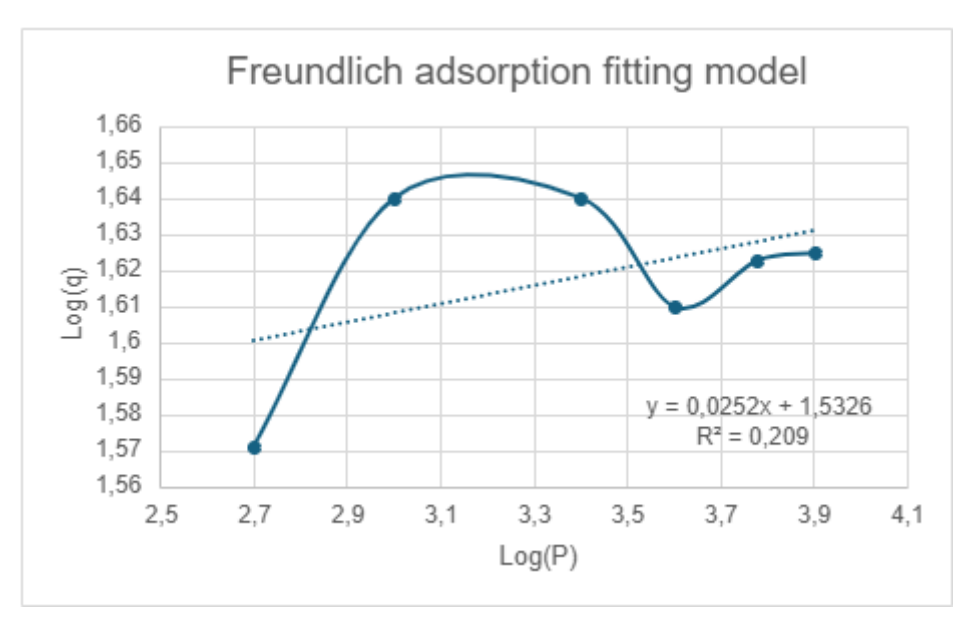


Figure 25: Graph of Freundlich model with fitted line equation.

| n (exponential factor)     | -8,04 |
|----------------------------|-------|
| KF (Freundlich's constant) | 3,62  |

Table 31: Fitting parameters of the Freundlich model.

This fit does not provide correct linearity. Therefore, is concluded that it is not an adequate method to describe this type of adsorption. Suggesting that the adsorbent surface is relatively homogeneous and that the adsorption energy is constant at all sites, characteristics well described by the Langmuir model. However, the fitting parameters can be viewed in table 31.

## Hydrogen sulphide

Adsorption of  $H_2S$  was tested on IFA2. The concentration range for the isothermal tests is less wide and limited due to the lower concentration in the cylinder and technical issues. The range between 250,00 and 1000,00 ppm, can be representative of the concentration of hydrogen sulphide in natural gas (this value greatly depends on the producing region) [37]. The fly ash could then alternatively be used as a cheap adsorbent for the removal of this gas. Known for causing corrosion problems on walls if it encounters water, as well as health and environmental problems.

| H2S<br>(ppm) | Mass before adsorption (mg) | Mass after adsorption (mg) | %<br>adsorbed | Adsorption<br>capacity<br>(mg H <sub>2</sub> S/g FA) |
|--------------|-----------------------------|----------------------------|---------------|--|
| 250,00       | 22,80                       | 23,16                      | 0,01          | 15,58  |
| 500,00       | 22,09                       | 22,45                      | 0,01          | 15,94  |
| 1000,00      | 22,61                       | 23,03                      | 0,02          | 18,24  |

Table 32: Adsorption isotherm of H<sub>2</sub>S.

Concentration effects are minimal, although a slight increase in adsorption, can be observed in Table 32. The effective modified procedure, with no moisture intake during the preparation of the sample before adsorption might be effective.

The tests with the same concentrations for the gas streams of the pollutants  $SO_2$  and  $H_2S$ , are compared. With a focus on the adsorption capacities, where  $SO_2$  results in a higher 37% uptake related to  $H_2S$ .

IFA2 appears to have active sites that preferentially bind with  $SO_2$ , as fly ash has a strong basic nature and high concentration of CaO. The explanation could rely on the higher acid behaviour of  $SO_2$ , smaller and more linear particles, stronger dipole interactions rather than  $H_2S$ .

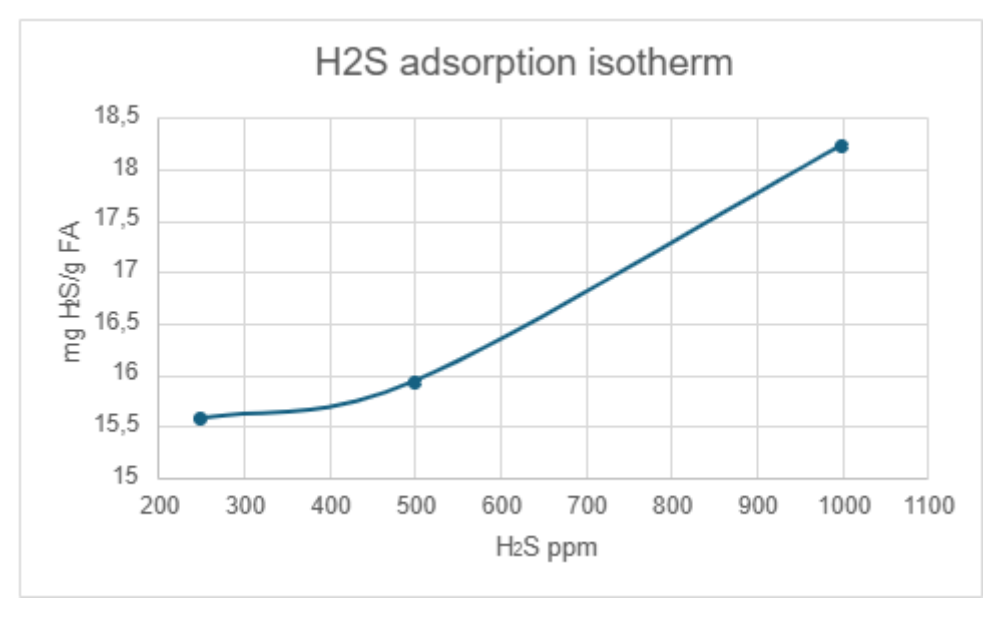


Figure 26: Isotherm graph adsorption of  $H_2S$  for IFA2.

Procedure for the calculation of the Langmuir and Freundlich model fitting is found in section 4.7.

Total pressure considered for the calculation is 1,0075 atm, as SO<sub>2</sub> adsorption tests.

# Langmuir model fitting

The Figure 27 shows a linear relationship, suggesting that the Langmuir model is adequate for describing adsorption behaviour in this inertized and activated ash. Although some other experiments need to be executed to confirm this behaviour.

|                     | P <sub>p</sub> /q |
|---------------------|-------------------|
| P <sub>p</sub> (Pa) | (Pa/(mgSO2/g FA)) |
| 251,425             | 16,14             |
| 502,85              | 31,55             |
| 1005,7              | 55,14             |

Table 33: Calculation results of partial pressure and partial pressure/adsorption capacity – data of the graph.

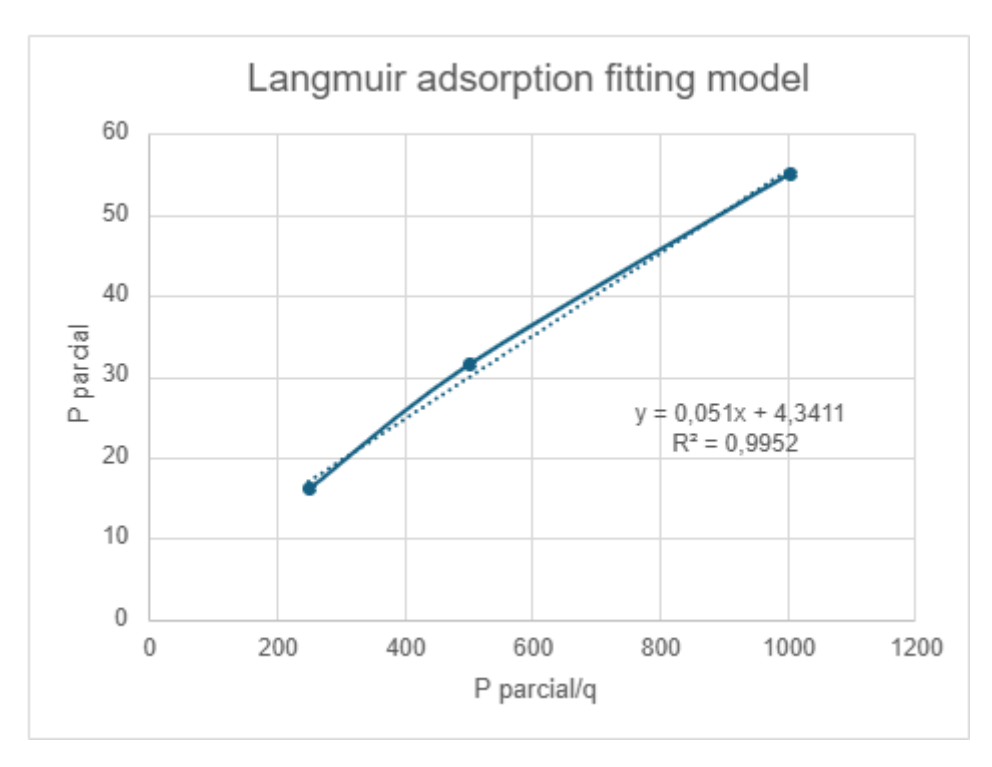


Figure 27: Graph of Langmuir model with fitted line equation.

The fitting parameters found in table 34, where the  $q_{max}$  represents the monolayer coverage with theoretically of every active site is occupied by one  $H_2S$  molecule. The value of maximum adsorption capacity is moderate falling in a normal/good range for treated fly ashes, which usually falls between 13 and 16 mg  $H_2S/g$  [37]. The  $H_2S$  adsorbent have an adsorption capacity of 100-485 mg/g range with the help of a sodium hydroxide solution [38]. The Langmuir equilibrium constant reflects the affinity between adsorbent and molecules, with smaller K (as in this case with a K=0,01 1/atm) meaning in weaker binding. Higher pressure might need to achieve significant adsorption and a physisorption dominates the interactions between active sites and  $H_2S$ , concluding with a probable reversible adsorption.

| q <sub>max</sub> : Maximum adsorption capacity (mg H <sub>2</sub> S/g FA) | 19,61 |
|---|-------|
| K: Langmuir's constant (1/atm)  | 0,01  |

Table 34: Fitting parameters of the Langmuir model.

# Freundlich model fitting

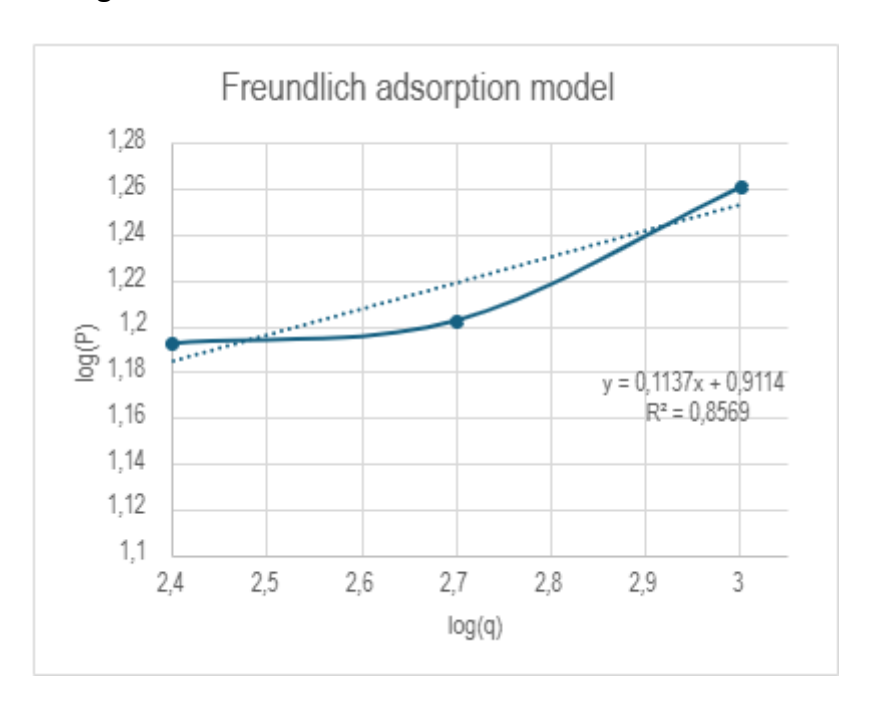


Figure 28: Graph of Freundlich model with fitted line equation.

| $\log (P_p)$ | $\log(q)$ |
|--------------|-----------|
| 2,40         | 1,19      |
| 2,70         | 1,20      |
| 3,00         | 1,26      |

Table 35: Calculation results of log(Pp) and log(q) – data of the graph.

From Table 35 and Figure 28, Freundlich model is excluded as a probable model describing the adsorption behaviour (low  $R^2$ ).

| n (exponential factor)     | 1,10 |
|----------------------------|------|
| KF (Freundlich's constant) | 1,12 |

Table 36: Calculated parameters from Freundlich fitted mode.

## **6 CONCLUSIONS AND FUTURE IMPROVEMENT**

This work successfully developed a dual-function treatment for fly ash that reduces environmental toxicity and creates value-added adsorbent properties. Only IFA2 out of four milling tests achieved non-toxic classification. The peculiarity of this ash is previous batch inertization, where chlorine and lead concentrations were reduced to safe levels, while mechanochemical activation with smaller and mixed dimension balls transformed the treated ash into an effective adsorbent for  $SO_2$  and  $H_2S$  removal. For this reason, it is the only ash subjected to further examinations, aiming to analyse its adsorbent behaviour. For all the ball milled fly ashes, it was assessed how effective the mechanochemical treatment decreases the toxic leaching behaviour. The differences in the tests are the variety of the ash feedstock type and ball mill size, comparing untreated ash with already stabilized and bigger or smaller milling balls.

As regards the specific objectives of the project, it was possible to conclude that:

- The mechanochemical ball milling treatment demonstrated effectiveness in reducing lead and chloride concentrations in untreated fly ash, with larger milling balls yielding superior results due to their higher impact energy. However, the reductions achieved were insufficient to reclassify the material as non-hazardous waste, indicating that ball milling alone must be coupled with additional treatment steps, such as chemical inertization, to meet regulatory thresholds.
  - Pre-inertized fly ash exhibited markedly different behavior under mechanical treatment. Ball milling increased chloride release due to structural amorphization that liberated previously encapsulated chlorides, reversing the stabilization achieved but remaining a non-hazardous waste. Lead behavior encountered ball-size dependency, where larger balls induced structural disruption that increased lead release, classifying the ash as toxic. While smaller balls promoted structural reorganization without compromising inertization, resulted in IFA2.
  - These findings indicate that mechanochemical treatment is most effective when applied to untreated ash feedstock. Also, for already stabilized ashes, smaller ball sizes should be employed to minimize matrix disruption while still achieving the desired adsorbent activation.
- Acid-base titration revealed a high acid neutralization capacity of 20,30 mmol H<sup>+</sup>/g with three distinct buffering regions, indicating heterogeneous distribution of alkaline species across the ash matrix. High acid neutralization capacity hypothesizes the material as Type C fly ash, characteristic of alkaline residues. Relating to FA-ST-WAT, the ash feedstock, an

increase of acid neutralization capacity of 3 mmol H<sup>+</sup>/g FA has been reported after activation via ball milling with NaOH. The causes could be milling, with exposition of previously encapsulated alkaline cores. In addition, the reagent might disrupt the inert aluminosilicate glass matrix, liberating lime and portlandite.

- From BET analysis, IFA2 exhibits a low-medium surface area. The pore size falls into the meso-porous range structure and the pore volume is low, deducing a limited internal void space with dense material matrix (more suitable for construction application rather than adsorption). The pores could be isolated or situated in shallow surfaces with thick pore walls. The isothermal shows a type II curve and a type IV hysteresis, with a mesoporous range uptake and a delay in the desorption indicating slit-like pores. Similar bet values and isotherm have been obtained for the non-activated fly ash. A common reason is that fracture and agglomeration happen simultaneously during ball milling, with NaOH acting as a binding agent. The result is a dense aggregate of the primary nanoparticles, might subjected to plastic deformation. The increased ANC in IFA2, demonstrate that adsorption sites are more active even if the surface area is quite the same.
- The activated fly ash demonstrated a better adsorption than FA-ST-WAT as expected. Good adsorption performances for both target pollutants, with SO<sub>2</sub> adsorption following Langmuir isotherm behaviour and achieving a maximum capacity of 42,02 mg SO<sub>2</sub>/g FA. Optimal uptake achieved within the 1000-2500 ppm concentration range typical of industrial flue gases, even if adsorption of water is happening concurrently. H<sub>2</sub>S adsorption yielded a lower maximum capacity of 19,61 mg H<sub>2</sub>S/g, though additional experimental validation is required for definitive confirmation. For a better comparing, the moles per gram of fly ash are calculated, as SO<sub>2</sub> presents a higher molecular mass. Respectively, 0,66 mol SO<sub>2</sub>/g FA and 0,58 mol H<sub>2</sub>S/g FA, verifying the slightly lower affinity for H<sub>2</sub>S compared to SO<sub>2</sub>. It can be attributed to the weaker Lewis acidity of H<sub>2</sub>S, resulting in less favourable interactions with the ash surface's basic sites and probable favourable reaction occurring in the adsorption sites.

IFA2 and FA-ST-WAT uptake of  $SO_2$  are compared, and good improvements are registered with the activation treatment using ball milling (adding an adsorption capacity of approximately 40 mg  $SO_2$ /g FA), only given by activation of adsorption sites.

While these capacities are lower than those of conventional adsorbents such as activated carbon and zeolites, the treated fly ash offers significant advantages for large-scale industrial applications where cost-effectiveness is a paramount. The energy-intensive production and

high material costs of traditional adsorbents, make fly ash-derived adsorbents an economically attractive alternative for bulk gas treatment, particularly for SO<sub>2</sub> removal. This approach simultaneously addresses safe management of hazardous fly ash waste and provision of affordable pollution control materials, according to circular economic principles.

For a deeper understanding and a scale up-feasibility in the integration of IFA2, the adsorption behaviour of H<sub>2</sub>S needs an expansion of the concentration range. Also, the isotherm for SO<sub>2</sub> adsorption needs to be re-evaluated, as it has a trend that deviates from normality. A better understating of how water or other parameters could influence and improve the adsorption process, for comparing with H<sub>2</sub>S tests, the same conditions are needed. To intuit the competitiveness of active ash sites and reproduce a better representation of a real flue gas composition, some experiments with simultaneous adsorption of H<sub>2</sub>S and SO<sub>2</sub> could be performed. A plus could be incorporating tests of desorption, indicating when to substitute and how to regenerate fly ashes for a possible re-use.

For improving the inertization and activation method, other coupled treatments could be suggested. As higher achievements have been reported, a first ball milling treatment with an increase of grinding time, potentially achieving better yielding. Coupled with a post alkali activation, aiming to increase the surface area through activation and re-creation of zeolitic sites.

The pairing of these processes, still produces an energy saving and low production of waste streams, sticking with the environmentally friendly and cost-effective policy.

# **BIBLIOGRAPHY**

- [1] Blissett, R.S., Rowson, N.A., (2012, July). A review of the multi-component utilization of coal fly ash. Fuel, 87, 1-23.
- [2] Vassilev, S. V., et al. (2023). Content, modes of occurrence, and significance of phosphorous in biomass and biomass ash. *Fuel*, 337.
- [3] Yildirim, I. Z., & Prezzi, M. (2011). Chemical, mineralogical, and morphological properties of steel slag. *Advances in Civil Engineering*, 2011, Article ID 463638.
- [4] Vogelsange, C., Umar, M., (2023). Municipal Solid Waste Fly ash-derived Zeolites as Adsorbents for recovery of nutrients and heavy metals. Water, 21, 3817.
- [5] Thomas, M. D. A. (2007). *Optimizing the use of fly ash in concrete*. Portland Cement Association.
- [6] Querol, J. C., Umana, A., Alastuey, A., Ayora, C., Lopez-Soler, A., & Plana, F. (2001). Extraction of soluble major and trace elements from fly ash in open and closed leaching systems. *Fuel*, 80(1), 1–11.
- [7] EOP Group. (2009). Cost Estimates for the Mandatory Closure of Surface Impoundments Used for the Management of Coal Combustion Byproducts at Coal-Fired Electric Utilities.
- [8] Qian, X., Koerner, R. M., & Gray, D. H. (2002). *Geotechnical aspects of landfill design and construction*. Prentice Hall.
- [9] Sakai, S., & Hiraoka, M. (2000). Municipal solid waste incinerator residue recycling by thermal processes. *Waste Management*, 20(2–3), 249–258.
- [10] Sánchez Redondo, I. (2023). *Valorización y aplicación de cenizas volantes procedentes de la planta de incineración de residuos sólidos urbanos de Tarragona* [Undergraduate thesis, Universidad Politécnica de Madrid].
- [11] Takacs, L. (2002). Self-sustaining reactions induced by ball milling. *Progress in Materials Science*, 47(4), 355–414.

- [12] Eurostat. (2021). Municipal waste statistics.
- [13] Fulvia, C. (2024). *Environmental processes and technologies*. [Course notes]. Politecnico di Torino.
- [14] European Environment Agency. (2022, June). Early warning assessment related to the 2025 targets for municipal waste and packaging waste: Italy.
- [15] European Environment Agency. (2022, June). Early warning assessment related to the 2025 targets for municipal waste and packaging waste: Spain.
- [16] Ministerio para la Transición Ecológica y el Reto Demográfico (MITECO). (2019). \*Plan Estatal Marco de Gestión de Residuos (PEMAR) 2016-2022\*.
- [17] Federambiente & ENEA. (2017). *Termovalorizzazione: impatto ambientale e potenziale energetico*.
- [18] Zhang, Q., & Saito, F. (2000). A review on mechanochemical syntheses of functional materials. *Advanced Powder Technology*, 23(5), 523–531.
- [19] Colombo, P., Brusatin, G., Bernardo, E., & Scarinci, G. (2003). Inertization and reuse of waste materials by vitrification and fabrication of glass-based products. *Current Opinion in Solid State and Materials Science*, 7(3), 225–239.
- [20] Hong, K.-J., Tokunaga, S., & Kajiuchi, T. (2000). Extraction of heavy metals from MSW incinerator fly ashes by chelating agents. *Journal of Hazardous Materials, B75*(1), 57–73.
- [21] Blanco Fernández, J. (2024). *Preparación de adsorbentes industriales a partir de cenizas volantes de incineradora de RSU* [Undergraduate thesis, Universidad Politécnica de Madrid].
- [22] Yuan, Q., Zhang, Y., Wang, T., Wang, J., & Romero, C. E. (2021). Mechanochemical stabilization of heavy metals in fly ash from coal-fired power plants via dry milling and wet milling. *Waste Management*, \*135\*, 428–436.
- [23] Retsch GmbH. (2020). Centrifugal Ball Mill S 100 [Instrument Database]. Evisa.

- [24] Shi, H.-S., & Kan, L.-L. (2009). Leaching behavior of heavy metals from municipal solid wastes incineration (MSWI) fly ash used in concrete. *Journal of Hazardous Materials*, 164(2–3), 750–754.
- [25] Metrohm. (2022). *Titolazioni di cloro con indicazione potenziometrica* (Application Bulletin No. AB-130).
- [26] Zewdie, D. T., Bizualem, Y. D., & Nurie, A. G. (2024). A review on removal CO<sub>2</sub>, SO<sub>2</sub>, and H<sub>2</sub>S from flue gases using zeolite-based adsorbent. *Discover Applied Sciences*, 6, 331.
- [27] Chen, Z., Lu, S., Tang, M., Ding, J., Buekens, A., Yang, J., Qiu, Q., & Yan, J. (2019). Mechanical activation of fly ash from MSWI for utilization in cementitious materials. *Waste Management*, \*88\*, 182–190.
- [28] Thommes, M., Kaneko, K., Neimark, A. V., Olivier, J. P., Rodríguez-Reinoso, F., Rouquerol, J., & Sing, K. S. W. (2015). Physisorption of gases, with special reference to the evaluation of surface area and pore size distribution (IUPAC Technical Report). *Pure and Applied Chemistry*, *87*(9–10), 1051–1069.
- [29] Li, M.-G., Sun, C.-J., Gau, S.-H., & Chuang, C.-J. (2010). Effects of wet ball milling on lead stabilization and particle size variation in municipal solid waste incinerator fly ash. *Journal of Hazardous Materials*, \*174\*(1–3), 586–591.
- [30] Saleh, T. A. (2022). Isotherm models of adsorption processes on adsorbents and nanoadsorbents. In *Interface Science and Technology* (Vol. 34, pp. 99–126). Elsevier.
- [31] Baláž, P., Achimovičová, M., Baláž, M., Billik, P., Cherkezova-Zheleva, Z., Criado, J. M., Delogu, F., Dutková, E., Gaffet, E., Gotor, F. J., Kumar, R., Mitov, I., Rojac, T., Senna, M., Streletskii, A., & Wieczorek-Ciurowa, K. (2013). Hallmarks of mechanochemistry: from nanoparticles to technology. *Chemical Society Reviews*, *42*(18), 7571–7637.
- [32] Brose, S., & Kwade, A. (2013). Impact of grinding media size and shape on the grinding efficiency. \*Minerals Engineering, 43-44\*, 2-6.
- [33] Chen, Z., Lu, S., Tang, M., Tang M., Ding J., Buekens, A., Yang, J., Qiu, Q., Yan, J., (2019). Mechanochemical activation of fly ash from MSWI for utilization in cementitious materials, Waste Management, 88, 182-190.

- [34] Altawil, H., & Olgun, M. (2025). Optimization of mechanical properties of geopolymer mortar based on Class C fly ash and silica fume: A Taguchi method approach. *Case Studies in Construction Materials*, \*22\*, e04332.
- [35] Ahmaruzzaman, M., (2010, June). A review on the utilization of fly ash. Progress in energy and combustion science, 36, 3, 327-363.
- [36] Liu, Y., Li, J., Zhao, Z., Hou, X., Zhang, H., Wen, C., Wang, X., Li, Y., & Wang, W. (2024). Study of a coal fly ash-based integrated CO<sub>2</sub> capture-mineralization material: Preparation method, modification mechanism, and CO<sub>2</sub> mineralization property. *Science of the Total Environment*, \*955\*, 177201.
- [37] Wu, H., Zhu, Y., Bian, S., Ko, J. H., Li, S. F. Y., & Xu, Q. (2018). H2S adsorption by municipal solid waste incineration (MSWI) fly ash with heavy metals immobilization. *Chemosphere*, \*195\*, 40–47.
- [38] Wang, S., Nam, H., Gebreegziabher, T. B., & Nam, H. (2019). Adsorption of acetic acid and hydrogen sulfide using NaOH impregnated activated carbon for indoor air purification. *Engineering Reports*, \*2\*(1), e12012.